Ye. Ye. Aleksandrov, V. O. Bohomolov, V. I. Klimenko, D. M. Leontiev

APPLIED THEORY OF VIBRATIONS for Students of Automotive Specializations at Higher Education Institutions

Study Guide

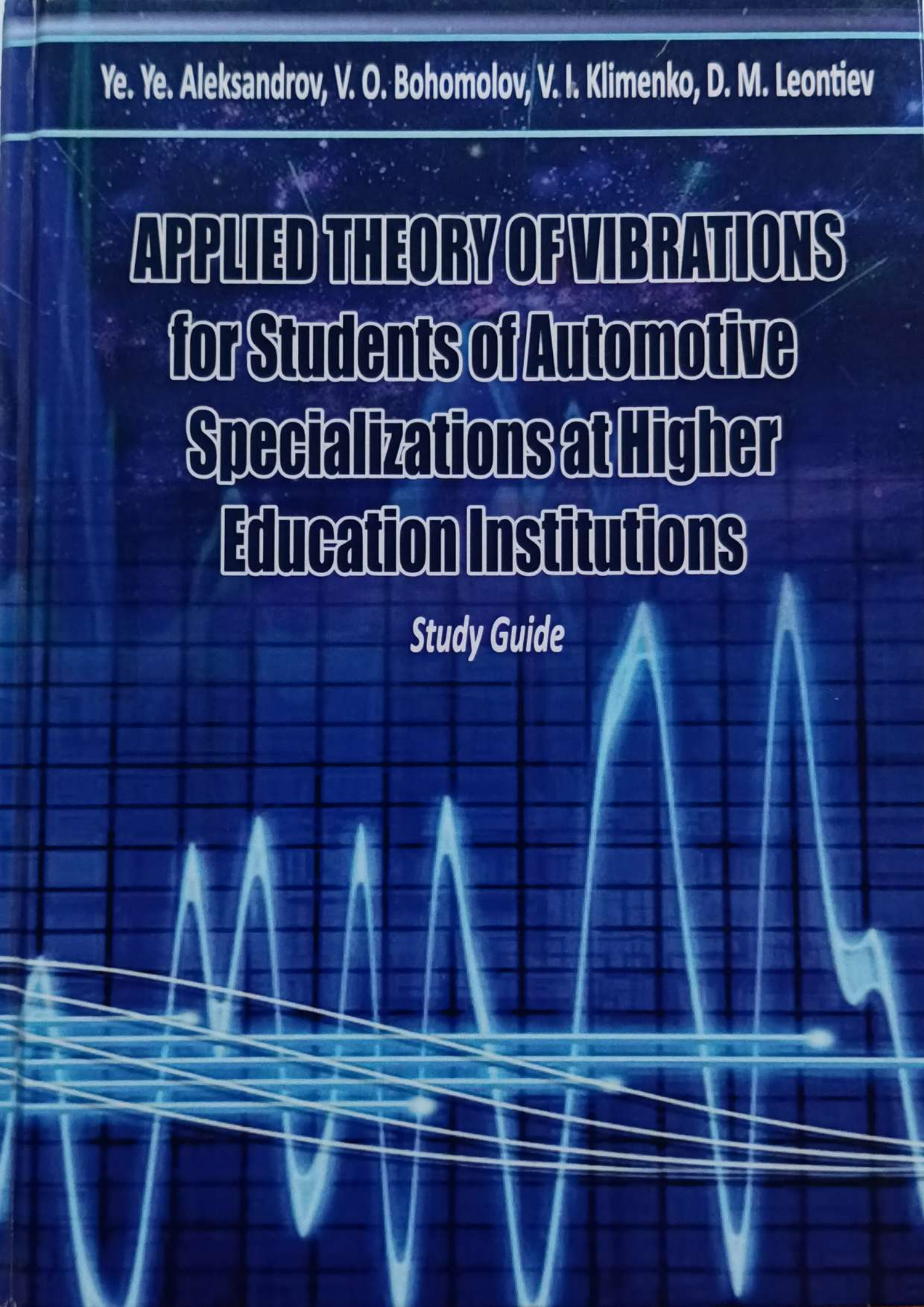

Ministry of Education and Science of Ukraine
Kharkiv National Automobile and Highway University

**Ye. Ye. Aleksandrov, V. O. Bohomolov,
V. I. Klimenko, D. M. Leontiev**

APPLIED THEORY OF VIBRATIONS for Students of Automotive Specializations at Higher Education Institutions

Study Guide

Kharkiv
KhNAHU
2026

UDC 629.3
BBK 30
A 46

Recommended by the Academic Council (Approval No. 80/25/6.22 dated 11/25/2025)
as a study guide for students of higher education institutions.

Reviewers:
O.O. Larin *– Corresponding Member of the National Academy of Sciences of Ukraine, D.Sc. (Eng.), Professor, Director of the Educational and Scientific Institute of Computer Modeling, Applied Physics and Mathematics, National Technical University "Kharkiv Polytechnic Institute"*
K.V. Avramov *– Corresponding Member of the National Academy of Sciences of Ukraine, D.Sc. (Eng.), Professor, Head of the Department of Nonlinear Mechanics and Mathematical Modeling of the Institute of Energy Machines and Systems, National Academy of Sciences of Ukraine*
R.O. Kaidalov *– D.Sc. (Eng.), Prof., Head of the Department for Organization of Educational and Scientific Activities of the Professional Training Directorate (J-7) of the Main Directorate of the National Guard of Ukraine*
M.A. Podryhalo *– D.Sc. (Eng.), Prof., Head of the Department of Mechanical Engineering Technology and Machine Repair, Kharkiv National Automobile and Highway University.*

Authors:
Ye.Ye. Aleksandrov, D.Sc. (Eng.), Professor, V.O. Bohomolov, D.Sc. (Eng.), Professor, V.I. Klymenko, D.Sc. (Eng.), Professor, D.M. Leontiev, D.Sc. (Eng.), Professor, KhNADU.

Ye. Ye. Aleksandrov

A 46 Applied theory of vibrations for students of automotive specializations at higher education institutions : 2nd Edition / Ye. Ye. Aleksandrov, V. O. Bohomolov, V.I. Klimenko, D. M. Leontiev – Kharkiv : 2nd Edition ФОП Бровін О.В., 2026. – 160 p.

ISBN 978-617-8587-36-9

The study guide covers free, forced, and random vibrations of the sprung part of a vehicle body, as well as self-oscillations of the sprung part with friction shock absorbers, and self-oscillations of the engine coolant temperature using the method of harmonic linearization of nonlinearities. It also explores free and forced elastic vibrations of a gun barrel mounted on the chassis of a military vehicle, and the influence of liquid sloshing on the directional stability of a fuel tanker truck.

This study guide is intended for students of automotive specialties at higher education institutions of the III and IV accreditation levels. It can also be used as a self-study resource by engineers in the fields of mechanical engineering and transportation.

Fig. 56. Table 5. Page 4. Bibliogr. 16 titles.

UDC 629.3
BBK 30

ISBN 978-617-8587-36-9

CONTENTS

Foreword

« It is perhaps no exaggeration to say that, among the processes used in engineering, vibrations occupy a prominent–often central–place in many respects. »

Academician M.D. Papalexi

Numerous examples can be cited to illustrate the importance of oscillatory processes in mechanical systems. In some cases, vibrations are detrimental; in others, they are beneficial and are deliberately utilized in modern engineering applications.

Vibrations often have the potential to disrupt the operating conditions of machines. For example, machine tool vibrations hinder the attainment of the required surface finish in machining parts, while oscillations of instruments mounted on moving objects (such as automobiles, aircraft, rockets, or ships) can compromise the accuracy of measuring motion parameters. In some cases, vibrations exert harmful physiological effects on individuals whose bodies are subjected to intense high-frequency oscillations, or they may cause “seasickness” in crew members under conditions of low-frequency oscillations of moving vehicles.

On the other hand, various technological processes based on artificially generated vibrations, or self-oscillations, are being increasingly introduced. The theory of vibrations makes it possible not only to explain the complex nature of such technical phenomena but also to determine the optimal values of vibration parameters that ensure the highest efficiency of the technological process.

Most dynamic processes occurring in various automotive assemblies are oscillatory in nature. Indeed, any road surface contains irregularities that induce forced vibrations of the sprung part of the vehicle body. During these vibrations, the dynamic weight of the automobile continuously changes in accordance with a specific law

$$G_d(t) = G + M_p \ddot{z}(t),$$

where G – the total weight of the vehicle; $G_d(t)$ – the dynamic weight; M_p – the mass of the sprung part of the body; $\ddot{z}(t)$ – the vertical acceleration of the sprung part of the body.

The continuous variation of a vehicle's dynamic weight leads to continuous changes in engine load torque and induces its forced elastic vibrations, which in turn are transmitted to the transmission shafts as well as to the angular velocity sensor of the crankshaft – an essential sensitive element of the all-mode fuel supply governor of the automobile engine. The forced vibrations of the centrifugal sensitive element's coupling in the all-mode fuel supply governor cause high-frequency oscillations of the rack in the diesel fuel pump, resulting in uneven fuel delivery to the diesel cylinders, which leads to increased engine vibrations, higher fuel consumption, and elevated exhaust smoke emissions.

The oscillations of a dynamic system and its individual assemblies may occur around a state of dynamic equilibrium. The dynamic equilibrium of an automobile can exist when moving on a perfectly horizontal surface without any irregularities, at a constant speed, with constant fuel supply, and with a constant angular velocity of the engine crankshaft. In this state of dynamic equilibrium, the dynamic weight of the vehicle equals its static weight, and the load torque transmitted to the crankshaft from the driving wheels equals the effective torque developed by the automobile engine.

Oscillations of the assemblies of a dynamic system in the vicinity of a state of dynamic equilibrium are possible only in the case of stable equilibrium. Therefore, an essential component of the course *"Applied Theory of Vibrations"* is the study of the elements of the theory of stability of motion in dynamic systems.

Ukraine, with its powerful industry, is a country where two scientific schools in the field of applied vibration theory emerged and successfully developed – namely, the scientific school of the Kyiv Polytechnic Institute under the leadership of Professor S.P. Timoshenko (1878–1972) and the scientific school of the Kharkiv Polytechnic Institute under the leadership of Professor I.M. Babakov (1890–1974), both renowned mechanical scientists. Many distinguished Ukrainian scholars have belonged, and still belong, to these schools, but their founders were not only great Ukrainian scientists; they were also outstanding educators who created some of the best textbooks on vibration theory for students and engineers. For example, the textbook by Stepan Prokopovych Timoshenko – who, together with V.I. Vernadsky, established the Ukrainian Academy of Sciences in 1918 and became one

of its first academicians, and who in 1928 was elected a foreign member of the USSR Academy of Sciences—was based on lectures delivered for mechanical engineers at the Westinghouse Electric and Manufacturing Company. This textbook was first published in the United States in 1928 under the title *"Vibration Problems in Engineering."* It went through four editions, three of which were translated and published by *Nauka* Publishing House in 1931, 1959, and 1985 under the title *"Kolébaniya v inzhenernom dele"* (*Vibrations in Engineering*), and were widely used by Ukrainian students as a textbook on applied vibration theory.

However, the textbook *"Theory of Vibrations"* by Ivan Mykhailovych Babakov gained even greater popularity among students and mechanical engineers. It was developed from the lectures that the author delivered for many years to students specializing in *"Dynamics and Strength of Machines"* at the Kharkiv Polytechnic Institute. This textbook went through four editions published by *Nauka* (1958, 1964, 1968, 2004), and was also published in Japan and China.

The above-mentioned textbooks, as well as the works of Latvian Academician Ya.G. Panovko, were extensively used by the authors in preparing this manuscript. This study guide is intended for students of automotive specializations at higher education institutions of the III and IV accreditation levels, as well as for engineers in the fields of *mechanical engineering* and *transportation*.

Chapter 1

OSCILLATIONS OF LINEAR DYNAMIC SYSTEMS WITH ONE DEGREE OF FREEDOM

1.1. Free oscillations of linear systems with one degree of freedom.

Consider the fundamental schematic of a car suspension system, which is shown in Figure 1.1.

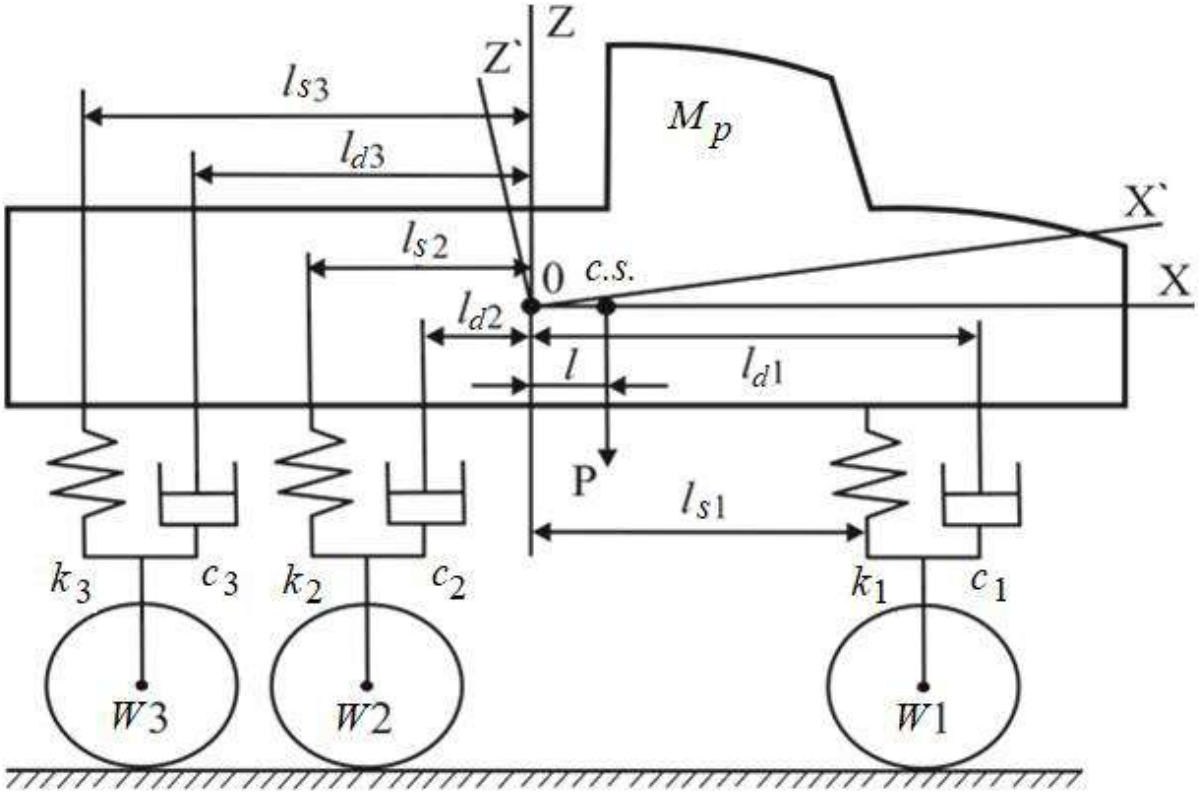

Fig. 1.1 **Fundamental schematic of a three-axle vehicle suspension**

The front axle of the vehicle will be considered the first axle, and the two rear axles will be considered the second and third axles, respectively. The following notations are used in Figure 1.1: M_p – sprung part of the vehicle's body (mass); $W1$, $W2$, $W3$ – Wheels of the first, second, and third axles, respectively; c_1, c_2, c_3 – dampers (shock absorbers) of the first, second, and third axles; k_1, k_2, k_3 – springs of the corresponding vehicle axles; *c.s.* – center of stiffness (elastic center) of the body; $0X$ – longitudinal principal axis of inertia of the sprung part of the body; $0Z$ – vertical principal axis of inertia of the sprung part of the

body; l_{s1}, l_{s2}, l_{s3} – horizontal distance from the center of gravity of the sprung part of the body to the spring attachment points; l_{d1}, l_{d2}, l_{d3} – horizontal distance from the center of gravity of the sprung part of the body to the damper attachment points; l – distance of the elastic center (*c.s.*) from the center of gravity (0).

The term "center of stiffness" (c.s.) of a vehicle's suspension refers to a point such that when a vertical external force P is applied to it, the sprung part of the body moves in a vertical direction, remaining parallel to its original position.

When the force $P = M_p \cdot g$ is applied to the center of stiffness, the sprung part of the body moves downward by a distance z. In this case, the additional elastic forces from all the springs, which balance the force P, satisfy Equation (1.1).

$$z\sum_{i=1}^{n} 2c_i = P \tag{1.1}$$

where n – the number of vehicle axles; c_i – the stiffness of the corresponding spring.

On the other hand, the moments of the additional spring forces about the proper transverse axis $0Y$ of the sprung part of the body are equal to the moment of the force P

$$\sum_{i=1}^{n_1} 2c_i z l_{si} - \sum_{j=1}^{n_2} 2c_j z l_{sj} = Pl, \tag{1.2}$$

where n_1 – number of front springs (in our case $n_1 = 1$); n_2 – number of rear springs (in our case $n_2 = 2$).

We will assume that all vehicle springs are identical: $c_i = c_j$.

Then equation (1.2) takes the form:

$$2c_i z(l_{s1} - l_{s2} - l_{s3}) = Pl. \tag{1.3}$$

The displacement of the center of stiffness relative to the center of gravity is equal to:

$$l = \frac{2c_i z(l_{s1} - l_{s2} - l_{s3})}{P}. \tag{1.4}$$

Taking into account equation (1.1), we write equation (1.4) in the form:

$$l = \frac{l_{s1} - l_{s2} - l_{s3}}{3}. \qquad (1.5)$$

If $l_{s1} = l_{s2} + l_{s3}$, then $l = 0$ and the center of stiffness coincides with the center of gravity. In this case, the vehicle suspension is called symmetric.

The oscillations of the sprung mass of the vehicle body are characterized by the periods of vertical and angular oscillations, as well as the amplitudes, velocities, and accelerations of the oscillatory motion. These quantities are referred to as the **ride comfort parameters** of the vehicle.

The oscillation periods of the vehicle body, or more precisely, the oscillation periods of its sprung part, primarily affect the **crew's performance**. Practice has established that the most favorable oscillation periods for the crew fall within the range of (0.5÷1.8) seconds. If the oscillation period is $T < 0.5$ seconds, rapid crew fatigue is observed due to jolting. Prolonged oscillations of the sprung part with a period $T > 1.8$ seconds also fatigue the crew, as in such cases, members may experience symptoms of **motion sickness**.

The amplitudes, velocities, and accelerations should be as small as possible. The smaller the oscillation amplitude, the lower the velocity and acceleration of the oscillatory motion. Therefore, the vehicle suspension should, if possible, prevent intense rocking of the sprung part, which is achieved through the targeted selection of spring and damper characteristics.

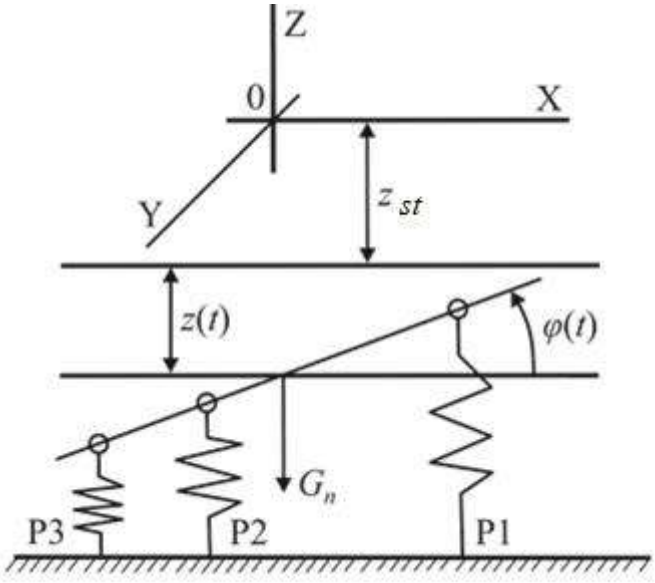

Fig. 1.2 **Calculation schematic of a vehicle suspension**

Referring to Figure 1.2, consider the calculation schematic of a vehicle suspension, the principle diagram of which is shown in Figure 1.1. Initially, assume that the dampers c_1, c_2, and c_3 are absent in the schematic. The forces acting on the vehicle body from the springs are determined by equation:

$$P_i(t) = c\delta_i(t) = c[z_{st} - z(t) - l_{si}\varphi(t)], \tag{1.6}$$

where the following notations are adopted: $\delta_i(t)$ – vertical displacement of the attachment point of the i-th spring; c – equivalent spring stiffness; z_{st} – static deflection of the spring under static load; $z(t)$ – generalized coordinate of the vertical oscillations of the vehicle body; $\varphi(t)$ – generalized coordinate of the pitch (longitudinal angular) oscillations of the body; l_{si} – horizontal distance from the center of gravity of the vehicle's sprung mass to the attachment point of the i-th spring.

Using d'Alembert's principle, we write the differential equations for the vertical and pitch oscillations of the vehicle body.

$$-P + \sum_{i=1}^{6} P_i(t) = M_p \ddot{z}(t); \tag{1.7}$$

$$\sum_{i=1}^{6} P_i(t) l_{si} = I_y \ddot{\varphi}(t), \tag{1.8}$$

where P – the sprung mass of the vehicle, I_y is the moment of inertia of the sprung mass M_p about its central transverse axis.

Let us substitute relation (1.6) into differential equations (1.7) and (1.8), we write the equations:

$$-P + 6cz_{st} - 6cz(t) - 2c\varphi(t)\sum_{i=1}^{3} l_{si} = M_p \ddot{z}(t); \tag{1.9}$$

$$2cz_{st}\sum_{i=1}^{3} l_{si} - 2cz(t)\sum_{i=1}^{3} l_{si} - 2c\varphi(t)\sum_{i=1}^{3} l_{si}^2 = I_y \ddot{\varphi}(t). \tag{1.10}$$

Given that the static weight P is balanced by the static deformation of the springs, we write the equation:

$$P = 6cz_{st},$$

and equation (1.9) is written in the form:

$$\ddot{z}(t)+\frac{6c}{M_p}z(t)+\frac{2c\sum_{i=1}^{3}l_{pi}}{M_p}\varphi(t)=0. \qquad (1.11)$$

In the position of static equilibrium, the moments from the front and rear springs balance each other, that is:

$$2cz_{st}\sum_{i=1}^{3}l_{pi}=0,$$

and equation (1.10) is written in the form:

$$\ddot{\varphi}(t)+\frac{2c\sum_{i=1}^{3}l_{pi}^2}{I_y}\varphi(t)+\frac{2c\sum_{i=1}^{3}l_{pi}}{I_y}z(t)=0. \qquad (1.12)$$

Let us introduce the notation:

$$a=\frac{6c}{M_p};\ b=\frac{2c\sum_{i=1}^{3}l_{pi}}{M_p};\ d=\frac{2c\sum_{i=1}^{3}l_{pi}^2}{I_y};\ f=\frac{2c\sum_{i=1}^{3}l_{pi}}{I_y}. \qquad (1.13)$$

Then the differential equations of oscillation for the vehicle's sprung mass M_p with its own central moment of inertia about the vehicle's transverse axis I_y are written in the form:

$$\ddot{z}(t)+az(t)+b\varphi(t)=0; \qquad (1.14)$$

$$\ddot{\varphi}(t)+d\varphi(t)+fz(t)=0. \qquad (1.15)$$

Both equations (1.14) and (1.15) are coupled, meaning they can only be solved together as a system. Physically, this mutual coupling indicates that the vertical and angular oscillations of the sprung mass occur simultaneously: a vertical disturbance causes an angular displacement, and an angular disturbance inevitably leads not only to angular but also to vertical oscillations.

When considering the calculation schematic of the vehicle suspension (Fig. 2), an assumption was made about the absence of dampers, i.e., devices designed to suppress oscillations by introducing additional resistance into the suspension structure. In automotive engineering, dampers with resistance proportional to the velocity of the damper's attachment point to the vehicle body are most commonly used. This velocity, using formula (1.6), can be written as equation (1.16).

$$\delta_i(t) = z_{st} - z(t) - l_{ai}\varphi(t). \tag{1.16}$$

The velocity of the attachment point of the i-th damper can be obtained by differentiating relation (1.16) with respect to time, where l_{ai} denotes the distance from the center of gravity of the sprung part of the body to the attachment point of the *i*-th damper.

$$\frac{d\delta_i(t)}{dt} = -\dot{z}(t) - l_{ai}\dot{\varphi}(t). \tag{1.17}$$

As a result, the damping force and damping moment of the *i*-th damper are expressed by the relations:

$$P_{ai}(t) = -\mu[\dot{z}(t) + l_{ai}\dot{\varphi}(t)]; \tag{1.18}$$

$$M_{ai}(t) = -\mu l_{ai}[\dot{z}(t) + l_{ai}\dot{\varphi}(t)], \tag{1.19}$$

where μ – is the average damping coefficient of the shock absorber.

Let us introduce the notation:

$$m = \frac{6\mu}{M_p};\ q = \frac{2\sum_{i=1}^{3}\mu l_{ai}}{M_p};\ r = \frac{2\mu\sum_{i=1}^{3} l_{ai}}{I_y};\ s = \frac{2\mu\sum_{i=1}^{3} l_{ai}^2}{I_y}. \tag{1.20}$$

As a result, the differential equations for the free oscillations of the vehicle suspension take the form:

$$\ddot{z}(t) + m\dot{z}(t) + az(t) + q\dot{\varphi}(t) + b\varphi(t) = 0; \tag{1.21}$$

$$\ddot{\varphi}(t) + s\dot{\varphi}(t) + d\varphi(t) + r\dot{z}(t) + fz(t) = 0. \tag{1.22}$$

If the attachment points of the springs and shock absorbers coincide, and the vehicle suspension is symmetric, then $q=b=r=f=0$, and the system of differential equations (1.21), (1.22) splits into two independent differential equations:

$$\ddot{z}(t)+m\dot{z}(t)+az(t)=0; \tag{1.23}$$

$$\ddot{\varphi}(t)+s\dot{\varphi}(t)+d\varphi(t)=0. \tag{1.24}$$

Let us consider a form of notation common to both equations (1.23) and (1.24):

$$\ddot{q}(t)+2n\dot{q}(t)+k^2q(t)=0. \tag{1.25}$$

The characteristic equation corresponding to the differential equation (1.25) is written as:

$$p^2+2np+k^2=0. \tag{1.26}$$

The roots of the characteristic equation (1.26) are:

$$p_{1,2}=-n\pm\sqrt{n^2-k^2}. \tag{1.27}$$

When $n<k$, a negative quantity appears under the square root sign, so relation (1.27) can be expressed as:

$$p_{1,2}=-n\pm j\sqrt{k^2-n^2}.$$

The general solution of the differential equation (1.25) is written as:

$$q(t)=e^{-nt}\left[C_1\sin\sqrt{k^2-n^2}t+C_2\cos\sqrt{k^2-n^2}t\right], \tag{1.28}$$

where the constants C_1 and C_2 are determined from the initial conditions q_0 and $\dot{q}(t)$.

Let us differentiate equation (1.28) with respect to time:

$$\begin{aligned}\dot{q}(t)=&-ne^{-nt}\left[C_1\sin\sqrt{k^2-n^2}t+C_2\cos\sqrt{k^2-n^2}t\right]+\\&+e^{-nt}\left[C_1\sqrt{k^2-n^2}\cos\sqrt{k^2-n^2}t-C_2\sqrt{k^2-n^2}\sin\sqrt{k^2-n^2}t\right].\end{aligned} \tag{1.29}$$

If we set $t = 0$ in equations (1.28) and (1.29), we obtain:

$$q_0 = C_2;\ \dot{q}_0 = -nC_2 + C_1\sqrt{k^2 - n^2},$$

from which

$$C_1 = \frac{\dot{q}_0 + nq_0}{\sqrt{k^2 - n^2}};\ C_2 = q_0.$$

As a result, the general solution of the differential equation (1.25) is written in the form:

$$q(t) = e^{-nt}\left[\frac{\dot{q}_0 + nq_0}{\sqrt{k^2 - n^2}}\sin\sqrt{k^2 - n^2}t + q_0\cos\sqrt{k^2 - n^2}t\right]. \quad (1.30)$$

Equation (1.30) can be represented in the form:

$$q(t) = Ae^{-nt}\sin\left(\sqrt{k^2 - n^2}t + \alpha\right), \quad (1.31)$$

where

$$A = \sqrt{C_1^2 + C_2^2} = \sqrt{\frac{\left(\dot{q}_0 + nq_0\right)^2}{k^2 - n^2} + q_0^2};$$

$$\alpha = \operatorname{arctg}\frac{C_2}{C_1} = \operatorname{arctg}\frac{q_0\sqrt{k^2 - n^2}}{\dot{q}_0 + nq_0}.$$

From the analysis of relations (1.30) and (1.31), it can be concluded that the free oscillations of the sprung part of the vehicle body have the form shown in Fig. 1.3 and decay quite rapidly. These oscillations occur at a constant frequency $\sqrt{k^2 - n^2}$ and with a constantly decreasing amplitude A.

The envelope curve in Fig. 3 is defined by the equation $A = A_0e^{-nt}$, where A_0 – is the initial ordinate of the envelope curve.

The period of free oscillations of the body is:

$$T = \frac{2\pi}{\sqrt{k^2 - n^2}}. \quad (1.32)$$

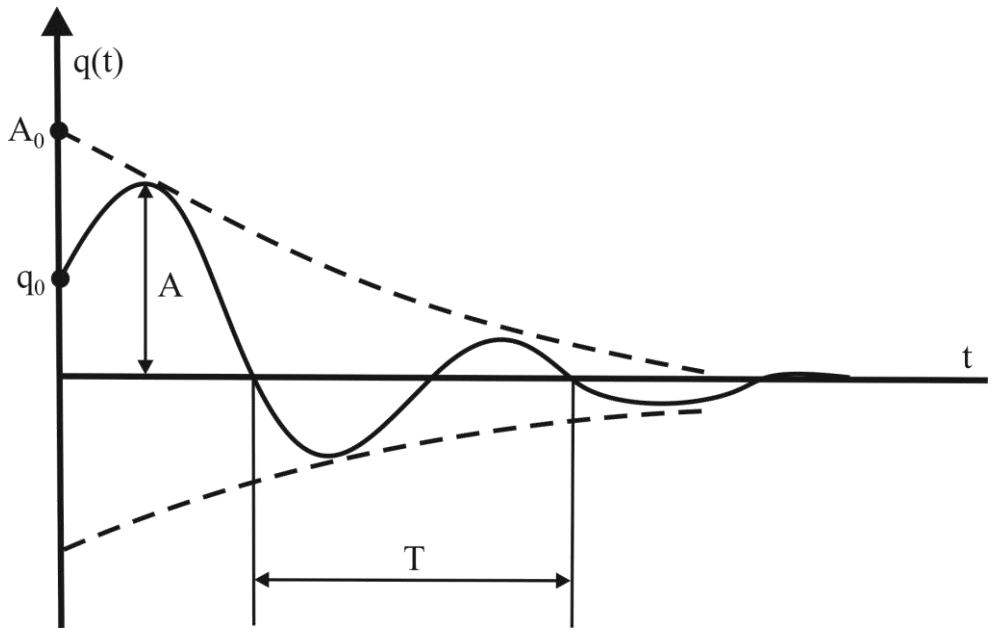

Fig. 1.3. **Free Oscillations of the Sprung Part of the Vehicle Body**

1.2. Forced oscillations of linear systems with one degree of freedom.

During vehicle motion, road surface irregularities continuously act upon the sprung part of the body through the springs and shock absorbers. If these road surface irregularities repeat periodically, the body's oscillations will follow certain patterns. With some assumptions, the nature of these irregularities can be considered sinusoidal, and thus the forces and moments acting on the sprung part of the vehicle body through the springs and shock absorbers will be periodic. As a result, the equations describing the forced oscillations of the sprung part of the vehicle body take the form:

$$\ddot{q}(t) + 2n\dot{q}(t) + k^2 q(t) = H \sin \omega t, \qquad (1.33)$$

where H – the equivalent amplitude of external disturbances from road irregularities; ω – the frequency of external disturbances, determined by the formula $\omega = 2 \cdot \pi \cdot v \cdot a^{-1}$; v – the vehicle's speed; a – the length of the sinusoidal irregularity (Fig. 1.4).

The period of the forced oscillations, equal to the time it takes for the vehicle to traverse the full length of the irregularity, is:

$$T = \frac{a}{v}.$$

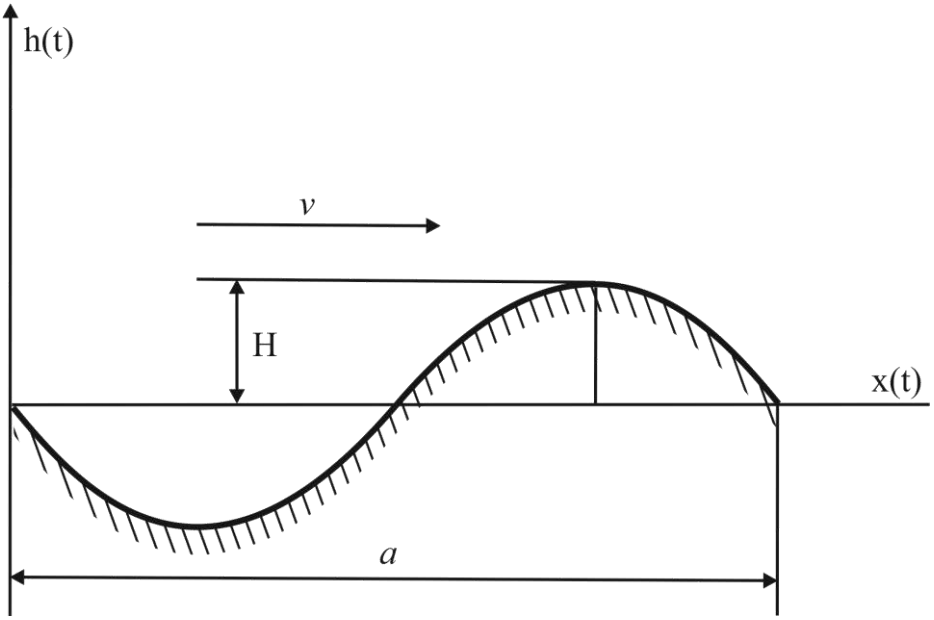

Fig. 1.4. **Sinusoidal irregularity of the road surface on which the vehicle is moving**

The general solution of the differential equation (1.33) is the sum of the general solution of the corresponding homogeneous equation (1.25) and a particular solution of equation (1.33).

$$q(t) = q_1(t) + q_2(t). \tag{1.34}$$

Let us represent the particular solution $q_2(t)$ in the form:

$$q_2(t) = M \sin \omega t + N \cos \omega t, \tag{1.35}$$

where M and N are constants that satisfy the linear algebraic equations obtained by substituting (1.35) into equation (1.33).

$$\begin{aligned} -N\omega^2 + 2M\omega n + Nk^2 = 0; \\ -M\omega^2 - 2N\omega n + Mk^2 = H. \end{aligned} \tag{1.36}$$

From the system (1.36), we find:

$$\begin{aligned} M &= H \frac{k^2 - \omega^2}{\left(k^2 - \omega^2\right)^2 + 4n^2\omega^2}; \\ N &= -H \frac{2n\omega}{\left(k^2 - \omega^2\right)^2 + 4n^2\omega^2}. \end{aligned} \tag{1.37}$$

As a result, the general solution of the differential equation (1.33) is written in the form:

$$q(t) = e^{-nt}\left[\frac{\dot{q}_0 + nq_0}{\sqrt{k^2 - n^2}}\sin\sqrt{k^2 - n^2}\,t + q_0\cos\sqrt{k^2 - n^2}\,t\right] + \\ + \frac{H}{\left(k^2 - \omega^2\right)^2 + 4n^2\omega^2}\left[\left(k^2 - \omega^2\right)\sin\omega t - 2n\omega\cos\omega t\right]. \tag{1.38}$$

The first term on the right side of solution (1.38), containing the factor e^{-nt}, represents the free oscillations discussed in the previous subsection. The second term, containing the frequency of the disturbing influence ω, represents the forced oscillations of the sprung part of the vehicle body.

Let us consider the dependence of the amplitude of the forced oscillations of the sprung part of the vehicle body on the frequency of the external disturbance ω:

$$A_3(\omega) = \frac{H}{\sqrt{\left(k^2 - \omega^2\right)^2 + 4n^2\omega^2}}. \tag{1.39}$$

Figure 1.5 shows the dependencies of the quantity (1.39) on the relative frequency of external disturbances:

$$\bar{\omega} = \frac{\omega}{k},$$

for different values of the parameter *n*.

Analysis of Fig. 5 leads to the conclusion that when the frequency of the external disturbance ω approaches the frequency of the system's free oscillations *k*, the amplitude of the forced oscillations $A_3(\omega)$ increases rapidly and becomes highly sensitive to changes in the damping coefficient *n*, especially when it is small. If

$$\bar{\omega} \to 1,$$

then resonance occurs in the system.

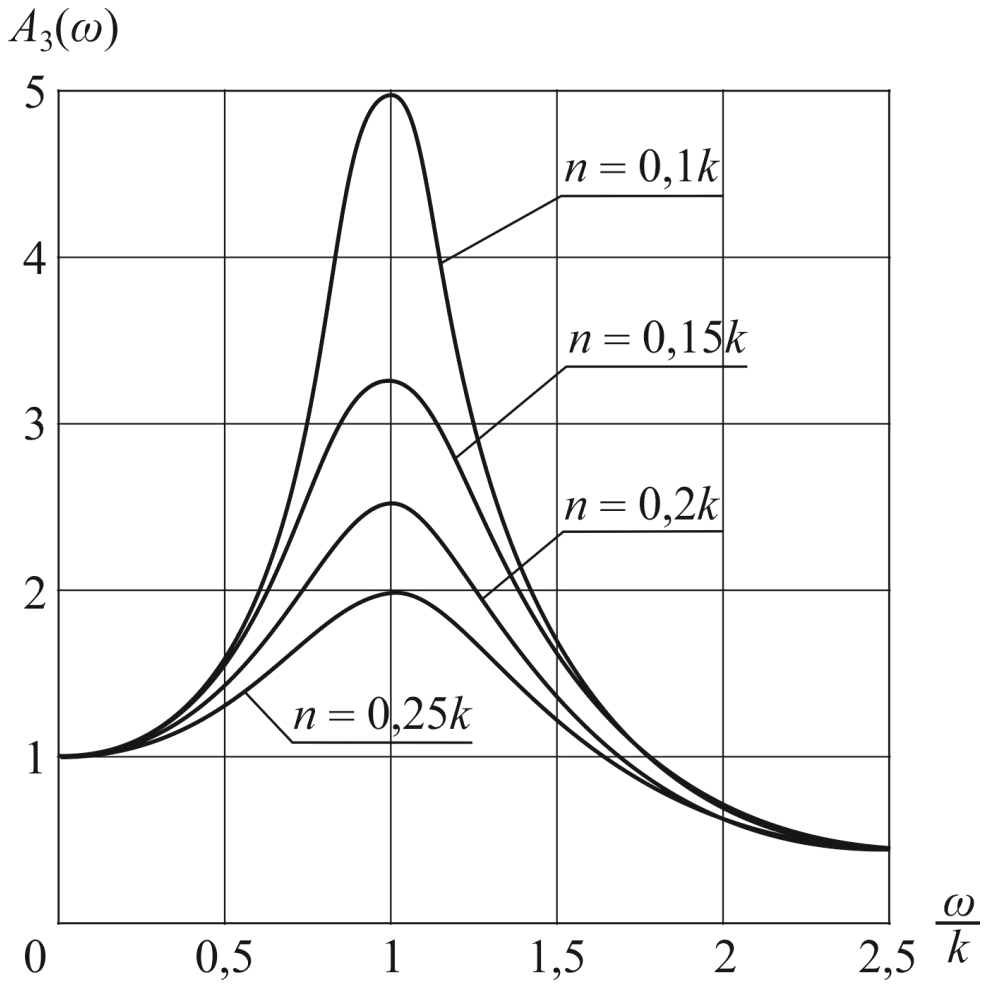

Fig. 1.5. **Dependence of the amplitude of forced oscillations on their relative frequency**

1.3. Random oscillations of linear systems with one degree of freedom.

In real road conditions, the distribution of surface irregularities is random (Fig. 1.6). A vehicle moving at a specific speed *v* can be considered as a mechanical dynamic system subjected to random external disturbances from the road surface.

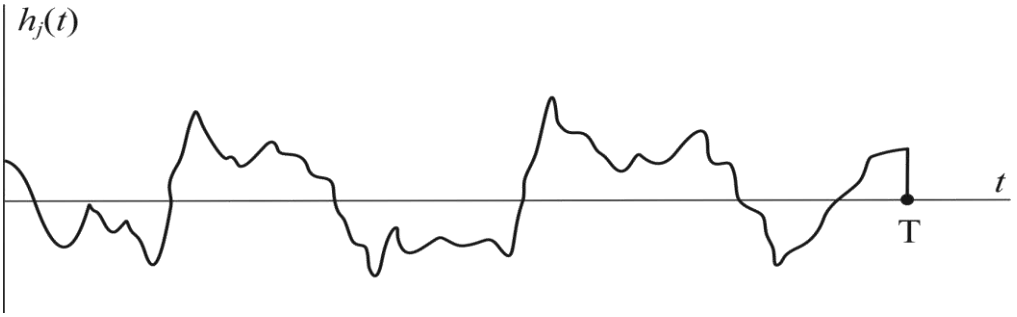

Fig. 1.6. **Stationary random process of road microprofile**

In this case, the random oscillatory processes of the sprung part of the vehicle body can be regarded as stationary, evolving relatively uniformly over time and exhibiting random oscillations around a certain mean value.

It is known that the correlation function of road surface irregularities is described by an approximating dependence:

$$R(\tau) = De^{-\alpha v\tau}\cos\beta\tau, \qquad (1.40)$$

where D is the variance of the irregularity heights; α, β are correlation coefficients, whose numerical values for different road surfaces are given in Table 1.

Table 1.1 – **Values of correlation coefficients and irregularity variance for different types of road surfaces**

Type of Road Surface	α, m^{-1}	β, m^{-1}	D, m^2
Asphalt Concrete	0,22	0,44	$5{,}5\cdot10^{-3}$
Paved (Cobblestone)	0,32	0,64	$8{,}0\cdot10^{-3}$
Dirt Road	0,47	0,94	$11{,}6\cdot10^{-3}$
Cross-Country Terrain	0,72	1,44	$20\cdot10^{-3}$

The relationship between the spectral density of a random process and its correlation function is determined by the Fourier transform:

$$S(\omega) = \int_{-\infty}^{\infty} R(\tau)e^{j\omega\tau}d\tau. \qquad (1.41)$$

Let us substitute equation (1.40) into equation (1.41). As a result, we obtain:

$$S(\omega) = D\left\{\frac{2\alpha v\left[v^2\left(\alpha^2+\beta^2\right)+\omega^2\right]}{\omega^4+2\omega^2v^2\left(\alpha^2-\beta^2\right)+v^4\left(\alpha^2+\beta^2\right)^2}\right\}. \qquad (1.42)$$

Figure 1.7 shows the spectral density curves (1.42), plotted for different vehicle speeds moving on various surfaces.

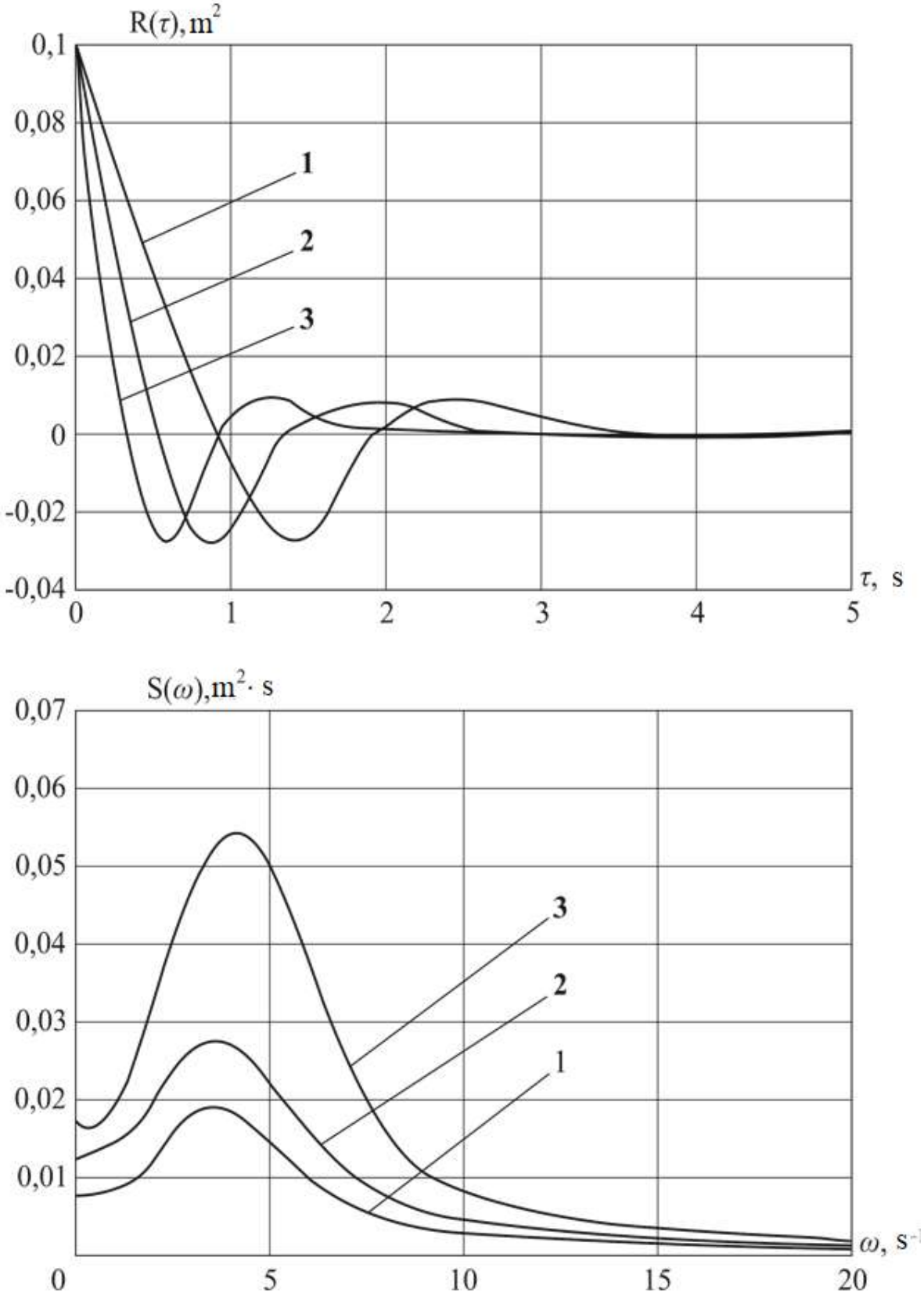

Fig. 1.7.a. **Correlation functions and spectral densities of the vehicle's running surface at v = 5 m·s^{-1}:**
1 – Asphalt Concrete; 2 – Paved (Cobblestone); 3 – Dirt Road

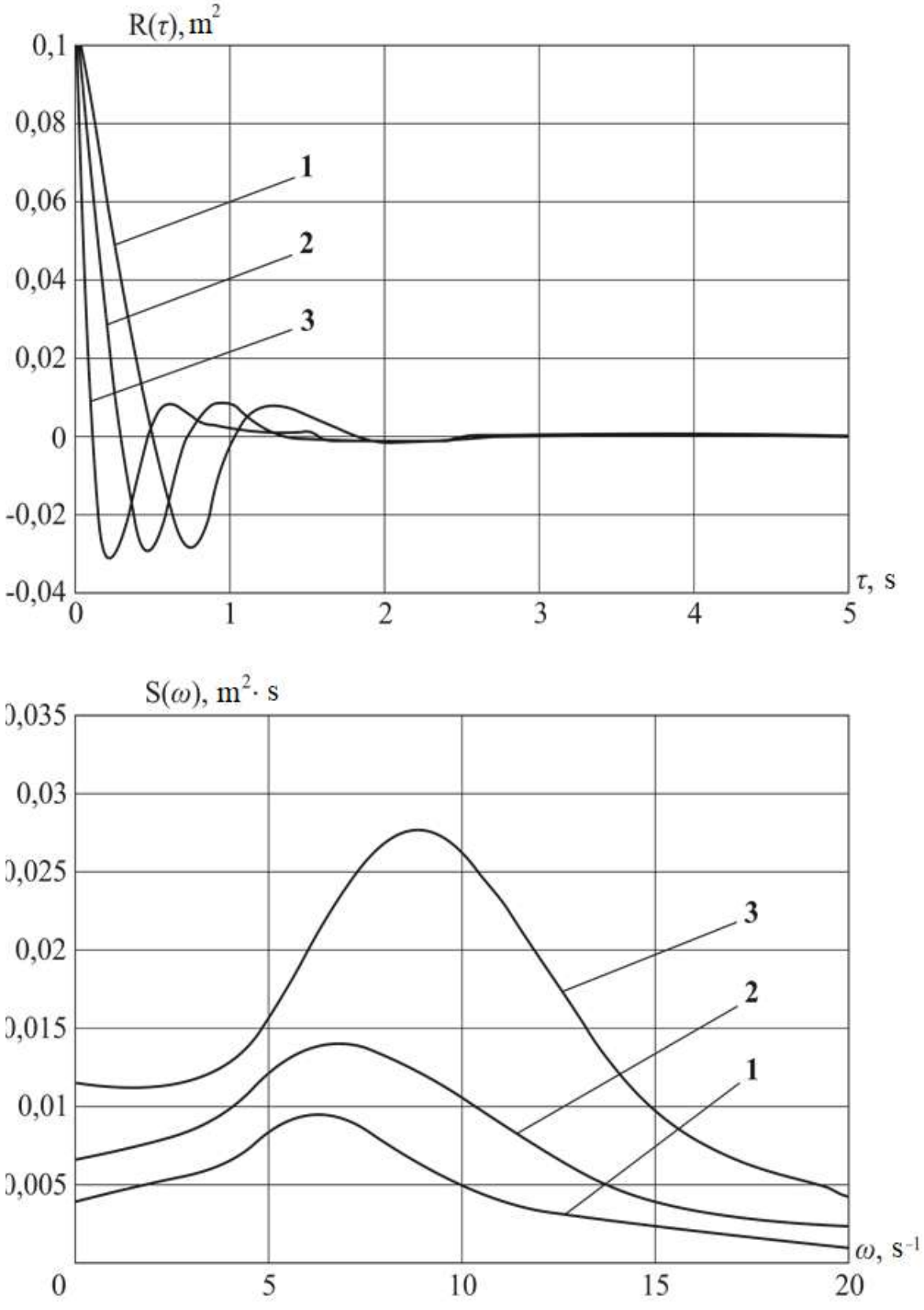

Fig. 1.7.b. **Correlation functions and spectral densities of the vehicle's running surface at v = 10 m·s^{-1}**:
1 – Asphalt Concrete; 2 – Paved (Cobblestone); 3 – Dirt Road

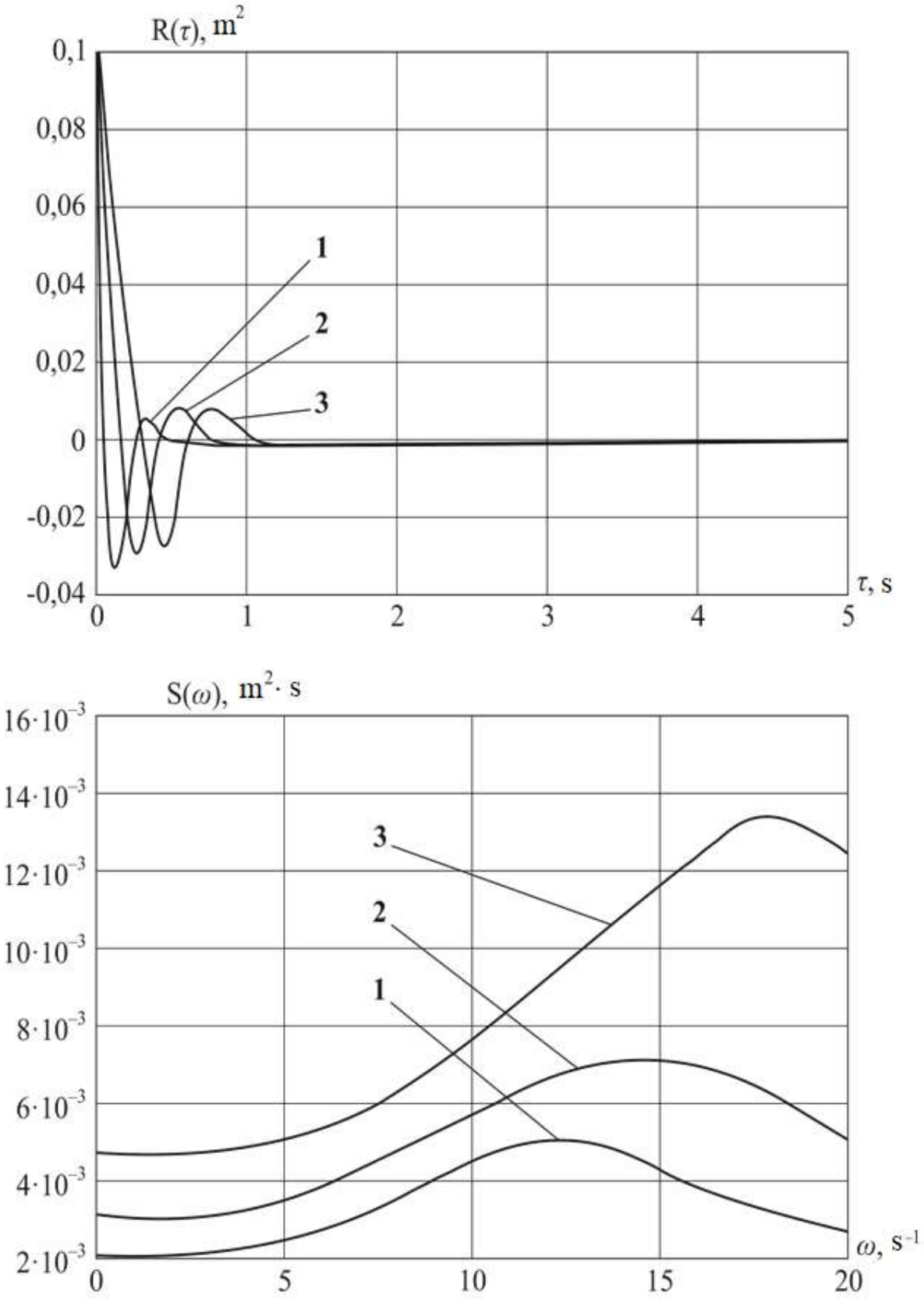

Fig. 1.7.c. **Correlation functions and spectral densities of the vehicle's running surface at $v = 20$ m·s^{-1}:**
1 – Asphalt Concrete; 2 – Paved (Cobblestone); 3 – Dirt Road

Analysis of the spectral density curves leads to the conclusion that they all have a clearly pronounced maximum, and the value of the resonant frequency is higher the greater the vehicle's speed.

It is known that the spectral densities of the input signal $x(t)$ and the output signal $y(t)$ of a dynamic element with transfer function $W(s)$ (Fig. 1.8) are related by the expression

$$S_y(\omega) = R^2(\omega) S_x(\omega), \tag{1.43}$$

where $R(\omega)$ is the amplitude-frequency characteristic of the dynamic element.

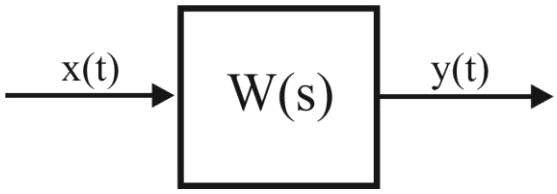

Fig. 1.8. **Linear dynamic element**

Assume that the input signal of the linear dynamic element represents unit "white noise":

$$x(t) = \xi(t),$$

whose spectral density is constant and equal to unity:

$$S_x(\omega) = S_\xi(\omega) = 1.$$

Then, according to relation (1.43), we have:

$$S_y(\omega) = R^2(\omega). \tag{1.44}$$

From the analysis of formula (1.44) and Fig. 1.7, it can be concluded that the considered dynamic element is an oscillatory one with the transfer function:

$$W(S) = \frac{k}{T_1^2 s^2 + T_2 s + 1}, \tag{1.45}$$

where k is the gain; T_1, T_2 are time constants.

A dynamic element with the transfer function (1.45) will be called a shaping dynamic element, i.e., an element that forms a specific

realization of the random function $y(t)$ when a realization of unit "white noise" $\xi(t)$ is applied to its input. In this case, the spectral density of the random function $y(t)$ must take the form (1.42). To achieve this, the parameters k, T_1, and T_2 must be chosen as follows.

In relation (1.45), we substitute $s = j\omega$:

$$W(j\omega) = \frac{k}{\left(1-\omega^2 T_1^2\right) + j\omega T_2}. \qquad (1.46)$$

To eliminate the complex number from the denominator of (1.46), we multiply the numerator and denominator of (1.46) by the complex conjugate $(1 - \omega^2 T_1^2) - j\omega T_2$. As a result, we obtain the frequency transfer function in the form:

$$W(j\omega) = \frac{\left(1-\omega^2 T_1^2\right)k}{\left(1-\omega^2 T_1^2\right)^2 + \omega^2 T_2^2} - j\frac{\omega T_2 k}{\left(1-\omega^2 T_1^2\right)^2 + \omega^2 T_2^2}. \qquad (1.47)$$

Let us introduce the notation:

$$U(\omega) = \frac{\left(1-\omega^2 T_1^2\right)k}{\left(1-\omega^2 T_1^2\right)^2 + \omega^2 T_2^2};\ V(\omega) = \frac{k\omega T_2}{\left(1-\omega^2 T_1^2\right)^2 + \omega^2 T_2^2}. \qquad (1.48)$$

Relations (1.48) are called the real and imaginary parts of the frequency transfer function (1.47), and the frequency transfer function of the shaping dynamic element itself is written as:

$$W(j\omega) = U(\omega) + jV(\omega),$$

and the square of the amplitude-frequency characteristic of the shaping dynamic element is thus equal to:

$$R^2(\omega) = U^2(\omega) + V^2(\omega) = \frac{k^2}{\left(1-\omega^2 T_1^2\right)^2 + \omega^2 T_2^2} = S_y(\omega). \qquad (1.49)$$

In equation (1.49), let us set $\omega = 0$:

$$k^2 = S_y(0). \qquad (1.50)$$

The maximum of function (1.49) is approximately reached when the expression in parentheses is zero:

$$1-\omega_p^2 T_1^2 = 0, \tag{1.51}$$

and the amplitude of the resonance peak is determined by the equation:

$$S_y(\omega_p) = \frac{k^2}{\omega_p^2 T_2^2}. \tag{1.52}$$

From relations (1.50) – (1.52), we obtain the values of the parameters of the shaping dynamic element with the transfer function (1.45):

$$k = \sqrt{S_y(0)};\ T_1^2 = \frac{1}{\omega_p^2};\ T_2 = \sqrt{\frac{S_y(0)}{\omega_p^2 S_y(\omega_p)}}. \tag{1.53}$$

The dependence of the characteristic points of the spectral densities shown in Figure 1.7 on the vehicle speed on asphalt concrete is given in Table 1.2, and the values of the shaping dynamic element parameters versus the vehicle speed are given in Table 1.3.

Table 1.2 – **Dependence of the characteristic points of the spectral density curves on the vehicle speed**

Vehicle Speed v, $\mathrm{m \cdot s^{-1}}$	$S_y(0)$, $\mathrm{m^2 \cdot s}$	ω_p, $\mathrm{s^{-1}}$	$S_y(\omega_p)$, $\mathrm{m^2 \cdot s}$
25	$0{,}396 \cdot 10^{-3}$	10,92	$0{,}963 \cdot 10^{-3}$
20	$0{,}495 \cdot 10^{-3}$	8,74	$1{,}207 \cdot 10^{-3}$
15	$0{,}660 \cdot 10^{-3}$	6,56	$1{,}604 \cdot 10^{-3}$
10	$0{,}990 \cdot 10^{-3}$	4,37	$2{,}407 \cdot 10^{-3}$
5	$1{,}980 \cdot 10^{-3}$	2,19	$4{,}813 \cdot 10^{-3}$

The differential equation of the shaping dynamic element is written in the form:

$$T_1^2 \ddot{h}_j(t) + T_2 \dot{h}_j(t) + h_j(t) = k\xi_j(t),\ (j = \overline{1,N}), \tag{1.54}$$

where $\xi_j(t)$, $(j=\overline{1,N})$ – j-th realization of unit "white noise"; $h_j(t)$, $(j=\overline{1,N})$ – current height of the road surface irregularities for the j-th realization of unit "white noise".

Table 1.3. – **Values of the parameters of the shaping dynamic element**

Vehicle Speed v, $\text{m}\cdot\text{s}^{-1}$	k	T_1, s	T_2, s
25	$1{,}98\cdot10^{-2}$	0,0916	0,0586
20	$2{,}21\cdot10^{-2}$	0,1440	0,0922
15	$2{,}56\cdot10^{-2}$	0,1524	0,0975
10	$3{,}15\cdot10^{-2}$	0,2288	0,1464
5	$4{,}39\cdot10^{-2}$	0,4566	0,2922

Figure 1.9 shows the random functions $h_j(t)$ of the road microprofile depending on the vehicle speed when moving on asphalt concrete.

These functions are solutions to the differential equations (1.54).

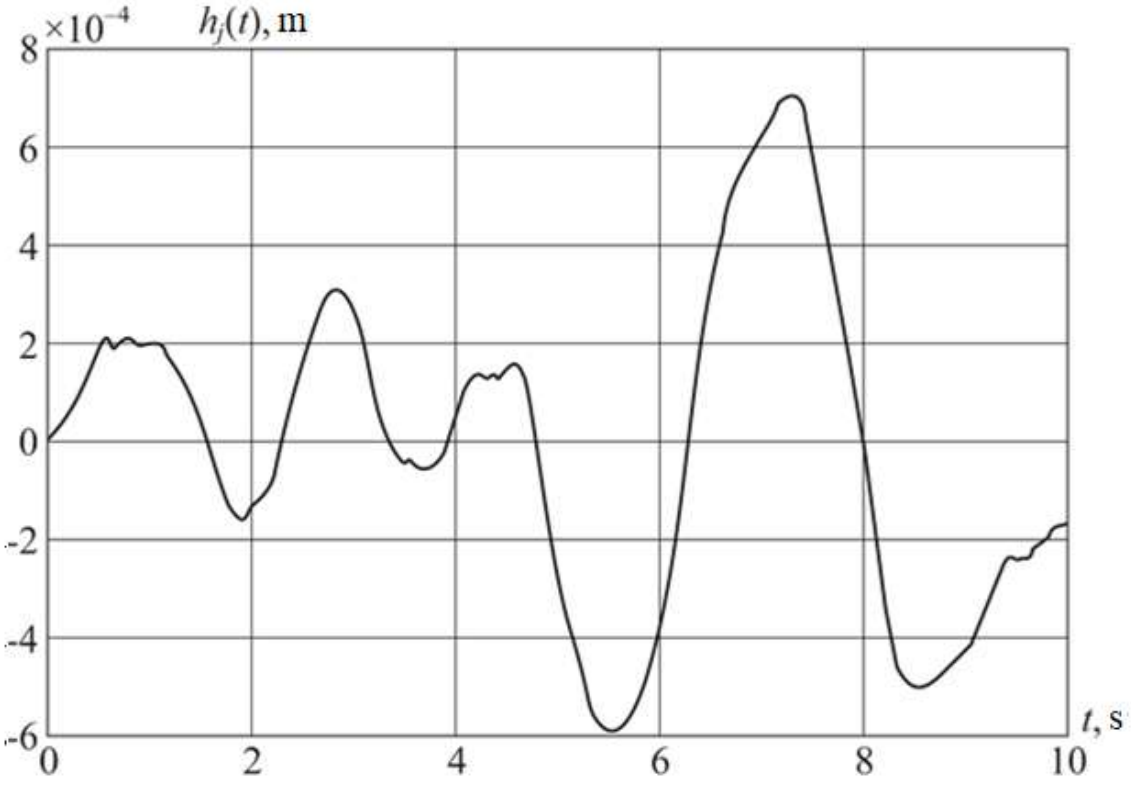

Fig. 1.9.a. **Random function $h_j(t)$ corresponding to a speed of 5 $\text{m}\cdot\text{s}^{-1}$**

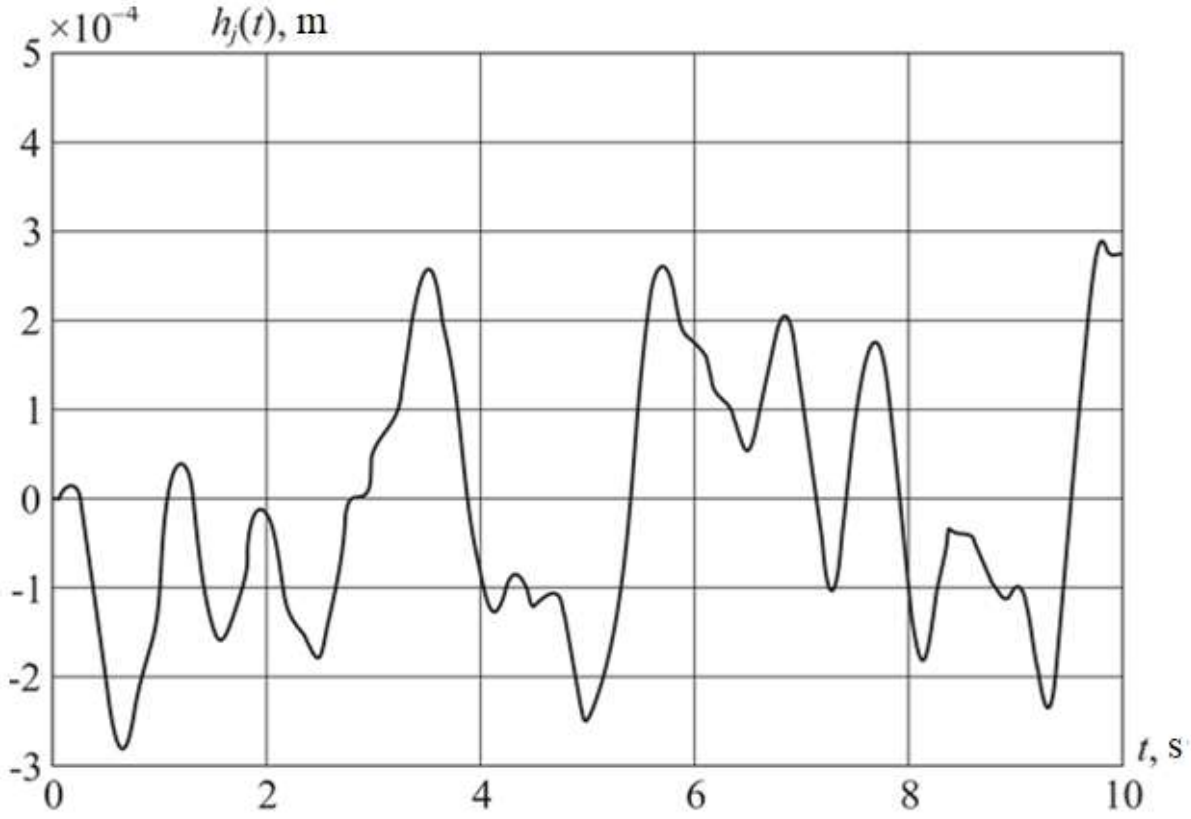

Fig. 1.9.b. **Random function $h_j(t)$ corresponding to a speed of 10 m·s^{-1}**

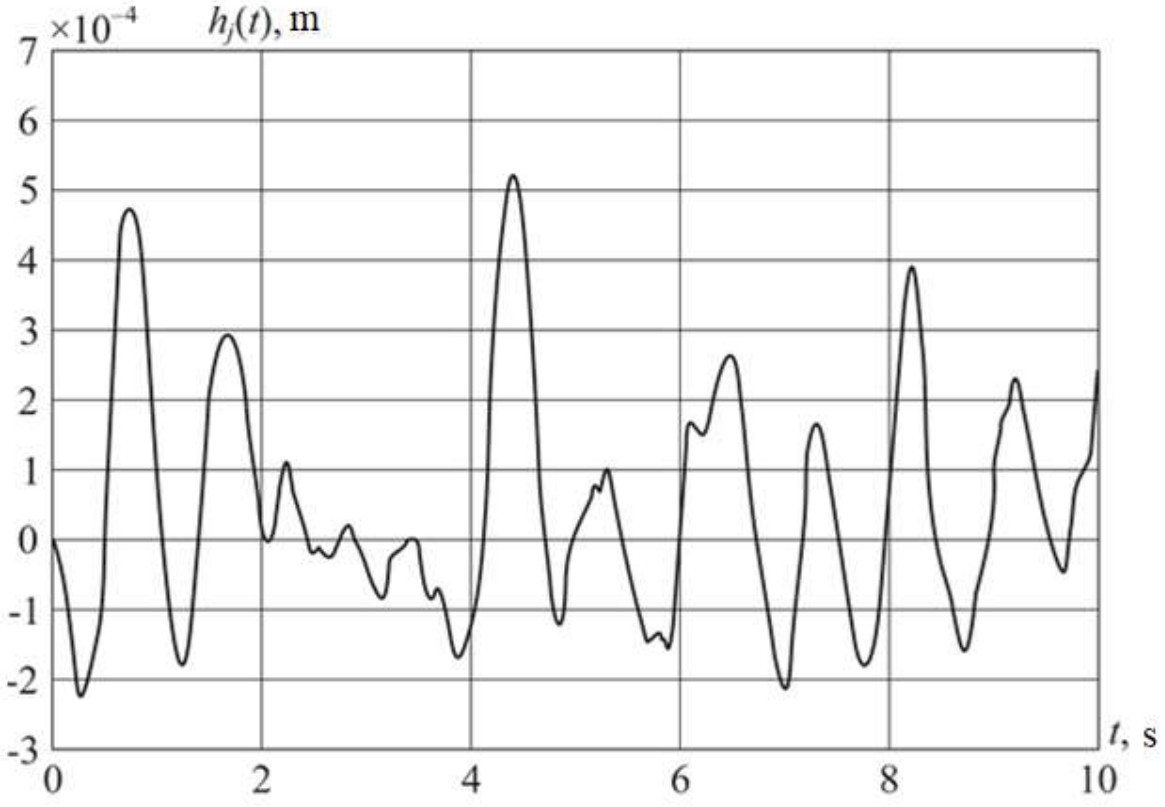

Fig. 1.9.c. **Random function $h_j(t)$ corresponding to a speed of 15 m·s^{-1}**

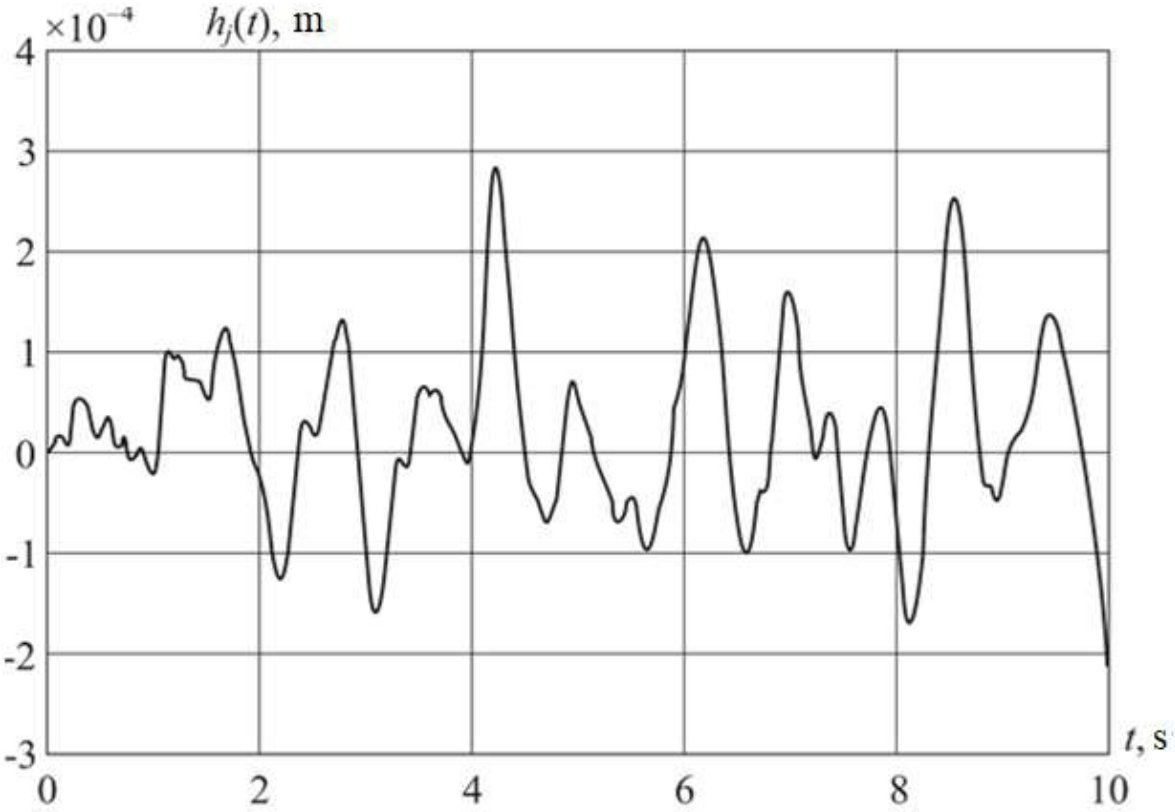

Fig. 1.9.d. **Random function $h_j(t)$ corresponding to a speed of 20 m·s^{-1}**

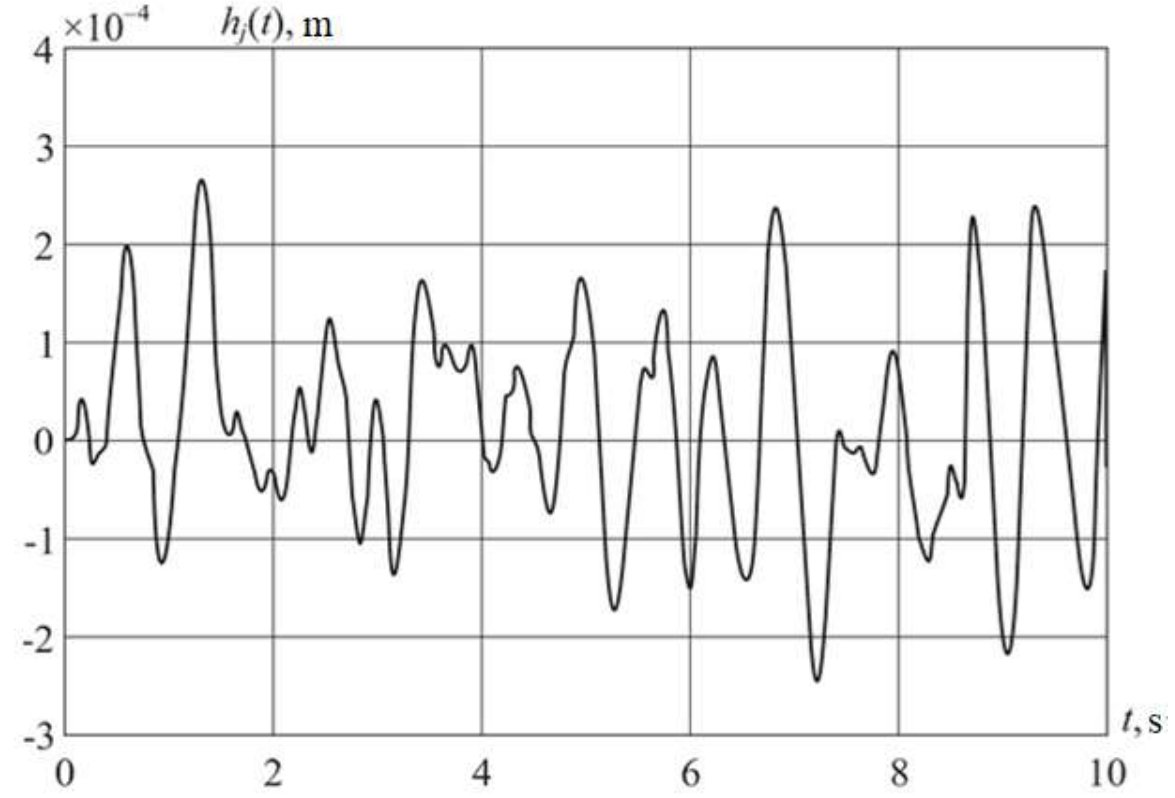

Fig. 1.9.e. **Random function $h_j(t)$ corresponding to a speed of 25 m·s^{-1}**

As the vehicle speed increases, the average frequency of oscillations of the random function $h_j(t)$ increases, while the average random amplitude of the function $h_j(t)$ decreases. As a result, the forced random oscillations of the sprung part of the vehicle body are described by the system of differential equations:

$$\begin{gathered}\ddot{z}_j(t)+m\dot{z}_j(t)+az_j(t)+q\dot{\varphi}_j(t)+b\varphi_j(t)= \\ =\frac{2c}{M_p}\left[\sum_{i=1}^{3}h_j\left(t+\frac{l_i}{v}\right)\right]+\frac{2\mu}{M_p}\left[\sum_{i=1}^{3}\dot{h}_j\left(t+\frac{l_i}{v}\right)\right]; \\ \ddot{\varphi}_j(t)+s\dot{\varphi}_j(t)+d\varphi_j(t)+r\dot{z}_j(t)+fz_j(t)= \\ =\frac{2c}{I_y}\left[\sum_{i=1}^{3}l_ih_j\left(t+\frac{l_i}{v}\right)\right]+\frac{2\mu}{I_y}\left[\sum_{i=1}^{3}l_i\dot{h}_j\left(t+\frac{l_i}{v}\right)\right]; \\ \left(j=\overline{1,N}\right)\end{gathered} \tag{1.55}$$

where the random function $h_j\left(t+\frac{l_i}{v}\right)$ and its time derivative $\dot{h}_j\left(t+\frac{l_i}{v}\right)$ satisfy the differential equation (1.54).

Assume that the suspension under consideration is symmetric. Then the mathematical model of the disturbed motion of the sprung part of the vehicle body, according to equation (1.55), splits into two independent equations:

$$\begin{gathered}\ddot{z}_j(t)+m\dot{z}_j(t)+az_j(t)= \\ =\frac{2c}{M_p}\left[\sum_{i=1}^{3}h_j\left(t+\frac{l_i}{v}\right)\right]+\frac{2\mu}{M_p}\left[\sum_{i=1}^{3}\dot{h}_j\left(t+\frac{l_i}{v}\right)\right];\end{gathered} \tag{1.56}$$

$$\begin{gathered}\ddot{\varphi}_j(t)+s\dot{\varphi}_j(t)+d\varphi_j(t)= \\ =\frac{2c}{I_y}\left[\sum_{i=1}^{3}l_ih_j\left(t+\frac{l_i}{v}\right)\right]+\frac{2\mu}{I_y}\left[\sum_{i=1}^{3}l_i\dot{h}_j\left(t+\frac{l_i}{v}\right)\right];\end{gathered} \tag{1.57}$$

$$\left(j=\overline{1,N}\right).$$

Equations (1.56) together with equation (1.54) represent the mathematical model of the disturbed motion or random vertical

oscillations of the sprung part of the vehicle, while equations (1.57) together with equation (1.54) represent the mathematical model of the disturbed motion or random pitch (longitudinal angular) oscillations of the sprung part of the vehicle.

Let us consider the random vertical oscillations of the sprung part of the vehicle body, described by the differential equations (1.56) and (1.54), which need to be reduced to the normal Cauchy form. Let us introduce the state vector, whose components represent the generalized coordinates and generalized velocities of the mathematical model (1.56), (1.54):

$$X_j(t) = \begin{bmatrix} x_{j1}(t) \\ x_{j2}(t) \\ x_{j3}(t) \\ x_{j4}(t) \end{bmatrix} = \begin{bmatrix} z_j(t) \\ \dot{z}_j(t) \\ h_j(t) \\ \dot{h}_j(t) \end{bmatrix}. \qquad (1.58)$$

Then the mathematical model (1.56), (1.54) is written in the normal Cauchy form:

$$\begin{aligned} \dot{x}_{j1}(t) &= x_{j2}(t); \\ \dot{x}_{j2}(t) &= -a x_{j1}(t) - m x_{j2}(t) + \\ &\quad + \frac{2c}{M_p}\left[\sum_{i=1}^{3} x_{j3}\left(t + \frac{l_i}{v}\right)\right] + \frac{2\mu}{M_p}\left[\sum_{i=1}^{3} x_{j4}\left(t + \frac{l_i}{v}\right)\right]; \qquad (1.59) \\ \dot{x}_{j3}(t) &= x_{j4}(t); \\ \dot{x}_{j4}(t) &= -\frac{1}{T_1^2} x_{j3}(t) - \frac{T_2}{T_1^2} x_{j4}(t) + \frac{k}{T_1^2} \xi_j(t). \end{aligned}$$

1.4. MATLAB software package for investigating random oscillations of dynamic systems.

The interactive MATLAB program (an abbreviation for Matrix Laboratory) is a highly efficient language for technical and scientific computing. MATLAB supports mathematical calculations, visualization of computational results, and programming within an easy-to-learn

operating environment. Being matrix-oriented, the MATLAB language significantly simplifies computations in the field of linear algebra, such as solving systems of linear equations. MATLAB is particularly valuable due to the availability of a large number of additional application-specific toolboxes, designed to solve problems in various fields of science and engineering (simulation, control system synthesis and analysis, neural networks and genetic algorithms, fuzzy logic, etc.).

One such MATLAB package is SIMULINK, which is used for modeling and analyzing a vast array of physical and mathematical systems, including systems with nonlinear elements and systems that operate in both continuous and discrete time.

As an extension of MATLAB, SIMULINK adds many features for dynamic systems while retaining all the core capabilities of MATLAB.

Using MATLAB enables the graphical modeling of systems, avoiding many of the nuances associated with conventional programming.

One of the most important tasks in studying the dynamics of technical systems is solving differential equations. MATLAB implements several methods to solve this problem. The most common method for solving differential equations is the 4th-order Runge-Kutta method, for which the standard function **ode45** is used.

The system of differential equations is written as a separate file, whose name is included in the list of one of the function's parameters; other parameters include the start of the integration interval, the end of the integration interval, and the *vector/matrix* of initial conditions.

To create the file for the system of differential equations, the latter must be presented in the normal Cauchy form.

The format of the **ode45** function is:

[T,Y] = ode45(‘m-file‘,[t0 t1],y0),

where [T, Y] is the solution matrix, T is the time vector, Y is the matrix of solution vectors, *m_file* is the name of the file containing the system of differential equations, t_0 is the start of the integration interval, t_1 is the end of the integration interval, and y_0 is the vector of initial conditions.

To display the results in the form of a graph, the **plot** command is used:

>>plot(T,Y)

The output of the *i*-th solution y_i is performed in the following format:

>>plot(T,Y(:,i))

Let's consider an example of solving the system of differential equations (1.59), which describes the oscillations of the vehicle's center of gravity while moving on a road surface modeled by system (1.54). The complexity of solving system (1.59) lies in the fact that its right-hand side contains delayed values describing the height of the road surface irregularities. The **ode45** function in its standard form does not support solving such equations. Therefore, we will first model the irregularities over the entire integration interval of the system under consideration by solving system (1.54), and then use the obtained values along with a specially developed algorithm to solve system (1.59).

To solve the differential equation (1.54) in the MATLAB integrated environment using the Runge-Kutta method, it must be reduced to the normal Cauchy form. This was done by making the appropriate variable substitution (1.58), resulting in the relations given by the 3rd and 4th equations of system (1.59). These equations must first be written into an m-file function, i.e., a file with the .m extension. To do this, select the **New** command from the **File** menu. The structure of the m-file has the code presented in Listing 1.1.

Listing 1.1 – **Solving the differential equation (1.54)**

```
function yp=sys159_fun_h(t,y)
global K T1 T2
yp(1)=y(2);
yp(2)=(-y(1)-T2*y(2)+K*awgn(0,1))/(T1^2);
yp=yp`;
```

To save this file, you need to select the command in the menu **File → Save As…**. The filename must match the function name. In our case, it is sys159_fun_h.m.

Next, to solve the entire system (1.59), the first two equations of this system need to be written into a similar m-file function.

An additional algorithm has been developed to handle variables with time delays. As a result, the second m-file function has the code presented in Listing 1.2.

Listing 1.2 – **Solving the system of equations (1.59)**

```
function yp=sys159_fun_z(t,y)
global V a m c mu Mp lp
global th h jh hk htk maxhj
for ik=1:3,
        while jh(ik)<=maxhj,
                if (t+lp(ik)/V)<=th(jh(ik)),
                        hk(ik)=h(jh(ik),1);
                        htk(ik)=h(jh(ik),2);
                        break;
                end
                jh(ik)=jh(ik)+1;
        end
end
sumh=hk(1)+hk(2)+hk(3);
sumht=htk(1)+htk(2)+htk(3);
yp(1)=y(2);
yp(2)=-a*y(1)-m*y(2)+2*c/Mp*sumh+2*mu/Mp*sumht;
yp=yp`;
```

File name – sys159_fun_z.m.

After preparing the function files for the right-hand sides of the system of differential equations using the method described above, you can execute the **ode45** function in the command line by first specifying the input data and initial conditions. It is advisable to record all commands in a command m-file, as shown in Listing 1.3.

Listing 1.3 – **Execution of the ode45 function**

```
global V a m c mu Mp lp
global th h jh hk htk maxhj
global K T1 T2
Vm=[25 20 15 10 5];
Km=[0.0198 0.0221 0.0256 0.0315 0.0439];
T1m=[0.0916 0.144 0.1524 0.2288 0.4566];
T2m=[0.0586 0.0922 0.0975 0.1464 0.2922];
i=5;
V=Vm(i)
K=Km(i)
T1=T1m(i)
```

```
T2=T2m(i)
lp=[2 -0.66 -1.34];
Mp=20000; c=330000; mu=51000;
a=6*c/Mp; m=6*mu/Mp;
Tk=10;
h0=[0 0];
[th,h] = ode45('sys159_fun_h',[0 Tk],h0);
figure(1)
plot(th,h(:,1),'-b','LineWidth',1)
grid on
maxhj=length(th)
jh=[1 1 1];
hk=[h(1,1) h(1,1) h(1,1)];
htk=[h(1,2) h(1,2) h(1,2)];
z0=[0 0];
[tz,z]=ode45('sys159_fun_z',[0 Tk],z0);
figure(2)
plot(tz,z(:,1),'black',tz,z(:,2),'-g','LineWidth',1.5)
grid on
```

As a result of applying the given program to the system of equations (1.59), we obtain the functions $x_{j3}(t) = h_j(t)$, shown in Fig. 1.8, as well as the functions $x_{j1}(t) = Z_j(t)$ and $x_{j2}(t) = \dot{Z}_j(t)$, which are shown in Fig. 1.10.

Using the MATLAB programming language with the standard **ode45** function to solve the specific system of differential equations (1.59) has two drawbacks. First, the system contains variables with time delays, which requires the development of a special algorithm. Second, modeling the "white noise" input to the dynamic element that simulates road surface irregularities using standard functions significantly increases the program's execution time for calculating the system's oscillatory processes, reaching up to one hour for a 10-second integration interval depending on the computer's processor type, which is very inconvenient for students performing laboratory work.

Considering the above drawbacks, a second method for investigating oscillations in the technical system using MATLAB is proposed, based on simulation in the **Simulink** package environment.

Let's build a model using equations (1.54) and (1.56). The block diagram of the model is shown in Fig. 1.10.

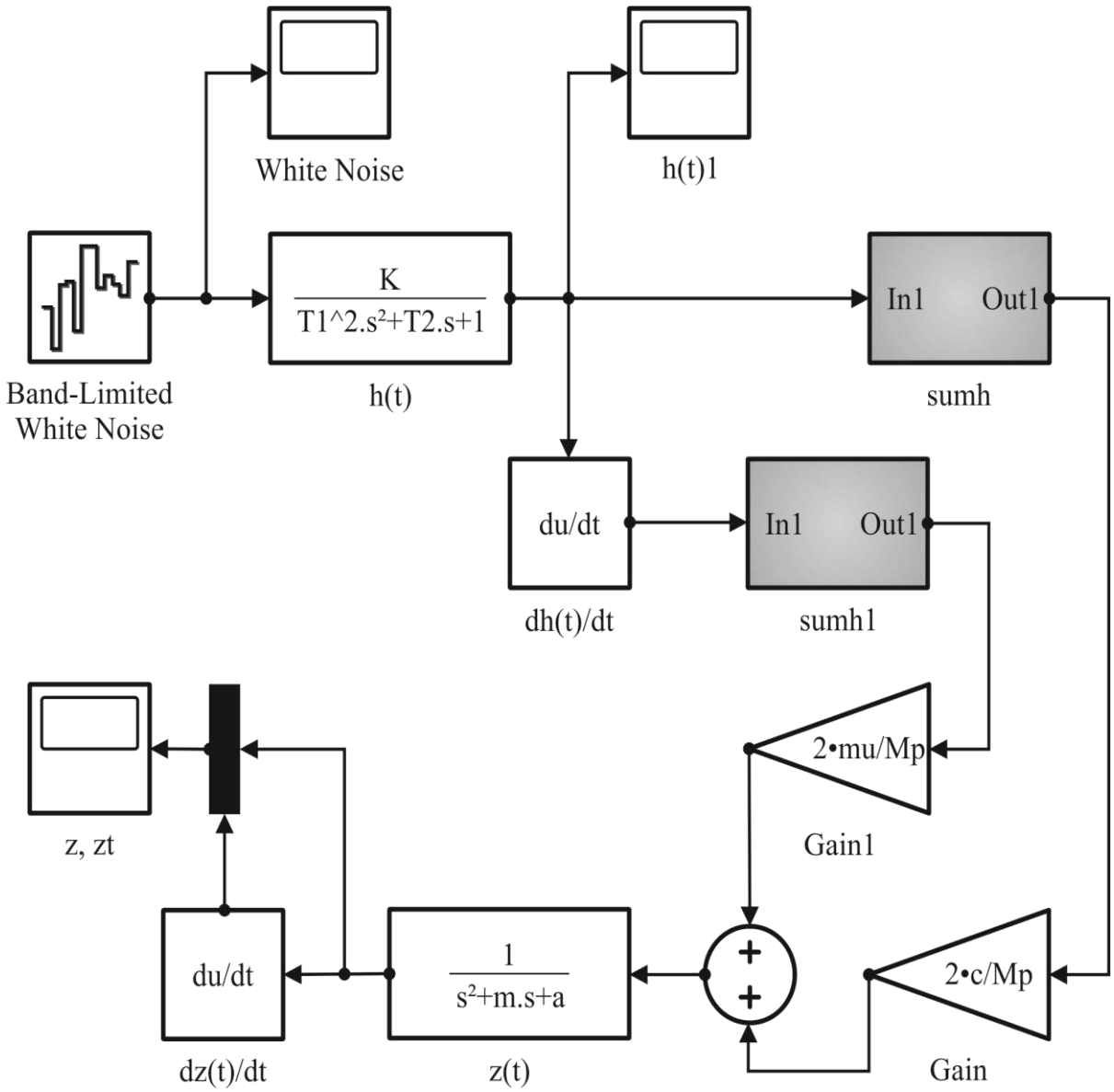

Fig. 1.10.a. **Block diagram of the model in the Simulink environment**

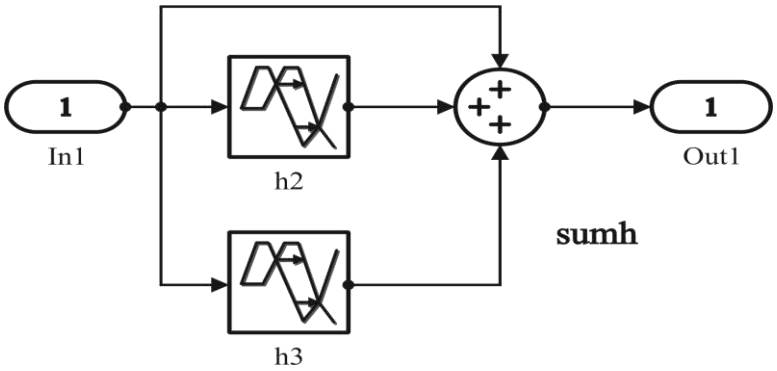

Fig. 1.10.b. **Block diagram of the model in the Simulink environment**

The **Band-Limited White Noise** block is located in the **Simulink/Sources** library. Parameters: Noise power: [0.005]; Sample time: 0.01.

The **Transfer Fcn** (transfer function) block is located in the **Simulink/Continuous** library. Parameters are the numerator and denominator coefficients, which must be specified as vectors. Coefficients should be entered in descending order of powers of **s**. Parameters for the variable **h(t)**: Numerator coefficients: [K]; Denominator coefficients: [T1^2 T2 1]. Parameters for the variable **z(t)**: Numerator coefficients: [1]; Denominator coefficients: [1 m a].

The **du/dt** (derivative) block is located in the **Simulink/Continuous** library.

To model sums of variables with delays (**sumh**, **sumh1**), **Subsystem** blocks from the **Simulink/Commonly Used Blocks** library are used. The internal structure of both blocks is shown in the lower part of Fig. 1.9. Each block includes **Transport Delay** elements (from the **Simulink/Continuous** library). Parameter for block **h2**: Time delay: (lp(1)-lp(2))/V; for block **h3**: Time delay: (lp(1)-lp(3))/V.

Amplifiers are set using **Gain** blocks, located in the **Simulink/Commonly Used Blocks** library.

Graphs of the variables **h(t)**, **z(t)**, and **ż(t)** are displayed using **Scope** blocks (from the **Simulink/Sinks** library).

Before running the model, create an m-file with the initial data (Listing 1.4).

Listing 1.4 – **Input data for calculation**

```
Vm=[25 20 15 10 5];
Km=[0.0198 0.0221 0.0256 0.0315 0.0439];
T1m=[0.0916 0.144 0.1524 0.2288 0.4566];
T2m=[0.0586 0.0922 0.0975 0.1464 0.2922];
i=1;
V=Vm(i)
K=Km(i)
T1=T1m(i)
T2=T2m(i)
lp=[2 -0.66 -1.34];
```

```
Mp=20000; c=330000; mu=51000;
a=6*c/Mp; m=6*mu/Mp;
```

Let's run this file. As a result, the values of all parameters will appear in the MATLAB Workspace, from where they are then used during the model execution. The results of the model execution are close to those obtained by the program calculation.

At the same time, the model execution time is only a few seconds, which is significantly faster than using the MATLAB programming language with the standard **ode45** function.

Figure 1.11 shows the random processes of vertical oscillations of the vehicle's sprung mass while moving on the random microprofile shown in Figure 1.8. The random processes were obtained using the Simulink model. Analysis of Figure 1.10 leads to the conclusion that an increase in the vehicle's speed on a random surface leads to an increase in the frequency and a decrease in the amplitude of the vertical oscillations of the sprung part of the vehicle body.

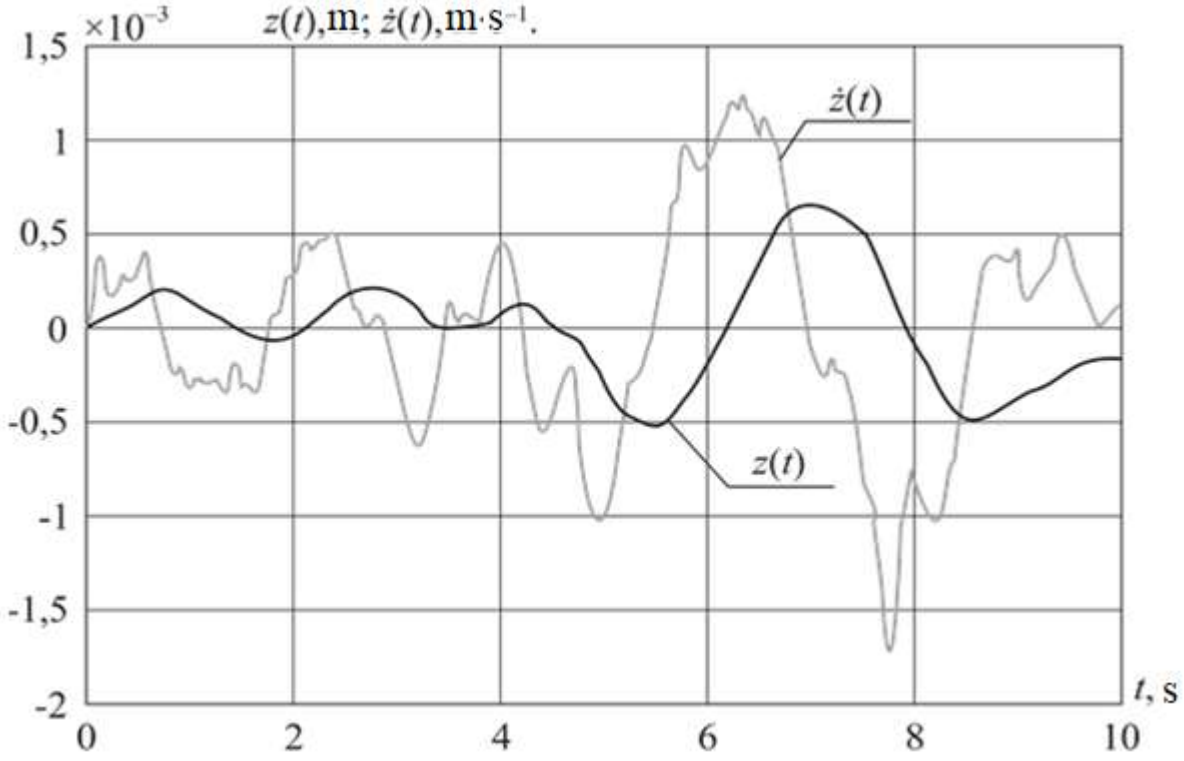

Fig. 1.11.a. **Random processes of vertical oscillations of the vehicle's sprung mass at v = 5 m·s^{-1}**

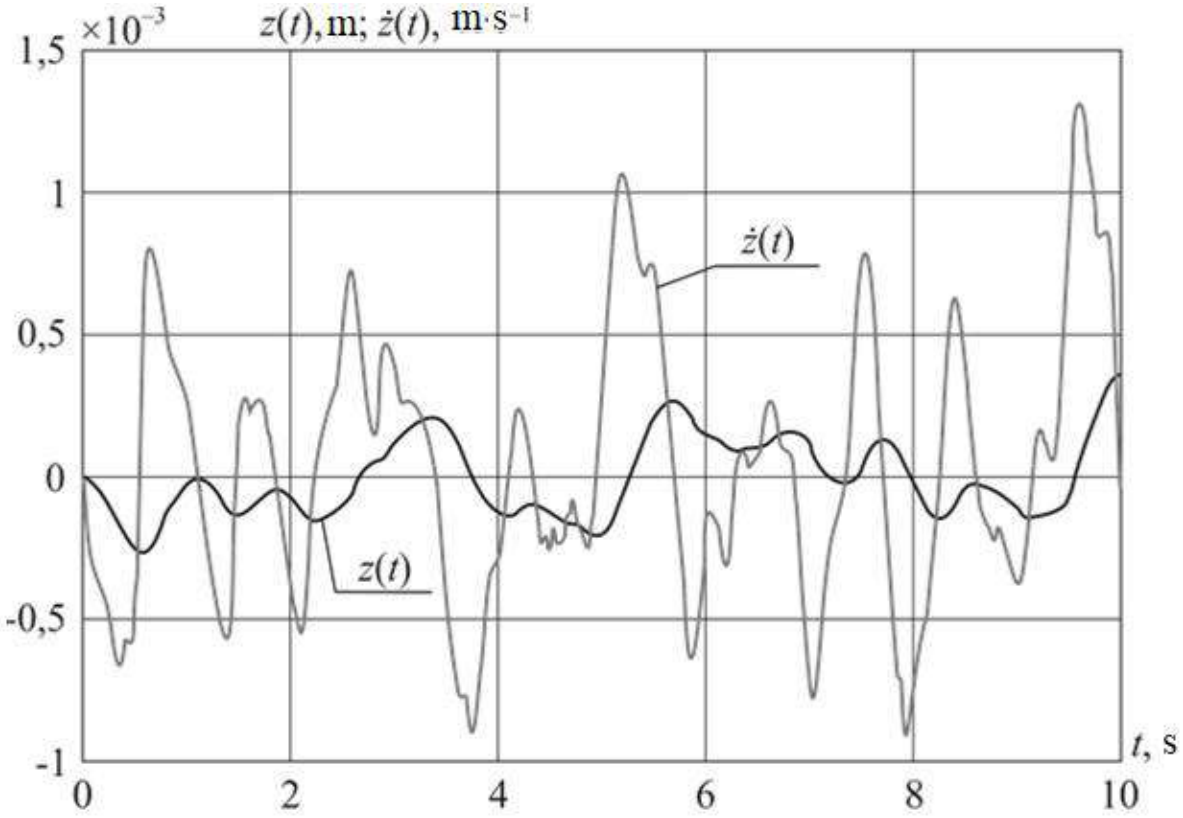

Fig. 1.11.b. **Random processes of vertical oscillations of the vehicle's sprung mass at v = 10 m·s^{-1}**

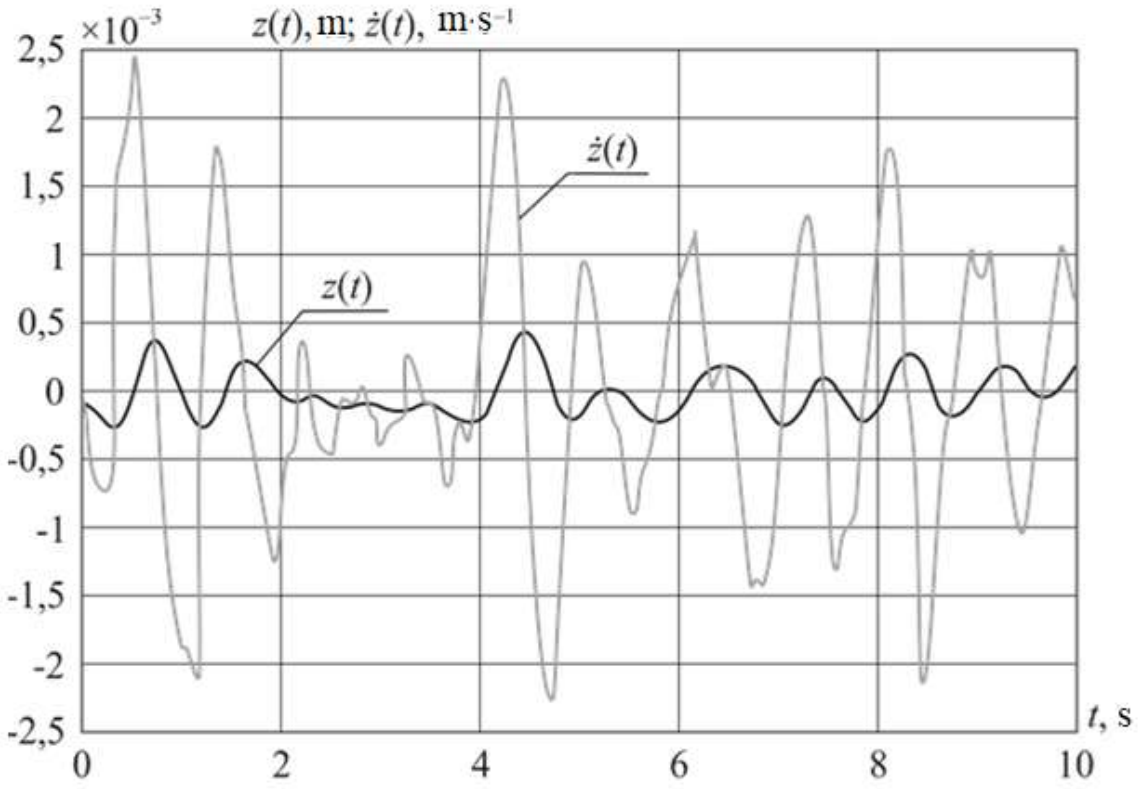

Fig. 1.11.c. **Random processes of vertical oscillations of the vehicle's sprung mass at v = 15 m·s^{-1}**

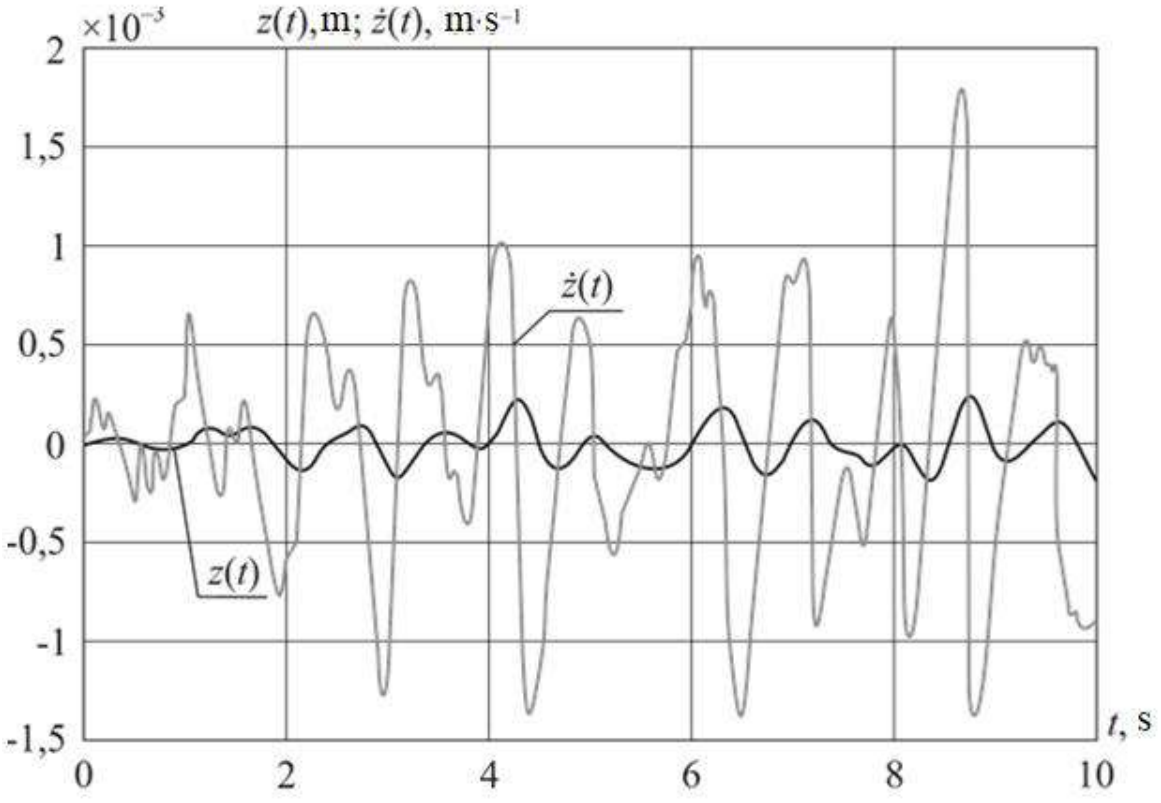

Fig. 1.11.d. **Random processes of vertical oscillations of the vehicle's sprung mass at v = 20 m·s^{-1}**

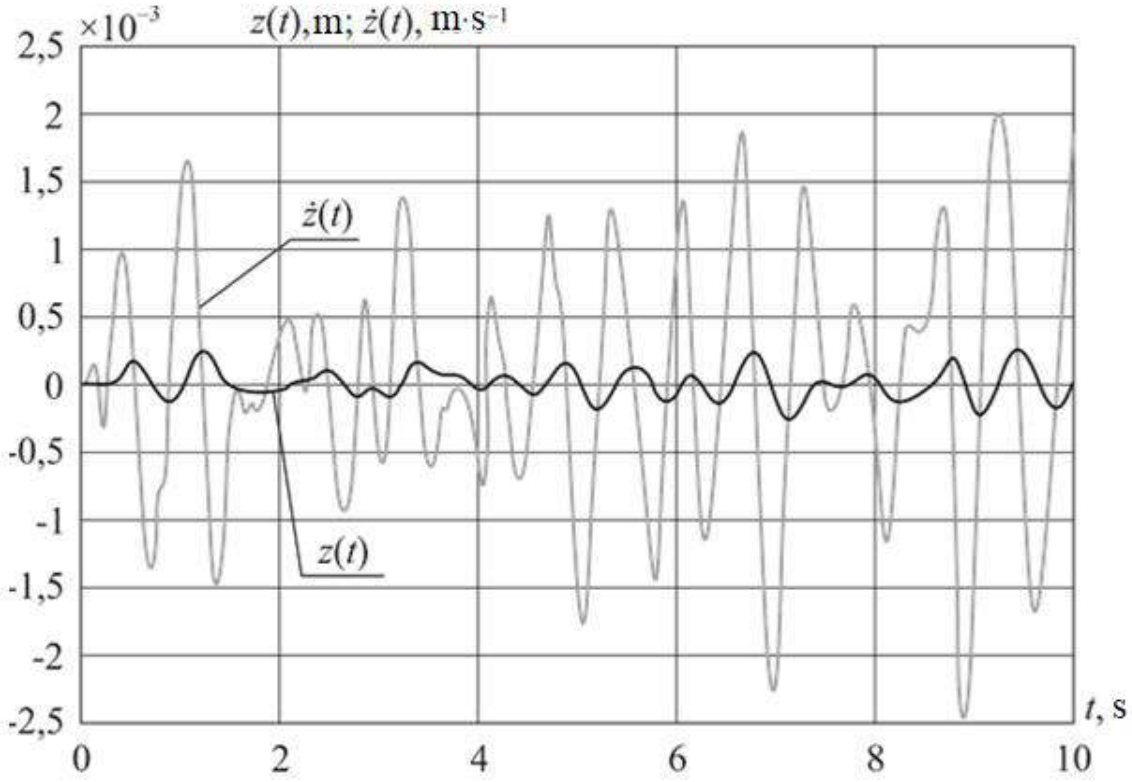

Fig. 1.11.e. **Random processes of vertical oscillations of the vehicle's sprung mass at v = 25 m·s^{-1}**

Control questions for the chapter 1.

1. Define the center of stiffness (elastic center) of a vehicle.
2. Specify the range of oscillation periods of the vehicle's sprung mass most favorable for the crew.
3. Define a symmetric vehicle suspension.
4. Write the formula for free oscillations of the vehicle's sprung mass with a symmetric suspension.
5. Define forced oscillations of the vehicle body.
6. When does resonance occur in forced oscillations of the sprung mass?
7. Under what conditions do random oscillations of the sprung mass arise?
8. Write the equation for the correlation function of road surface irregularities.
9. Write the formula for the spectral density of road surface irregularities.
10. Define a shaping dynamic element.

Chapter 2

OSCILLATIONS OF LINEAR DYNAMIC SYSTEMS WITH TWO DEGREES OF FREEDOM.

2.1. Free oscillations of linear systems with two degrees of freedom.

Let us consider a vehicle with an asymmetric suspension, the free oscillations of whose sprung mass are described by differential equations (1.21) and (1.22). The state vector of the dynamic system (1.21), (1.22) is represented as:

$$X(t)=\begin{bmatrix} x_1(t) \\ x_2(t) \\ x_3(t) \\ x_4(t) \end{bmatrix}=\begin{bmatrix} z(t) \\ \dot{z}(t) \\ \varphi(t) \\ \dot{\varphi}(t) \end{bmatrix}$$

and write the system (1.21), (1.22) in the normal Cauchy form:

$$\begin{aligned} &\dot{x}_1(t)=x_2(t); \\ &\dot{x}_2(t)=-ax_1(t)-mx_2(t)-bx_3(t)-qx_4(t); \\ &\dot{x}_3(t)=x_4(t); \\ &\dot{x}_4(t)=-fx_1(t)-rx_2(t)-dx_3(t)-sx_4(t). \end{aligned} \qquad (2.1)$$

Let us write the system (2.1) in vector-matrix form:

$$\dot{X}(t)=AX(t), \qquad (2.2)$$

where A is the system matrix (state matrix) of the system (2.1)

$$A=\begin{bmatrix} 0 & 1 & 0 & 0 \\ -a & -m & -b & -q \\ 0 & 0 & 0 & 1 \\ -f & -r & -d & -s \end{bmatrix}. \qquad (2.3)$$

The characteristic equation of the system (2.1) has the following form (2.4).

$$\det[A - Ep] = \begin{vmatrix} -p & 1 & 0 & 0 \\ -a & -m-p & -b & -q \\ 0 & 0 & -p & 1 \\ -f & -r & -d & -s-p \end{vmatrix} = 0. \qquad (2.4)$$

Expanding the determinant (2.4), we obtain:

$$\begin{gathered} p^4 + (m+s)p^3 + (a+d+ms-qr)p^2 + \\ +(as+md-br-fq)p + ad - fb = 0. \end{gathered} \qquad (2.5)$$

Obtaining an analytical solution for a fourth-degree algebraic equation is extremely complex; therefore, it is advisable to study oscillatory processes by directly integrating the system (2.1) under non-zero initial conditions:

$$x_{10} = z(0) = z_0;$$

$$x_{20} = \dot{z}(0) = \dot{z}_0;$$

$$x_{30} = \varphi(0) = \varphi_0;$$

$$x_{40} = \dot{\varphi}(0) = \dot{\varphi}_0.$$

Figure 2.1 shows the solutions of the system of differential equations (2.1) with the initial conditions:

$$z(0) = x_{10} = -0.05\ m;\ \dot{z}(0) = x_{20} = 0\ m \cdot s^{-1};$$

$$\varphi(0) = x_{30} = 0.05\ \text{rad};\ \dot{\varphi}(0) = x_{40} = 0\ s^{-1}.$$

Figure 2.2 shows the solutions of the same system under the initial conditions:

$$z(0) = x_{10} = -0.05\ m;\ \dot{z}(0) = x_{20} = 0\ m \cdot s^{-1};$$

$$\varphi(0) = x_{30} = 0\ \text{rad};\ \dot{\varphi}(0) = x_{40} = 0\ s^{-1}.$$

Analysis of Figure 2.1 and Figure 2.2 leads to the conclusion that the natural oscillations of the system (2.1) are damped.

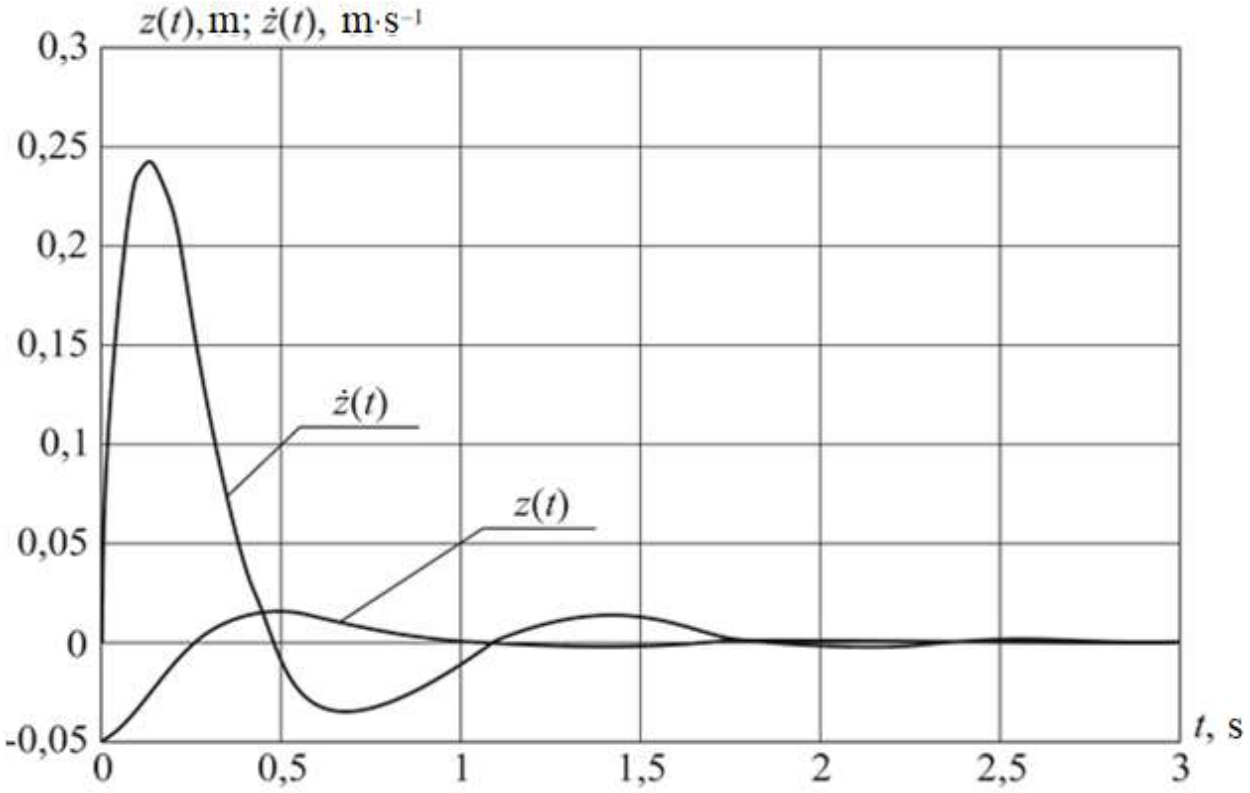

Fig. 2.1.a. **Solution of the system (2.1)**

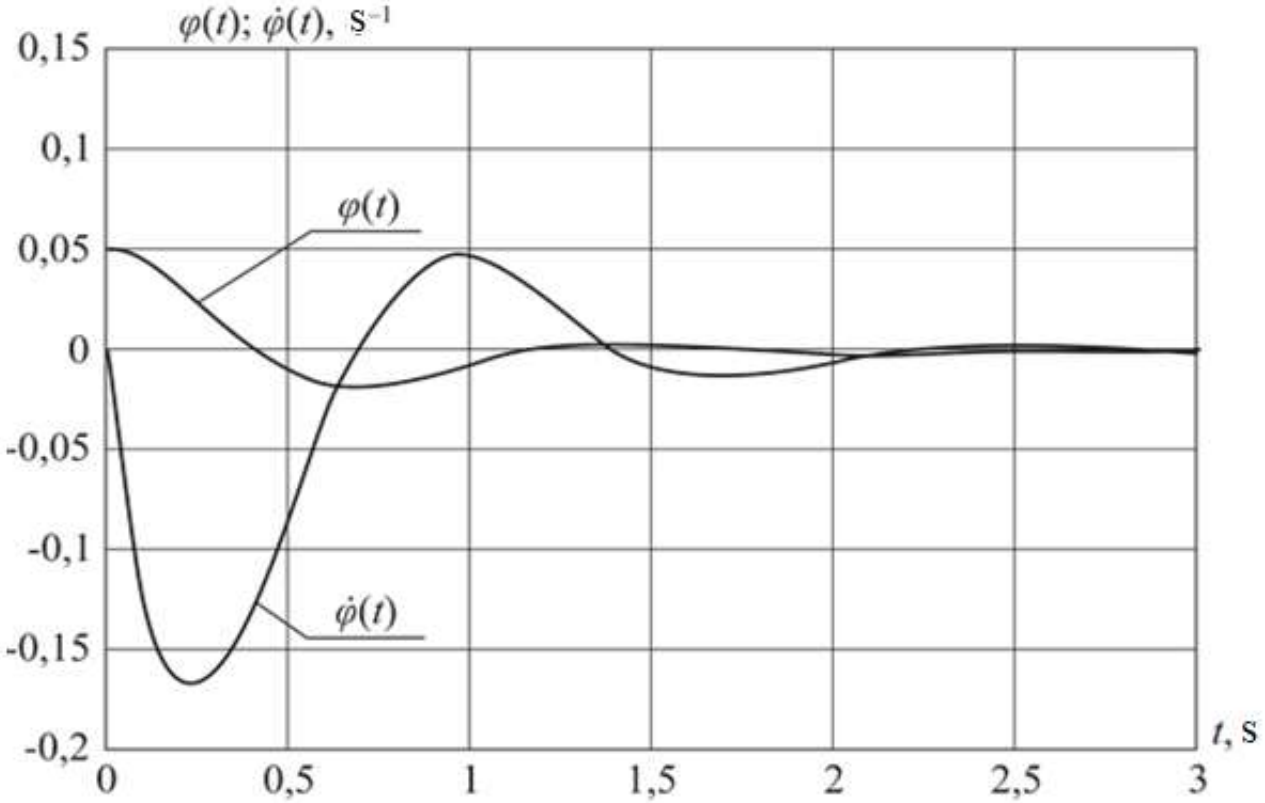

Fig. 2.1.b. **Solution of the system (2.1)**

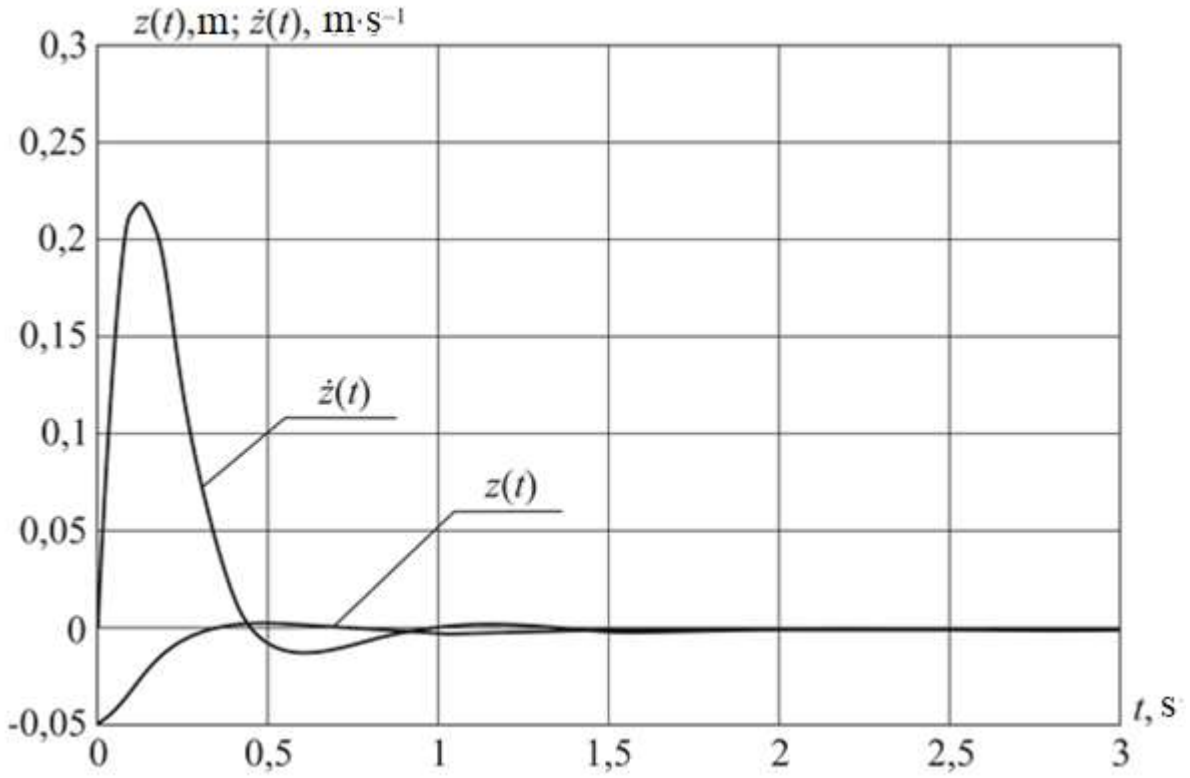

Fig. 2.2.a. **Solution of the system (2.1)**

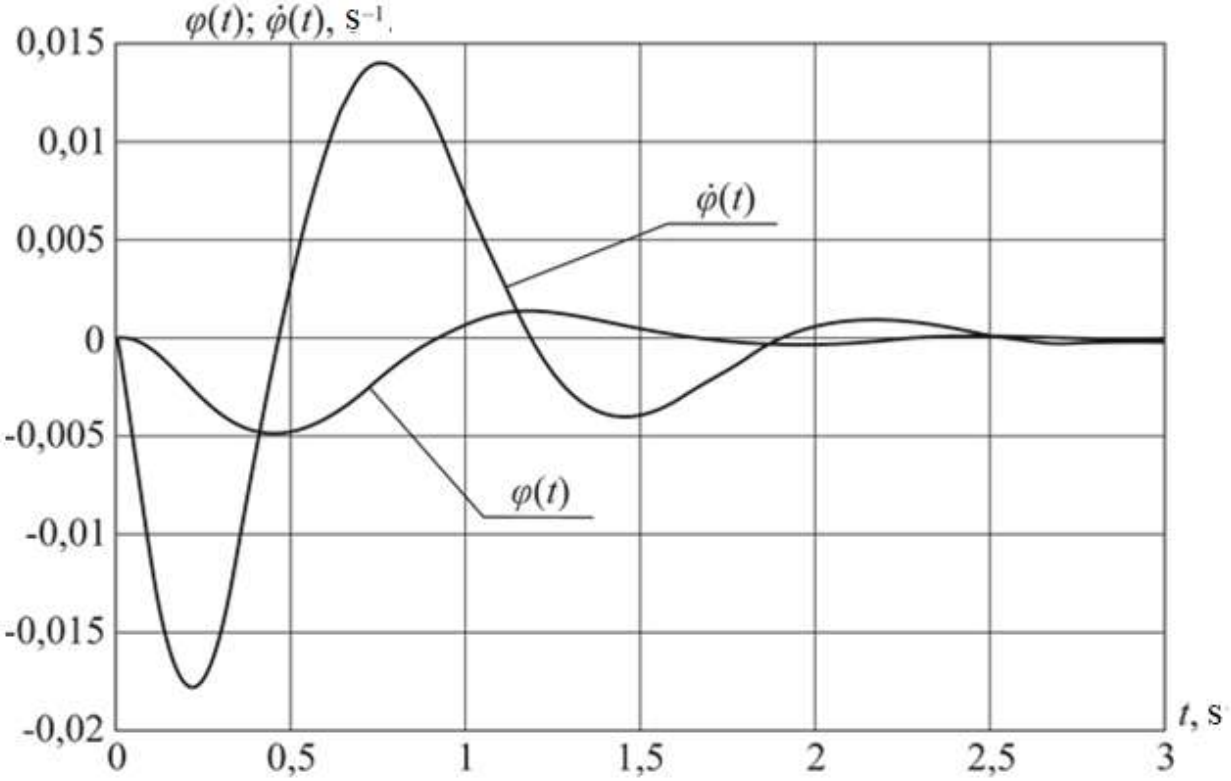

Fig. 2.2.b. **Solution of the system (2.1)**

2.2. Forced oscillations of linear systems with two degrees of freedom.

We will assume that the microprofile of the vehicle's running surface is sinusoidal, i.e., in equations (1.55) we take:

$$h(t) = \frac{H}{2}\sin\omega t, \tag{2.6}$$

where H is the amplitude, and ω is the frequency of the sinusoidal profile.

Let us differentiate equation (2.6) with respect to time:

$$\dot{h} = \frac{H\omega}{2}\cos\omega t. \tag{2.7}$$

Taking into account equation (2.6) and equation (2.7), the mathematical model of the disturbed motion of the sprung part of the vehicle body in the form of equation (1.55) takes the form:

$$\begin{gathered}
\ddot{z}(t) + m\dot{z}(t) + az(t) + q\dot{\varphi}(t) + b\varphi(t) = \\
= \frac{cH}{M_p}\sum_{i=1}^{3}\sin\omega\left(t + \frac{l_i}{v}\right) + \frac{\mu H\omega}{M_p}\sum_{i=1}^{3}\cos\omega\left(t + \frac{l_i}{v}\right); \\
\ddot{\varphi}(t) + s\dot{\varphi}(t) + d\varphi(t) + r\dot{z}(t) + fz(t) = \\
= \frac{cH}{I_y}\sum_{i=1}^{3} l_i \sin\omega\left(t + \frac{l_i}{v}\right) + \frac{\mu H\omega}{I_y}\sum_{i=1}^{3} l_i \cos\omega\left(t + \frac{l_i}{v}\right).
\end{gathered} \tag{2.8}$$

Let us write the system of equations (2.8) in vector-matrix form:

$$\dot{X}(t) = AX(t) + F(t),$$

where $X(t)$ is the state vector of the dynamic system; A is the system matrix (state matrix); $F(t)$ is the vector of external disturbances.

Matrix A has the form (2.3), and vector $F(t)$ is written as:

$$F(t)=\begin{bmatrix} \dfrac{H}{M_p}\left[c\sum_{i=1}^{3}\sin\omega\left(t+\dfrac{l_i}{v}\right)+\mu\omega\sum_{i=1}^{3}\cos\omega\left(t+\dfrac{l_i}{v}\right)\right] \\ \dfrac{H}{I_y}\left[c\sum_{i=1}^{3}l_i\sin\omega\left(t+\dfrac{l_i}{v}\right)+\mu\omega\sum_{i=1}^{3}l_i\cos\omega\left(t+\dfrac{l_i}{v}\right)\right] \end{bmatrix}^{0}. \qquad (2.9)$$

Figure 2.3 shows the oscillatory processes constructed using the Simulink software package and described by the fourth-order system of differential equations (2.8).

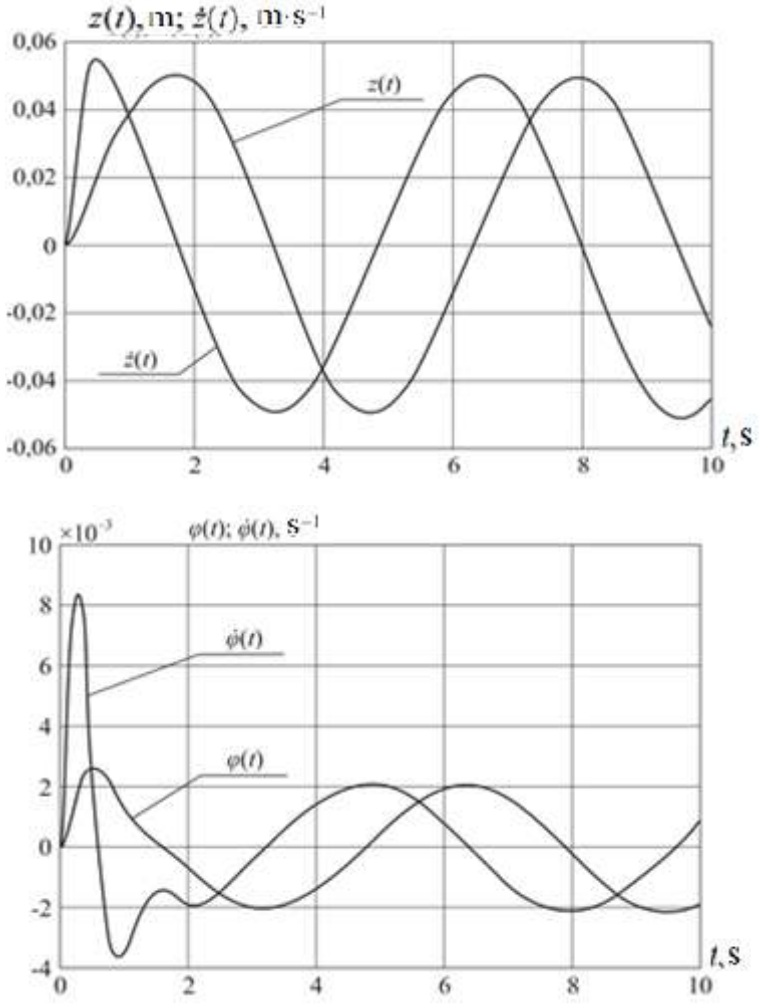

Fig. 2.3.a. **Processes of forced oscillations of the sprung part of the vehicle body, corresponding to a sinusoidal profile frequency of ω = 1 s⁻¹;**

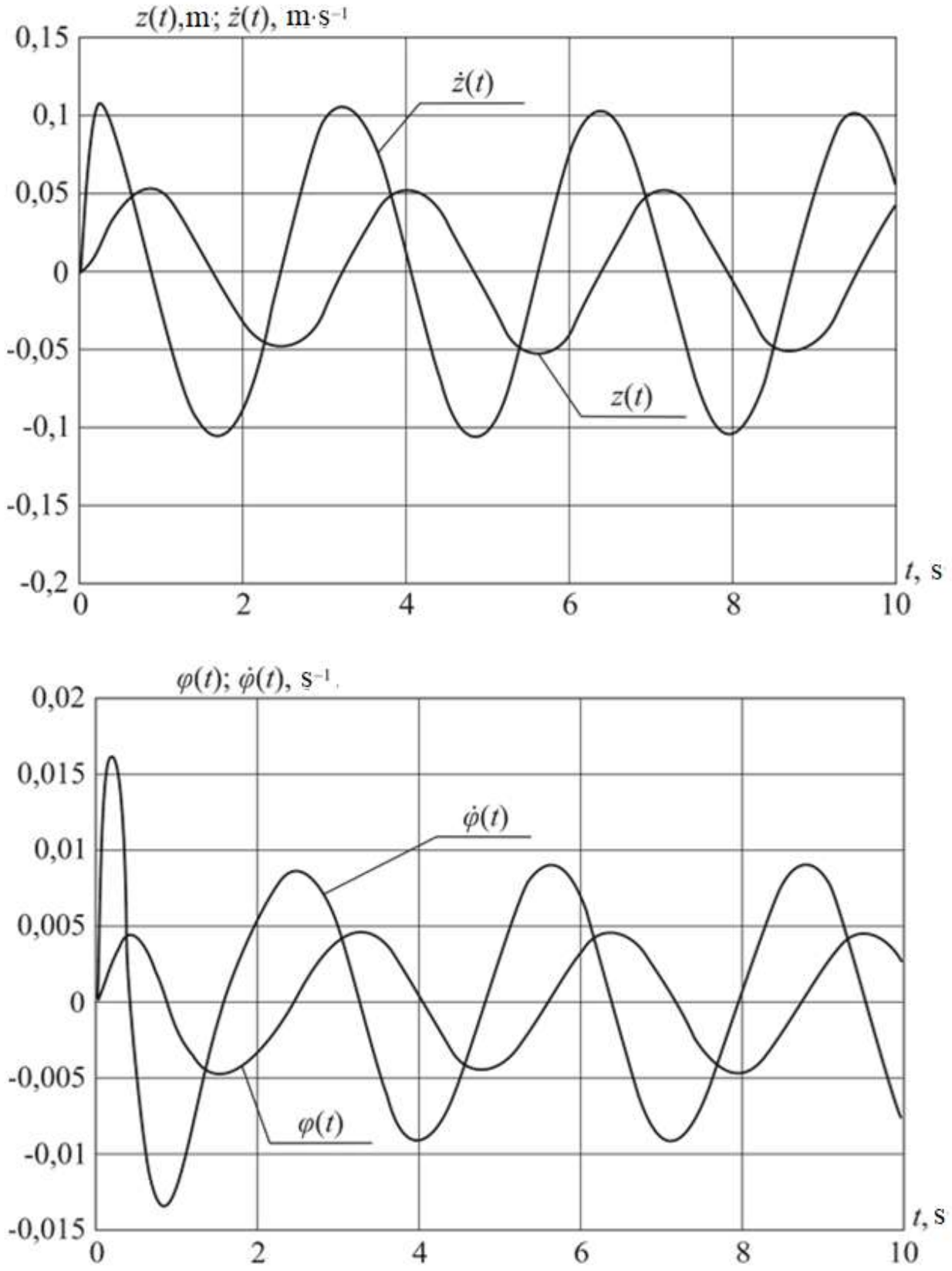

Fig. 2.3.b. **Processes of forced oscillations of the sprung part of the vehicle body, corresponding to a sinusoidal profile frequency of ω = 2 s⁻¹;**

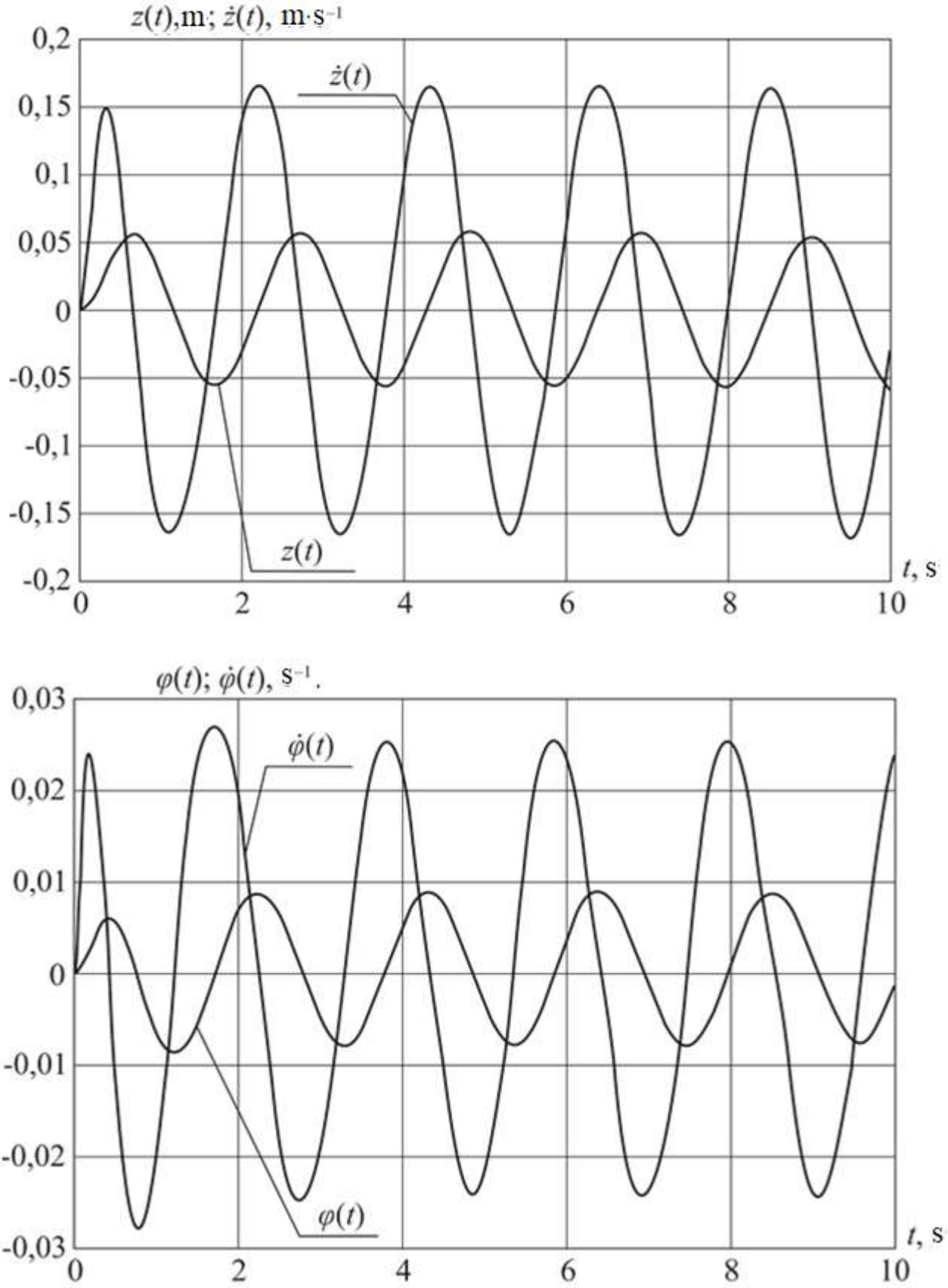

Fig. 2.3.c. **Processes of forced oscillations of the sprung part of the vehicle body, corresponding to a sinusoidal profile frequency of ω = 3 s⁻¹;**

Analysis of Figure 2.3 leads to the conclusion that the natural oscillations of the sprung part of the vehicle body decay quite rapidly, and forced oscillations with frequency ω become established in the system. This frequency is determined by the sinusoidal profile of the path irregularities and the vehicle's speed.

2.3. Random oscillations of linear systems with two degrees of freedom.

Let us return to the dynamic system (1.55), which describes random forced oscillations of the sprung part of the vehicle. When developing the mathematical model of system (1.55), an assumption was made that the random microprofile of the running surface is the same on the left and right sides of the vehicle.

This allowed us to analyze the forced vertical and pitch oscillations of the sprung part of the vehicle body. This assumption enables the exclusion of roll (lateral angular) oscillations of the sprung body from consideration. However, in practice, roll oscillations of the sprung body necessarily occur precisely because the random microprofile of the running surface differs between the right and left sides and is described by random functions of time $h_{kp}(t)$ and $h_{lp}(t)$ $(k,l=\overline{1,N})$, which are solutions to the differential equations:

$$\begin{gathered} T_1^2\ddot{h}_{kp}(t)+T_2\dot{h}_{kp}(t)+h_{kp}(t)=k\xi_{kp}(t); \\ (k=\overline{1,N}); \\ T_1^2\ddot{h}_{lp}(t)+T_2\dot{h}_{lp}(t)+h_{lp}(t)=k\xi_{lp}(t); \\ (l=\overline{1,N}). \end{gathered} \tag{2.10}$$

In studies investigating the ride comfort of a multi-axle vehicle containing 3 springs and 3 shock absorbers on each side, the following mathematical model of the disturbed motion of its sprung part is used:

$$\ddot{z}_{kl}(t)+\frac{6\mu}{M_p}\dot{z}_{kl}(t)+\frac{6c}{M_p}z_{kl}(t)+\frac{2\mu}{M_p}\sum_{j=1}^{3}l_j\dot{\varphi}_{kl}(t)+$$

$$+\frac{2c}{M_p}\sum_{i=1}^{3}l_i\varphi_{kl}(t)=\frac{c}{M_p}\left[\sum_{i=1}^{3}h_{kp}\left(t+\frac{l_i}{v}\right)+\sum_{i=1}^{3}h_{lp}\left(t+\frac{l_i}{v}\right)\right]+$$

$$+\frac{\mu}{M_p}\left[\sum_{j=1}^{3}\dot{h}_{kp}\left(t+\frac{l_j}{v}\right)+\sum_{j=1}^{3}\dot{h}_{lp}\left(t+\frac{l_j}{v}\right)\right];$$

$$\ddot{\varphi}_{kl}(t)+\frac{2\mu}{I_y}\sum_{j=1}^{3}l_j^2\dot{\varphi}_{kl}(t)+\frac{2c}{I_y}\sum_{i=1}^{3}l_i^2\varphi_{kl}(t)+\frac{2\mu}{I_y}\sum_{j=1}^{3}l_j\dot{z}_{kl}(t)+$$

$$+\frac{2c}{I_y}\sum_{i=1}^{3}l_iz_{kl}(t)=\frac{c}{I_y}\left[\sum_{i=1}^{3}l_ih_{kp}\left(t+\frac{l_i}{v}\right)+\sum_{i=1}^{3}l_ih_{lp}\left(t+\frac{l_i}{v}\right)\right]+$$

$$+\frac{\mu}{I_y}\left[\sum_{j=1}^{3}l_j\dot{h}_{kp}\left(t+\frac{l_j}{v}\right)+\sum_{j=1}^{3}l_j\dot{h}_{lp}\left(t+\frac{l_j}{v}\right)\right];$$

$$\ddot{\theta}_{kl}(t)+\frac{3\mu B^2}{2I_x}\dot{\theta}_{kl}(t)+\frac{3cB^2}{2I_x}\theta_{kl}(t)=$$

$$=\frac{cB}{2I_x}\left[\sum_{i=1}^{3}h_{kp}\left(t+\frac{l_i}{v}\right)-\sum_{i=1}^{3}h_{lp}\left(t+\frac{l_i}{v}\right)\right]+$$

$$+\frac{\mu B}{2I_x}\left[\sum_{j=1}^{3}\dot{h}_{kp}\left(t+\frac{l_j}{v}\right)-\sum_{j=1}^{3}\dot{h}_{lp}\left(t+\frac{l_j}{v}\right)\right]. \qquad (2.11)$$

The sixth-order system of differential equations (2.11) differs from the fourth-order system (1.55) by the presence of an additional differential equation for the generalized coordinate $\theta(t)$, which represents the roll angle (rotation) of the vehicle's sprung mass about its own central longitudinal axis of inertia *OX*, which is perpendicular to the *OZ* and *OY* axes shown in Figures 1.1 and 1.2. If the microprofile of the running surface is identical on the left and right sides of the vehicle, the right-hand side of the third differential equation in system (2.11) becomes zero, indicating the absence of roll (lateral angular) oscillations of the vehicle's sprung mass.

Let us introduce a tenth-order state vector:

$$X(t)=\begin{bmatrix} x_1(t)\\ x_2(t)\\ x_3(t)\\ x_4(t)\\ x_5(t)\\ x_6(t)\\ x_7(t)\\ x_8(t)\\ x_9(t)\\ x_{10}(t)\end{bmatrix}=\begin{bmatrix} z_{kl}(t)\\ \dot{z}_{kl}(t)\\ \varphi_{kl}(t)\\ \dot{\varphi}_{kl}(t)\\ \theta_{kl}(t)\\ \dot{\theta}_{kl}(t)\\ h_{kp}(t)\\ \dot{h}_{kp}(t)\\ h_{lp}(t)\\ \dot{h}_{lp}(t)\end{bmatrix}.$$

Taking into account the notations introduced earlier in equations (1.13) and (1.20), as well as the new notations:

$$u=\frac{3\mu B^2}{2I_x};\ w=\frac{3cB^2}{2I_x},$$

the system of differential equations (2.11), (2.10) can be written in the normal Cauchy form:

$$\dot{x}_1(t)=x_2(t);$$

$$\dot{x}_2(t)=-mx_2(t)-ax_1(t)-qx_4(t)-bx_3(t)+$$
$$+\frac{c}{M_p}\left[\sum_{i=1}^{3}x_7\left(t+\frac{l_i}{v}\right)+\sum_{i=1}^{3}x_9\left(t+\frac{l_i}{v}\right)\right]+$$
$$+\frac{\mu}{M_p}\left[\sum_{j=1}^{3}x_8\left(t+\frac{l_j}{v}\right)+\sum_{j=1}^{3}x_{10}\left(t+\frac{l_i}{v}\right)\right];$$

$$\dot{x}_3(t)=x_4(t);$$

$$\dot{x}_4(t) = -sx_4(t) - dx_3(t) - rx_2(t) - fx_1(t) +$$
$$+\frac{c}{I_y}\left[\sum_{i=1}^{3} l_i x_7\left(t+\frac{l_i}{v}\right)+\sum_{i=1}^{3} l_i x_9\left(t+\frac{l_i}{v}\right)\right]+$$
$$+\frac{\mu}{I_y}\left[\sum_{j=1}^{3} l_j x_8\left(t+\frac{l_j}{v}\right)+\sum_{j=1}^{3} l_j x_{10}\left(t+\frac{l_j}{v}\right)\right];$$
$$\dot{x}_5(t) = x_6(t);$$
$$\dot{x}_6(t) = -ux_6(t) - wx_5(t) + \tag{2.12}$$
$$+\frac{cB}{2I_x}\left[\sum_{i=1}^{3} x_7\left(t+\frac{l_i}{v}\right)-\sum_{i=1}^{3} x_9\left(t+\frac{l_i}{v}\right)\right]+$$
$$+\frac{\mu B}{2I_x}\left[\sum_{j=1}^{3} x_8\left(t+\frac{l_j}{v}\right)-\sum_{j=1}^{3} x_{10}\left(t+\frac{l_j}{v}\right)\right];$$

$$\dot{x}_7(t) = x_8(t);$$

$$\dot{x}_8(t) = -\frac{1}{T_1^2}x_7(t) - \frac{T_2}{T_1^2}x_8(t) + \frac{k}{T_1^2}\xi_{kp}(t);\ (k=\overline{1,N});$$

$$\dot{x}_9(t) = x_{10}(t);$$

$$\dot{x}_{10}(t) = -\frac{1}{T_1^2}x_9(t) - \frac{T_2}{T_1^2}x_{10}(t) + \frac{k}{T_1^2}\xi_{lp}(t);\ (l=\overline{1,N})$$

Figure 2.4 shows the random processes of forced oscillations of the vehicle's sprung part under zero initial conditions and different vehicle speeds.

Analysis of the random oscillatory processes presented in Fig. 2.4 indicates an increase in the average frequency and a decrease in the average amplitude of the vehicle body's oscillations as the speed of movement over the random surface increases.

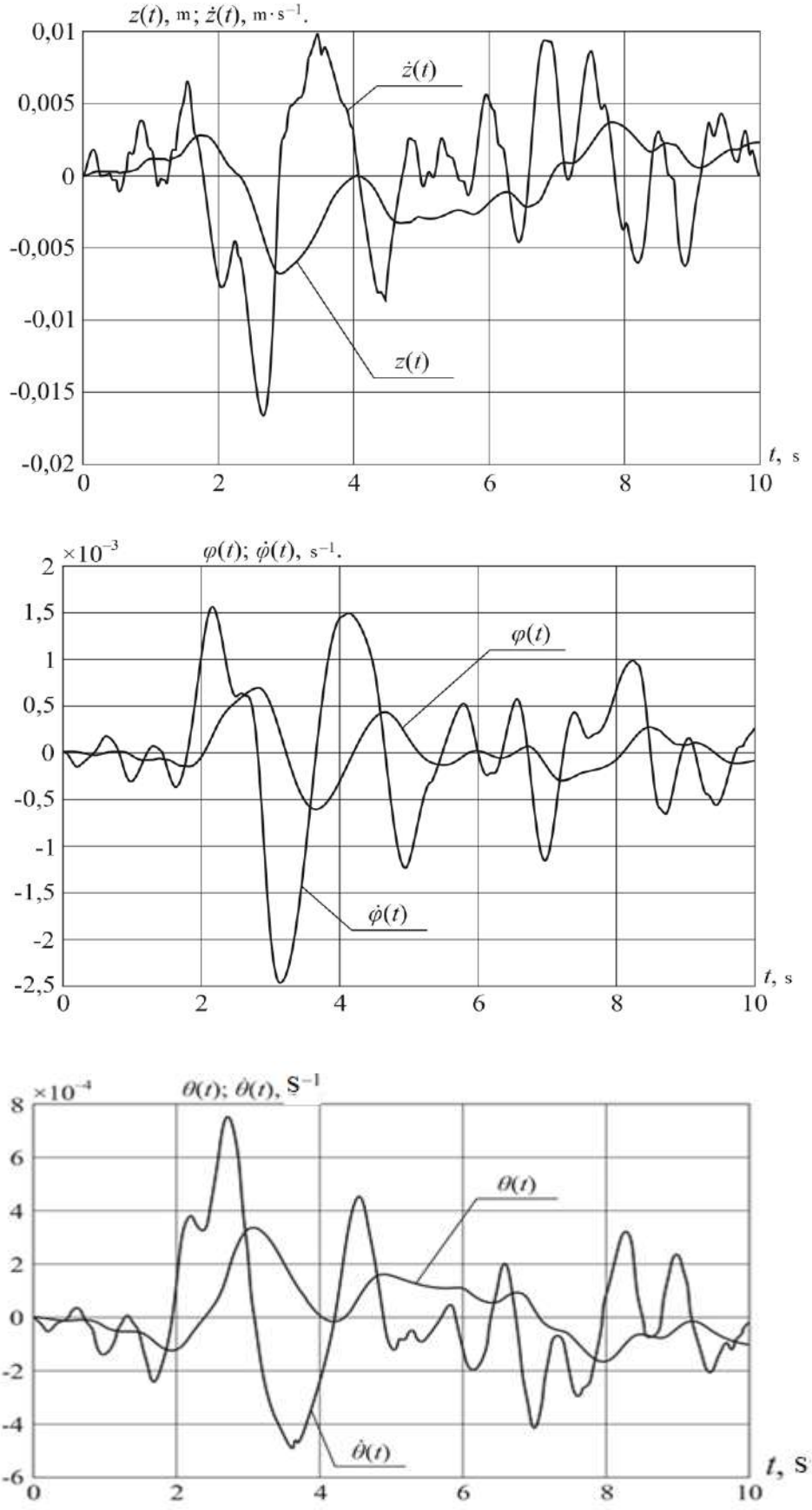

Fig. 2.4.a. **Random oscillatory processes of the sprung part of the vehicle body, corresponding to a travel speed of $v = 5$ m·s⁻¹**

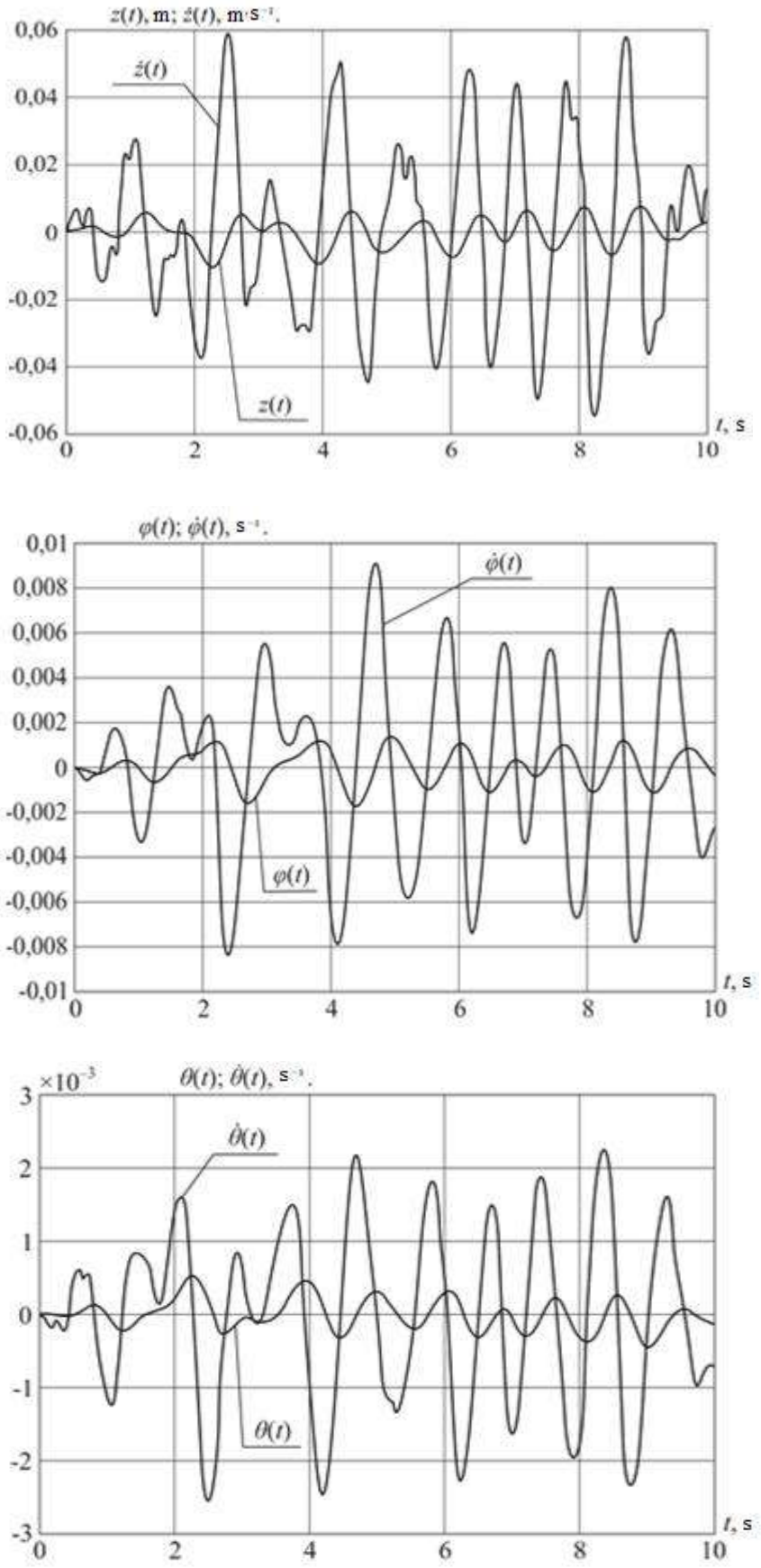

Fig. 2.4.b. **Random oscillatory processes of the sprung part of the vehicle body, corresponding to a travel speed of v = 15 m·s⁻¹**

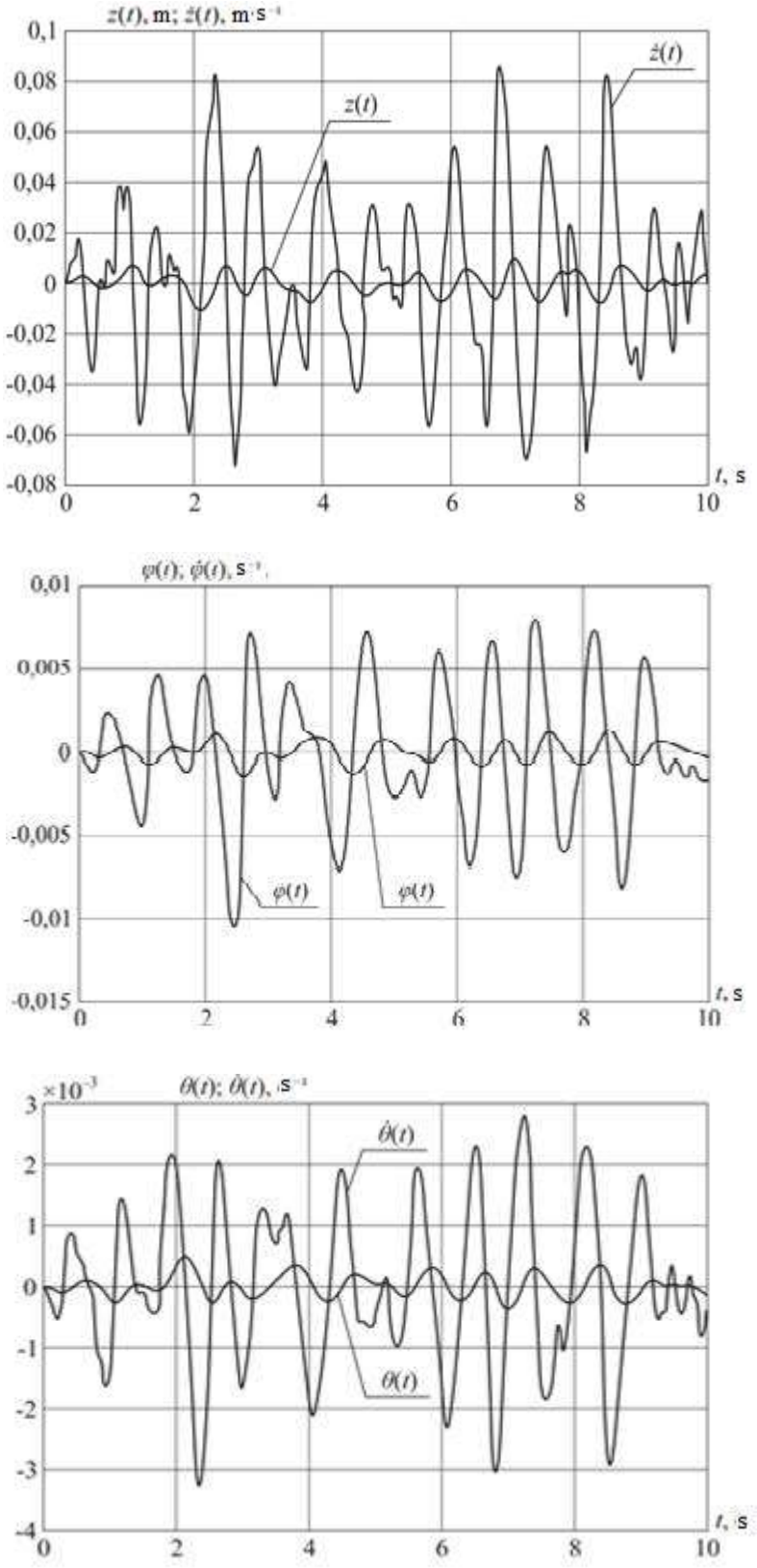

Fig. 2.4.c. **Random oscillatory processes of the sprung part of the vehicle body, corresponding to a travel speed of $v = 25$ m·s⁻¹**

Control questions for the chapter 2.

1. What is the difference between oscillatory systems with one degree of freedom and those with two degrees of freedom?
2. Describe the procedure for reducing the mathematical model of disturbed motion of an oscillatory system to the normal Cauchy form.
3. Define the state vector of a dynamic system.
4. Define the system matrix of a dynamic system.
5. Define the characteristic equation of a dynamic system.
6. List the generalized coordinates and velocities of a vehicle’s sprung mass.
7. Under what condition does resonance occur in the forced oscillations of the vehicle’s sprung mass?

Chapter 3
OSCILLATIONS OF NONLINEAR DYNAMIC SYSTEMS

3.1. Main nonlinearities in dynamic systems.

The theory of oscillations in linear dynamic systems has seen significant development and widespread application in engineering practice. This is primarily due to three reasons: first, methods for the analysis and synthesis of this class of systems have been developed, offering sufficient generality and convenience for engineering computations; second, the results obtained through the linearization of dynamic systems often prove satisfactory, albeit inherently approximate; and third, in recent decades, with the rapid advancement of computing technology and programming, numerous application software packages, such as MATLAB and Mathcad, have been created, focusing primarily on solving problems related to the analysis and synthesis of dynamic systems, especially linear ones.

The results achieved by linearizing nonlinear dynamic systems may be validated or refuted by practice, depending on the extent to which the linearized nonlinearities influence the dynamic processes. For a detailed and comprehensive study of real technical systems, linear mathematical models are often overly simplified. In such cases, it is advisable to examine the dynamic properties of nonlinear mathematical models, which has become feasible thanks to modern software products.

The theory of nonlinear dynamic systems, based on nonlinear mathematical models of their disturbed motion, is a much broader scientific field than the theory of linear systems. The study of nonlinear mathematical models allows for the identification of fundamentally new phenomena that may not be observed in linear systems. Here, it is essential to highlight the phenomenon of self-oscillations, which represents periodic motion. This motion arises not due to external periodic influences but as a result of the inherent dynamic properties of the system itself. The problem of self-oscillations in control systems is of great practical importance. Sometimes they are intentionally utilized to improve the dynamic properties of a system, while in other cases, their emergence is undesirable. Therefore, it is crucial to be able to determine the conditions for their occurrence and their parameters.

A nonlinear dynamic system is defined as a system whose mathematical model contains at least one nonlinear differential equation. In general, a nonlinear dynamic system is described by a mathematical model of the following form:

$$\begin{aligned}
&\dot{x}_1(t) = \varphi_1\left[x_1(t), x_2(t), \ldots, x_n(t)\right] + f_1(t);\\
&\dot{x}_2(t) = \varphi_2\left[x_1(t), x_2(t), \ldots, x_n(t)\right] + f_2(t);\\
&\vdots\\
&\dot{x}_n(t) = \varphi_n\left[x_1(t), x_2(t), \ldots, x_n(t)\right] + f_n(t).
\end{aligned} \tag{3.1}$$

In vector-matrix form, equation (3.1) is written as:

$$\dot{X}(t) = \Phi[X(t)] + F(t), \tag{3.2}$$

where the system state vector $X(t)$, the external disturbance vector $F(t)$, and the vector function $\Phi[X(t)]$ have the form:

$$X(t) = \begin{bmatrix} x_1(t) \\ x_2(t) \\ \vdots \\ x_n(t) \end{bmatrix};\ F(t) = \begin{bmatrix} f_1(t) \\ f_2(t) \\ \vdots \\ f_n(t) \end{bmatrix};$$

$$\Phi[X(t)] = \begin{bmatrix} \varphi_1[x_1(t), x_2(t), \ldots, x_n(t)] \\ \varphi_2[x_1(t), x_2(t), \ldots, x_n(t)] \\ \vdots \\ \varphi_n[x_1(t), x_2(t), \ldots, x_n(t)] \end{bmatrix}.$$

Most nonlinear dynamic systems can be linearized by expanding the nonlinear vector function $\Phi[X(t)]$ into a Taylor series around an equilibrium point and subsequently discarding the nonlinear terms of the expansion due to their small magnitude compared to the linear terms.

The equilibrium point $x_{10}, x_{20}, \ldots, x_{n0}$ of the dynamic system (3.1) is found by solving the system of algebraic equations:

$$\begin{aligned}
&\varphi_1[x_{10}, x_{20}, \ldots, x_{n0}] = 0;\\
&\varphi_2[x_{10}, x_{20}, \ldots, x_{n0}] = 0;\\
&\vdots\\
&\varphi_n[x_{10}, x_{20}, \ldots, x_{n0}] = 0.
\end{aligned} \tag{3.3}$$

Let us introduce the relative generalized coordinates of the dynamic system (3.1):

$$y_i(t) = x_i(t) - x_{i0};\ (i = \overline{1,n}). \tag{3.4}$$

Typically, when constructing a mathematical model of the disturbed motion of a dynamic system (3.1), its generalized coordinates are chosen such that their values in the state of stable equilibrium are zero:

$$x_{i0} = 0;\ (i = \overline{1,n}). \tag{3.5}$$

Then, according to (3.5), we have:

$$y_i(t) = x_i(t);\ (i = \overline{1,n}),$$

and the mathematical model of the linearized dynamic system (3.2) takes the form:

$$\dot{X}(t) = \left(\frac{\partial \Phi[X(t)]}{\partial X} \right)_0 X(t) + F(t), \tag{3.6}$$

where each element of the system matrix of the linearized dynamic system (3.6) is:

$$A = \left(\frac{\partial \Phi[X(t)]}{\partial X} \right)_0$$

equals

$$a_{ij} = \left[\frac{\partial \varphi_i[x_1(t), x_2(t), \ldots, x_n(t)]}{\partial x_j(t)} \right]_0 \tag{3.7}$$

and represents the partial derivative of the i-th component of the vector function $\Phi[X(t)]$ with respect to the j-th component of the state vector of the dynamic system, evaluated at the equilibrium point.

As a result, the mathematical model of the disturbed motion of the linearized dynamic system (3.6) is written as:

$$\dot{X}(t) = AX(t) + F(t). \tag{3.8}$$

The system of differential equations (3.8) is called the system of the first approximation relative to system (3.2) or (3.1).

However, there are nonlinear dynamic systems for which linearization by expanding the nonlinear vector function $\Phi[X(t)]$ into a Taylor series and discarding the nonlinear terms is **not possible**. This applies to non-analytic vector functions $\Phi[X(t)]$. Examples of such systems include:

1. A vehicle suspension system with friction dampers.
2. A relay-based automatic control system for coolant temperature, the operation of which will be discussed in the following subsections.

Let us consider an oscillatory system with friction, where the friction characteristic is described by a nonlinear function of the generalized velocity:

$$F[\dot{q}(t)] = -a_1\dot{q}(t) + a_3\dot{q}^3(t). \tag{3.9}$$

The form of function (3.9) is shown in Figure 3.1.

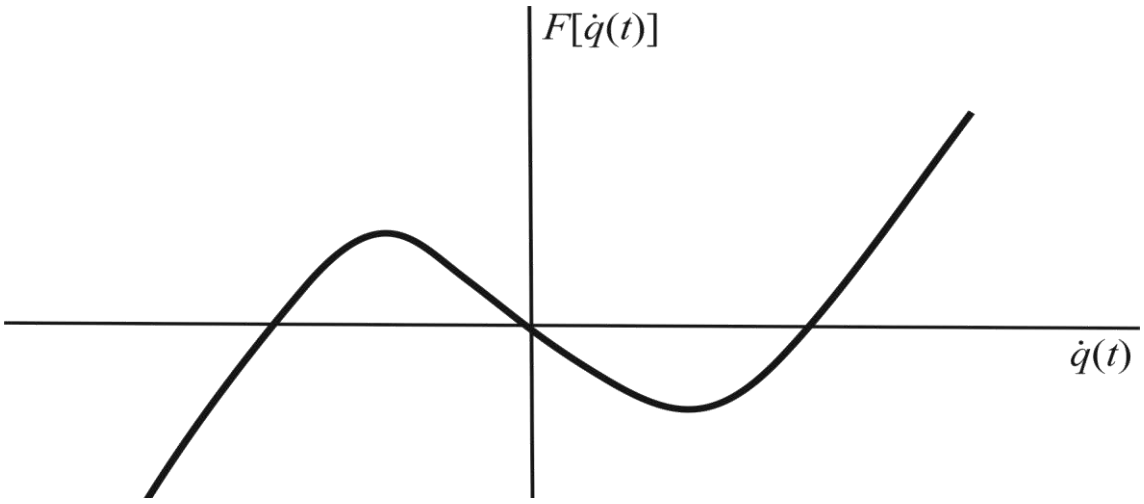

Fig. 3.1. **Shape of the nonlinear friction function**

The disturbed motion of the considered oscillatory system is described by the Rayleigh differential equation:

$$\ddot{q}(t) - a_1\dot{q}(t) + a_3\dot{q}^3(t) + cq(t) = 0. \qquad (3.10)$$

Assume $a_1 > 0$ and $a_3 > 0$, and write the nonlinear second-order equation (3.10) in the normal Cauchy form, i.e., as a system of two first-order differential equations. To do this, introduce a second-order state vector:

$$X(t) = \begin{bmatrix} x_1(t) \\ x_2(t) \end{bmatrix} = \begin{bmatrix} q(t) \\ \dot{q}(t) \end{bmatrix}.$$

As a result, we obtain:

$$\begin{aligned} \dot{x}_1(t) &= x_2(t); \\ \dot{x}_2(t) &= -cx_1(t) + a_1x_2(t) - a_3x_2^3(t). \end{aligned} \qquad (3.11)$$

Figure 3.2 shows the solutions of the system of differential equations under different initial conditions: $x_1(0) = x_{10} = 0{,}1;\ x_2(0) = 0.$

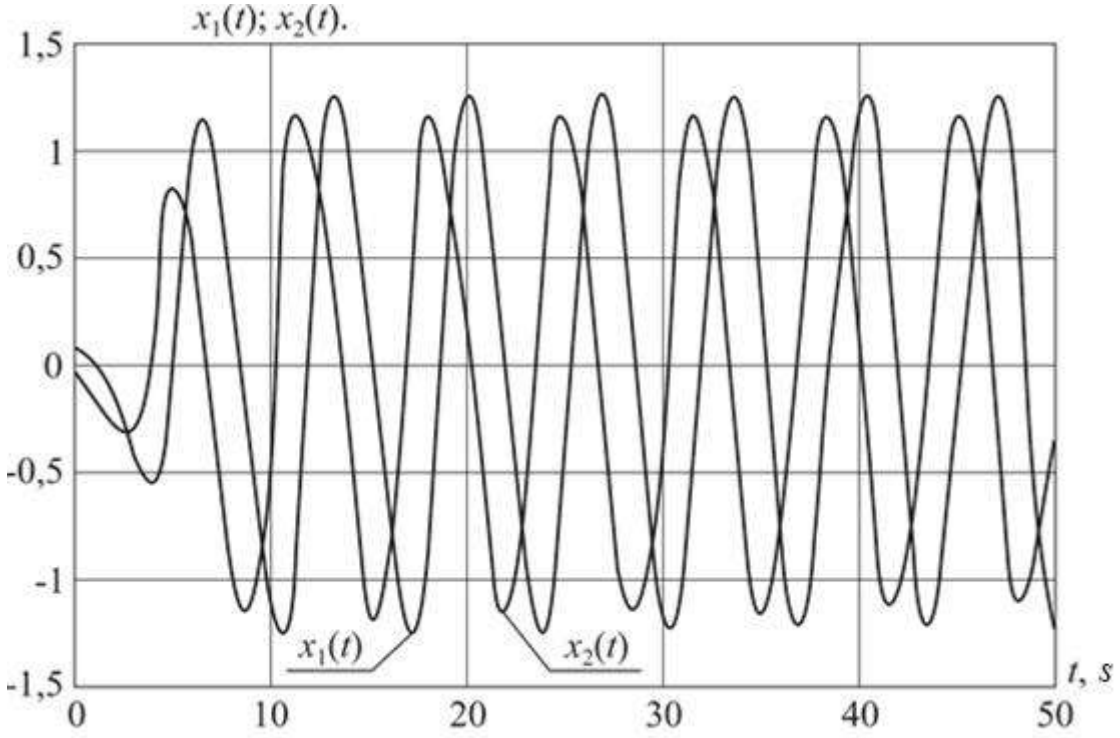

Fig. 3.2. **Oscillatory processes in the nonlinear dynamic system (3.11)**

Let us consider the Van der Pol equation:

$$\ddot{q}(t) - \mu[1 - q^2(t)]\dot{q}(t) + cq(t) = 0. \qquad (3.12)$$

Let us reduce equation (3.12) to the normal Cauchy form:

$$X(t) = \begin{bmatrix} x_1(t) \\ x_2(t) \end{bmatrix} = \begin{bmatrix} q(t) \\ \dot{q}(t) \end{bmatrix}$$

$$\begin{aligned} \dot{x}_1(t) &= x_2(t); \\ \dot{x}_2(t) &= -cx_1(t) + \mu[1 - x_1^2(t)]x_2(t). \end{aligned} \qquad (3.13)$$

Figure 3.3 shows the solutions of the Van der Pol equation, obtained by integrating the system (3.13) using the Runge-Kutta method implemented in the MathLAB software package.

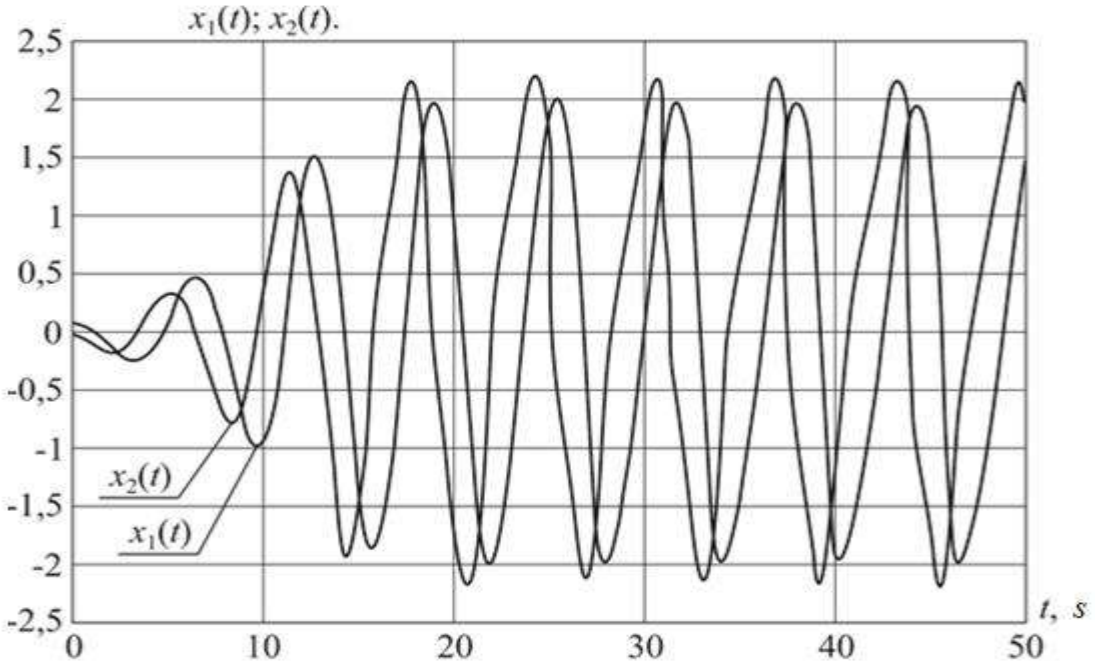

Fig. 3.3. **Oscillatory processes of system (3.13)**

3.2. Harmonic Linearization Method for Nonlinearities.

In the previous subsection, oscillations of nonlinear dynamic systems with analytical nonlinearities were considered. In such systems, undamped oscillations, or so-called limit cycles with constant oscillation amplitude, can arise. Such oscillations belong to stationary regimes or self-oscillation modes.

However, most technical dynamic systems contain non-analytical nonlinearities described by non-analytical functions. In such systems, self-oscillations typically arise, and their parameters are determined using the method of harmonic linearization, which consists of the following.

Imagine a nonlinear dynamic system as interconnected linear (LL) and nonlinear (NL) parts (Fig. 3.4).

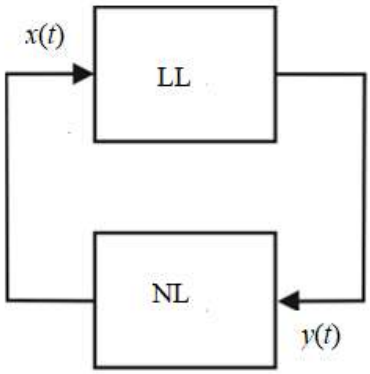

Fig. 3.4. **Nonlinear dynamic system**

Suppose that a non-sinusoidal periodic action **x(t)** is applied to the input of the linear part of the dynamic system. This action can be represented as a trigonometric Fourier series. Typically, the linear part of the system, whose disturbed motion is described by a linear differential equation:

$$A(p)y(t) = C(p)x(t), \tag{3.14}$$

acts as a high-frequency filter, meaning the amplitudes of the higher harmonics of the input signal $x(t)$ are significantly reduced when passing through the linear part of the dynamic system. Indeed, the transfer function of the linear part (LL) represents the ratio of the Laplace transform $\mathcal{L}\{y(t)\}$ of the output signal $y(t)$ to the Laplace transform $\mathcal{L}\{x(t)\}$ of the input signal $x(t)$ of the LL. Let us transform the differential equation (3.14) using the Laplace transform:

$$A(s)Y(s) = C(s)X(s), \tag{3.15}$$

where ***s*** – the complex variable of the Laplace transform;

$$Y(s) = \mathcal{L}\{y(t)\};$$

$$X(s) = \mathcal{L}\{x(t)\}.$$

The transfer function of the linear part of the dynamic system is written as:

$$W(s) = \frac{Y(s)}{X(s)} = \frac{C(s)}{A(s)}. \qquad (3.16)$$

In relation (3.16), we perform the substitution:

$$s = j\omega.$$

As a result, we obtain the relation for the frequency function of the linear part:

$$W_{\text{LL}}(j\omega) = \frac{C(j\omega)}{A(j\omega)} = U_{\text{LL}}(\omega) + jV_{\text{LL}}(\omega); \qquad (3.17)$$

where $U_{\text{LL}}(\omega)$ and $V_{\text{LL}}(\omega)$ – the real and imaginary parts of the frequency transfer function (3.17).

Then the amplitude-frequency response (AFR) of the linear part is determined by the relation:

$$M_{\text{LL}}(\omega) = \sqrt{U_{\text{LL}}^2(\omega) + V_{\text{LL}}^2(\omega)}. \qquad (3.18)$$

Typically, the amplitude-frequency response (AFR) of the linear part of a dynamic system has the form shown in Fig. 3.5, where ω_1 denotes the frequency of the first harmonic of the non-sinusoidal signal $x(t)$.

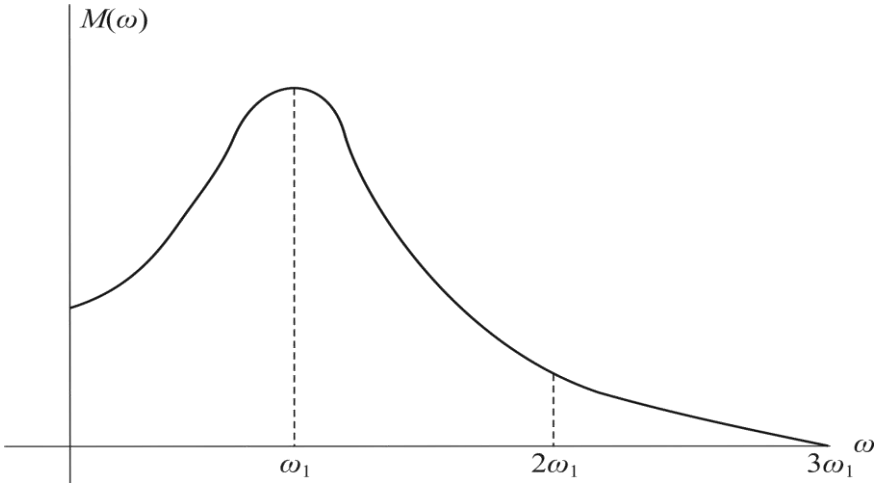

Fig. 3.5. **Amplitude-frequency response of the system's linear part**

Therefore, the higher harmonics of the output signal $y(t)$ of the linear part can be neglected, leaving only the first harmonic.

$$y(t) = A \cdot \sin \omega t, \tag{3.19}$$

where A and ω – are the sought amplitude and frequency of the periodic motion, respectively.

If the input to the nonlinear part (NL) of the system, whose behavior is described by the equation:

$$x(t) = F[y(t), \dot{y}(t)], \tag{3.20}$$

where $F[y(t), \dot{y}(t)]$ – is a nonlinear non-analytical function of its arguments, and the input signal is (3.19), then the output signal **x(t)** is a periodic non-sinusoidal function of time, which can be represented as a trigonometric Fourier series:

$$\begin{aligned} x(t) = \frac{a_0}{2} + a_1 \cos \omega t + b_1 \sin \omega t + a_2 \cos 2\omega t + \\ + b_2 \sin 2\omega t + \ldots + a_k \cos k\omega t + b_k \sin k\omega t + \ldots . \end{aligned} \tag{3.21}$$

The coefficients of the series (3.21) are calculated according to the formulas:

$$\begin{aligned} a_k &= \frac{1}{\pi} \int_0^{2\pi} F\left[A \sin \omega t, A\omega \cos \omega t\right] \cos k\omega t d\omega t; \\ b_k &= \frac{1}{\pi} \int_0^{2\pi} F\left[A \sin \omega t, A\omega \cos \omega t\right] \sin k\omega t d\omega t. \end{aligned} \tag{3.22}$$

Let $\varphi = \omega \cdot t$ and write relation (3.22) as:

$$a_k = \frac{1}{\pi} \int_0^{2\pi} F\left[A \sin \varphi, A\omega \cos \varphi\right] \cos k\varphi d\varphi; \tag{3.23}$$

$$b_k = \frac{1}{\pi} \int_0^{2\pi} F\left[A \sin \varphi, A\omega \cos \varphi\right] \sin k\varphi d\varphi. \tag{3.24}$$

We discard the higher harmonics of the Fourier series (3.21) with frequencies 2ω, 3ω, …, kω, … because they are poorly transmitted by the linear part of the system and have little influence on the output signal of the linear part.

$$x(t) = \frac{a_0}{2} + \frac{1}{\pi}\int_0^{2\pi} F\left[A\sin\varphi, A\omega\cos\varphi\right]\cos\varphi d\varphi \cos\omega t + \\ + \frac{1}{\pi}\int_0^{2\pi} F\left[A\sin\varphi, A\omega\cos\varphi\right]\sin\varphi d\varphi \sin\omega t = \\ = \frac{a_0}{2} + A\left[q(A)\sin\omega t + q_1(A)\cos\omega t\right], \tag{3.25}$$

where the quantities $q(A)$ and $q_1(A)$, called the harmonic linearization coefficients, are determined by the relations:

$$q(A) = \frac{1}{\pi A}\int_0^{2\pi} F\left[A\sin\varphi, A\omega\cos\varphi\right]\sin\varphi d\varphi; \tag{3.26}$$

$$q_1(A) = \frac{1}{\pi A}\int_0^{2\pi} F\left[A\sin\varphi, A\omega\cos\varphi\right]\cos\varphi d\varphi. \tag{3.27}$$

The time derivative of the input signal to the nonlinear part of the dynamic system is:

$$\frac{dy(t)}{dt} = py(t) = A\omega\cos\omega t. \tag{3.28}$$

Then, according to relations (3.19) and (3.28), we obtain:

$$x(t) = \frac{a_0}{2} + \left[q(A)y(t) + \frac{q_1(A)}{\omega}py(t)\right] = \\ = \frac{a_0}{2} + \left[q(A) + \frac{q_1(A)}{\omega}p\right]y(t). \tag{3.29}$$

Thus, the equation of the nonlinear element (3.20) has taken the form of a linear equation (3.29). The operation of transitioning from the nonlinear equation (3.20) to the linear one (3.29) is called harmonic

linearization. A characteristic feature of the harmonic linearization method is the dependence of the coefficients $q(A)$ and $q_1(A)$ on the unknown amplitude of the periodic solution (3.19).

Substitute equation (3.29) into the right-hand side of the differential equation (3.14). As a result, we obtain the differential equation of the disturbed motion of the closed, harmonically linearized dynamic system shown in Figure 3.5.

$$\left\{ A(p) - C(p)\left[q(A) + \frac{q_1(A)}{\omega} p \right] \right\} y(t) = C(p) \frac{a_0}{2}. \qquad (3.30)$$

The characteristic equation corresponding to the differential equation (3.30) is written as:

$$A(s) - C(s)\left[q(A) + \frac{q_1(A)}{\omega} s \right] = 0. \qquad (3.31)$$

In the characteristic equation of the harmonically linearized dynamic system (3.31), we perform the substitution $s = j \cdot \omega$:

$$A(j\omega) - C(j\omega)\left[q(A) + jq_1(A) \right] = 0. \qquad (3.32)$$

Let us transform relation (3.32) to the form:

$$\frac{C(j\omega)}{A(j\omega)} = \frac{1}{q(A) + jq_1(A)}. \qquad (3.33)$$

The left side of relation (3.33) contains only one parameter of the self-oscillations of the dynamic system – the frequency ω; the right side – only the unknown amplitude A. Furthermore, the left side of (3.33) represents the frequency transfer function of the linear part of the system, which can be expressed in the form (3.17), i.e., as the sum of real and imaginary parts.

The right side of relation (3.33), for $0 \le A \le \infty$, describes a curve in the complex plane.

$$\frac{1}{q(A) + jq_1(A)} = \frac{q(A)}{q^2(A) + q_1^2(A)} - j \frac{q_1(A)}{q^2(A) + q_1^2(A)}. \qquad (3.31)$$

In the complex plane (U, V), we construct the curves described by relations (3.17) and (3.34), with frequency values marked on curve (3.17) and amplitude values on curve (3.34). At the intersection point of the curves (if it exists), we determine the values of the amplitude and frequency of the self-oscillations of the dynamic system (Fig. 3.6). If no intersection point exists, then periodic regimes are absent in the system.

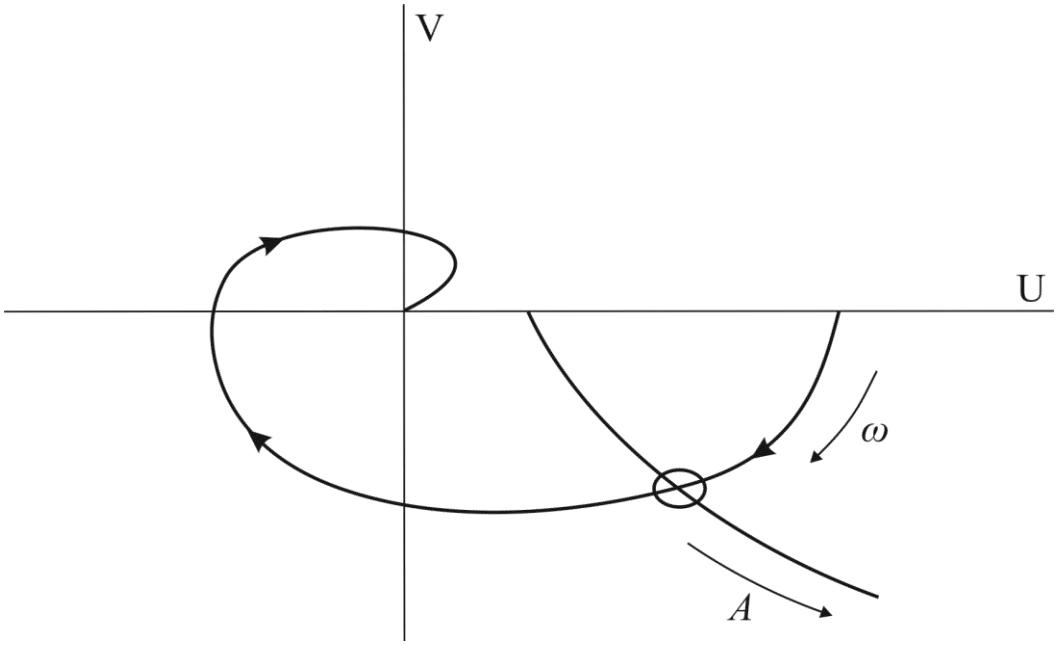

Fig. 3.6. **Determination of self-oscillation parameters of a nonlinear dynamic system**

3.3. Oscillations of a vehicle body with torsion bar suspension and friction dampers.

Let us consider the forced oscillations of a vehicle body with an independent torsion bar suspension and friction dampers. To solve this essentially nonlinear problem, we will apply the method of harmonic linearization of nonlinearities. Recent foreign literature sources have reported the use of friction dampers in military-purpose vehicles, which is explained by advancements in the development of friction materials characterized by increased wear resistance, high and stable values of the friction coefficient. The design of a friction damper is quite simple and allows for effective integration with a torsion bar suspension, making the issue of its use in military vehicles of undoubted practical interest.

The static characteristic of the i-th elastic element of the suspension, operating in parallel with the friction damper, is shown in Figure 3.7.

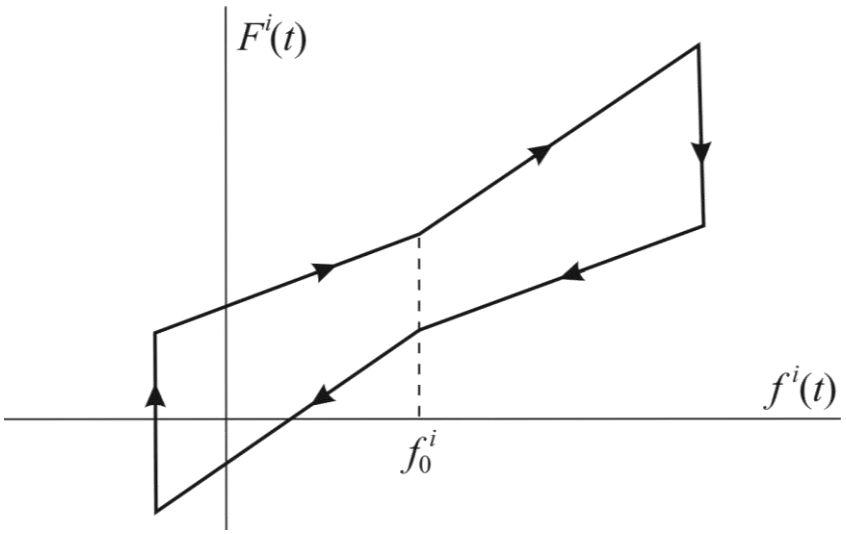

Fig. 3.7. **Static characteristic of the *i*-th suspension element**

The total deformation of the i-th suspension element can be represented as:

$$f^i(t) = f_0^i + f_\varphi^i(t) + f_\delta^i(t), \tag{3.32}$$

where f_0^i – static deformation of the i-th suspension element; $f_\varphi^i(t)$ – deformation of the *i*-th elastic element due to the angular displacement of the vehicle body

$$f_\varphi^i(t) = l_i \varphi(t), \tag{3.33}$$

where $\varphi(t)$ – generalized coordinate characterizing the angular displacement of the body; l_i – distance from the center of gravity of the body to the attachment point of the i-th torsion bar; $f_\delta^i(t)$ – deformation of the *i*-th elastic element caused by the wheels hitting road irregularities

$$f_\delta^i(t) = -\delta_m \sin(\omega t + \psi_i), \tag{3.34}$$

where δ_m – amplitude of the irregularities; ω – frequency of irregularity repetition; ψ_i – phase of vertical oscillations of the *i*-th wheel, equal to

$$\psi_i = 2\pi \frac{l_i}{a}, \tag{3.35}$$

where a – wavelength of the irregularities.

Taking into account formulas (3.33) and (3.34), the dynamic deformation of the *i*-th elastic suspension element is written as:

$$\Delta f_i(t) = f_{\varphi}^{i}(t) + f_{\delta}^{i}(t) = l_i\varphi(t) - \delta_m \sin(\omega t + \psi_i). \qquad (3.36)$$

The dynamic force acting on the vehicle body from the i-th elastic element has the form:

$$\Delta F^{i}(t) = F_{\varphi}^{i}(t) + F_{\delta}^{i}(t). \qquad (3.37)$$

In accordance with the harmonic linearization method, the nonlinear function $F_{\varphi}^{i}(t)$ can be represented as:

$$F_{\varphi}^{i}(t) = -\left[q^{i}(\varphi_m) + \frac{q_1^{i}(\varphi_m)}{\omega} p \right] l_i\varphi(t), \qquad (3.38)$$

where φ_m – amplitude of the forced oscillations of the vehicle body.

The "minus" sign in equation (3.38) indicates that the force from the elastic suspension element has a sign opposite to that of the deformation.

In relation (3.38), the term $q^{i}(\varphi_m)$ and $q_1{}^{i}(\varphi_m)$ denotes the harmonic linearization coefficients of the nonlinear function $F_{\varphi}^{i}(t)$, for the calculation of which we will construct Figure 3.8.

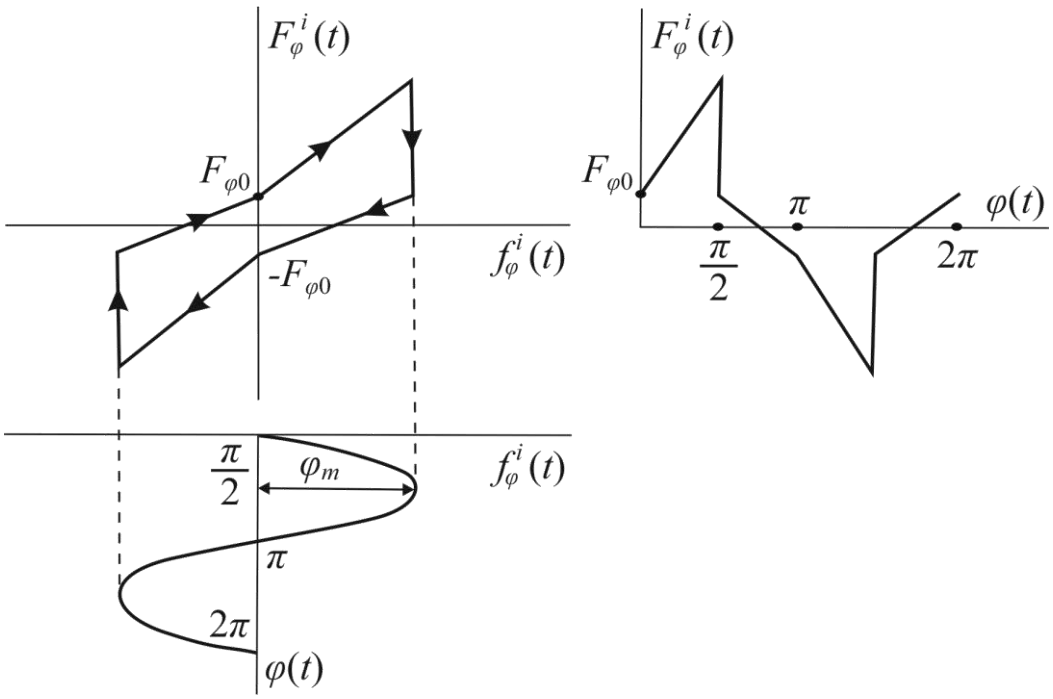

Fig. 3.8. **For the calculation of harmonic linearization coefficients**

In accordance with formulas (3.26) and (3.27), we calculate the harmonic linearization coefficients $q^i(\varphi_m)$ and $q_1{}^i(\varphi_m)$:

$$q_{\varphi}^{i}(\varphi_m)=\frac{2}{\pi\varphi_m l_i}\int_0^{\pi/2}\left[F_{\varphi 0}+\left(c_t+c\varphi\right)\varphi_m l_i\sin\theta\right]\sin\theta d\theta+$$
$$+\frac{2}{\pi\varphi_m l_i}\int_{\pi/2}^{\pi}\left[-F_{\varphi 0}+\left(c_t-c_{\varphi}\right)\varphi_m l_i\sin\theta\right]\sin\theta d\theta=c_t; \tag{3.39}$$

$$q_{1\varphi}^{i}(\varphi_m)=\frac{2}{\pi\varphi_m l_i}\int_0^{\pi/2}\left[F_{\varphi 0}+\left(c_t+c_{\varphi}\right)\varphi_m l_i\sin\theta\right]\cos\theta d\theta+$$
$$+\frac{2}{\pi\varphi_m l_i}\int_{\pi/2}^{\pi}\left[-F_{\varphi 0}+\left(c_t-c_{\varphi}\right)\varphi_m l_i\sin\theta\right]\cos\theta d\theta=\frac{4F_{\varphi 0}}{\pi\varphi_m l_i}+\frac{2c_{\varphi}}{\pi}, \tag{3.40}$$

where $F_{\varphi 0}$ – friction force of the friction damper at zero dynamic deformation of the elastic element; c_t – linear stiffness coefficient of the torsion shaft; c_{φ} – linear stiffness coefficient of the friction damper.

Taking into account relations (3.39) and (3.40), equation (3.38) takes the form:

$$F_{\varphi}^{i}(t)=-c_t l_i\varphi(t)-\left(\frac{4F_{\varphi 0}}{\pi\varphi_m\omega}+\frac{2c_{\varphi}l_i}{\omega\pi}\right)\dot{\varphi}(t). \tag{3.41}$$

Similarly, the nonlinear function $F_{\delta}{}^i$ can be represented as:

$$F_{\delta}^{i}=c_t\delta_m\sin(\omega t+\psi_i)+\left(\frac{4F_{\varphi 0}}{\pi\delta_m}+\frac{2c_{\varphi}}{\pi}\right)\delta_m\cos(\omega t+\psi_i).$$

The total moment of forces acting on the vehicle body from the suspension is equal to:

$$M(t)=2\sum_{i=1}^{n}\Delta F^{i}(t)l_i=-2c_t\varphi(t)\sum_{i=1}^{n}l_i^2-\left(\frac{8F_{\varphi 0}}{\pi\varphi_m\omega}\sum_{i=1}^{n}l_i+\frac{4c_{\varphi}}{\omega\pi}\sum_{i=1}^{n}l_i^2\right)\dot{\varphi}(t)+$$
$$+2c_t\delta_m\sum_{i=1}^{n}l_i\sin(\omega t+\psi_i)+\left(\frac{8F_{\varphi 0}}{\pi}+\frac{4c_{\varphi}\delta_m}{\pi}\right)\sum_{i=1}^{n}l_i\cos(\omega t+\psi_i). \tag{3.42}$$

For a symmetric torsion bar suspension, the following relations hold:

$$\sum_{i=1}^{n} l_i \sin(\omega t + \psi_i) = \cos\omega t \sum_{i=1}^{n} l_i \sin 2\pi \frac{l_i}{a};$$

$$\sum_{i=1}^{n} l_i \cos(\omega t + \psi_i) = -\sin\omega t \sum_{i=1}^{n} l_i \sin 2\pi \frac{l_i}{a};$$

$$\sum_{i=1}^{n} l_i = 0.$$

Due to these relations, we write equation (3.42) in the form:

$$M(t) = -2c_t \varphi(t) \sum_{i=1}^{n} l_i^2 - \frac{4c_\varphi}{\omega\pi} \sum_{i=1}^{n} l_i^2 \dot{\varphi}(t) +$$

$$+2c_t \delta_m \sum_{i=1}^{n} l_i \sin 2\pi \frac{l_i}{a} \cos\omega t - \qquad (3.43)$$

$$-\left(\frac{8F_{\varphi 0}}{\pi} + \frac{4c_\varphi \delta_m}{\pi} \right) \sum_{i=1}^{n} l_i \sin 2\pi \frac{l_i}{a} \sin\omega t.$$

Then the differential equation for the forced pitch oscillations of the vehicle body, taking into account equation (3.43), is written as:

$$I_y \ddot{\varphi}(t) + \left(\frac{4c_\varphi}{\omega\pi} \sum_{i=1}^{n} l_i^2 \right) \dot{\varphi}(t) + \left(2c_t \sum_{i=1}^{n} l_i^2 \right) \varphi(t) =$$

$$= 2c_t \delta_m \sum_{i=1}^{n} l_i \sin 2\pi \frac{l_i}{a} \cos\omega t - \qquad (3.44)$$

$$-\frac{\left(8F_{\varphi 0} + 4c_\varphi \delta_m\right)}{\pi} \sum_{i=1}^{n} l_i \sin 2\pi \frac{l_i}{a} \cdot \sin\omega t,$$

where I_y – is the moment of inertia of the vehicle body about its own transverse axis.

Let us introduce the notation:

$$k_\varphi^2 = \frac{2c_t \sum_{i=1}^{n} l_i^2}{I_y}; \; \text{З} = \frac{2c_\varphi \sum_{i=1}^{n} l_i^2}{I_y \omega \pi};$$

$$A = \frac{2c_t \delta_m \sum_{i=1}^{n} l_i \sin 2\pi \frac{l_i}{a}}{I_y};$$

$$B = -\frac{\left(8F_{\varphi 0} + 4c_\varphi \delta_m\right) \sum_{i=1}^{n} l_i \sin 2\pi \frac{l_i}{a}}{I_y \pi}.$$

Then the differential equation (3.44) takes the form:

$$\ddot{\varphi}(t) + 2\text{З}\dot{\varphi}(t) + k_\varphi^2 \varphi(t) = A\cos\omega t + B\sin\omega t. \qquad (3.45)$$

It is known that the amplitude of the forced component of the solution to the differential equation (3.45) is determined by the relation:

$$\varphi_m = \frac{\sqrt{A^2 + B^2}}{\sqrt{\left(k_\varphi^2 - \omega^2\right)^2 + 4\text{З}^2\omega^2}}. \qquad (3.46)$$

The frequency of irregularity repetition ω is related to the vehicle speed by the dependence:

$$\omega = \frac{2\pi}{a} v. \qquad (3.47)$$

Relations (3.46) and (3.47) allow us to obtain the dependencies of the amplitude of the forced oscillations of the body on its speed at different values of the parameter c_φ.

Let the parameters of the vehicle suspension system with torsion bar suspension and friction dampers have the following values: I_y = 1,3·10^5 N·m·s^2; l_1 = l_5 = 1,8 m; l_2 = l_4 = 0,85 m; l_3 = 0;

$c_t = 4{,}35 \cdot 10^5$ N·m^{-1}; $F_{\varphi 0} = 10^3$ N. The wavelength of the irregularities and their amplitude are: $a = 4$ m; $\delta_m = 0{,}75 \cdot 10^{-1}$ m.

Figure 3.9 shows the dependencies of the amplitude of the forced pitch oscillations of the vehicle body on its speed at the following values of the linear stiffness of the friction damper:$c_{\varphi 1} = 9{,}25 \cdot 10^5$ N·m^{-1}; $c_{\varphi 2} = 7 \cdot 10^5$ N·m^{-1}; $c_{\varphi 3} = 5 \cdot 10^5$ N·m^{-1}; $c_{\varphi 4} = 3 \cdot 10^5$ N·m^{-1}.

Analysis of the amplitude characteristics shown in Figure 3.9 indicates sufficiently high effectiveness of the vehicle torsion bar suspension with friction dampers.

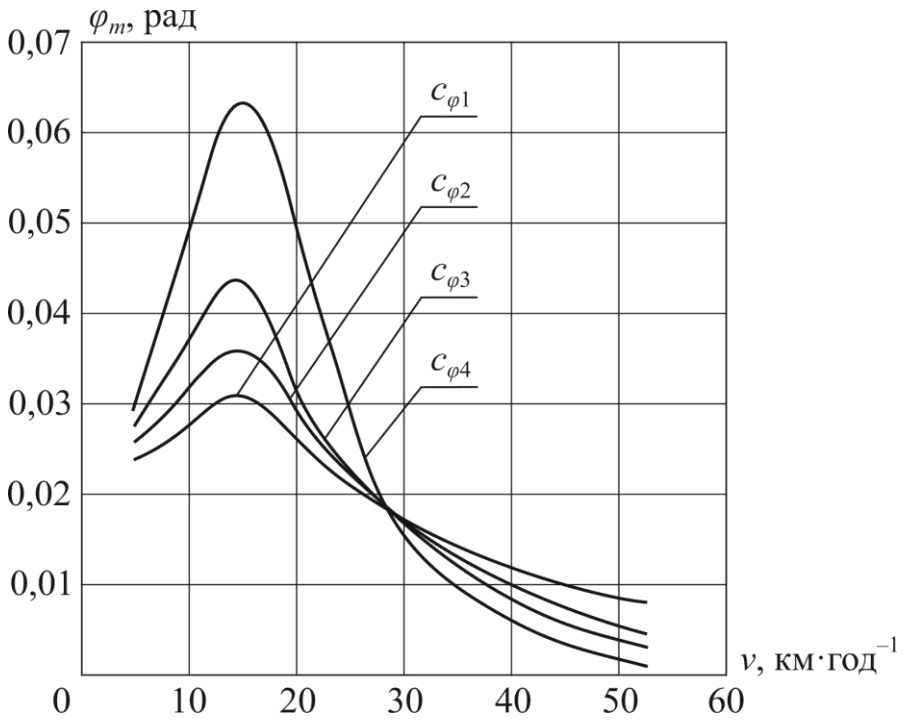

Fig. 3.9. **Amplitude characteristics of the vehicle suspension system with torsion bar and friction dampers**

3.4. Oscillations of the coolant temperature in a vehicle engine.

On some powerful truck engines, fans with automatic shut-off are used. The use of such fans improves the vehicle's traction properties and increases its average speed, reduces operational fuel consumption, ensures less noisy engine operation, accelerates its warm-up after starting, contributes to reliable maintenance of the optimal coolant temperature regime, and extends the service life of fan belts.

Figure 3.10 shows the schematic diagram of the automatic control system for the coolant temperature of an internal combustion engine. The deviation of the coolant temperature $\Delta T(t)$ from the nominal value T_0 is measured by a thermistor connected to a bridge circuit (1). The voltage from the measuring diagonal of the bridge is supplied to the control winding of a two-position relay (2). The relay contacts (2) control the operation of the DC motor (3).

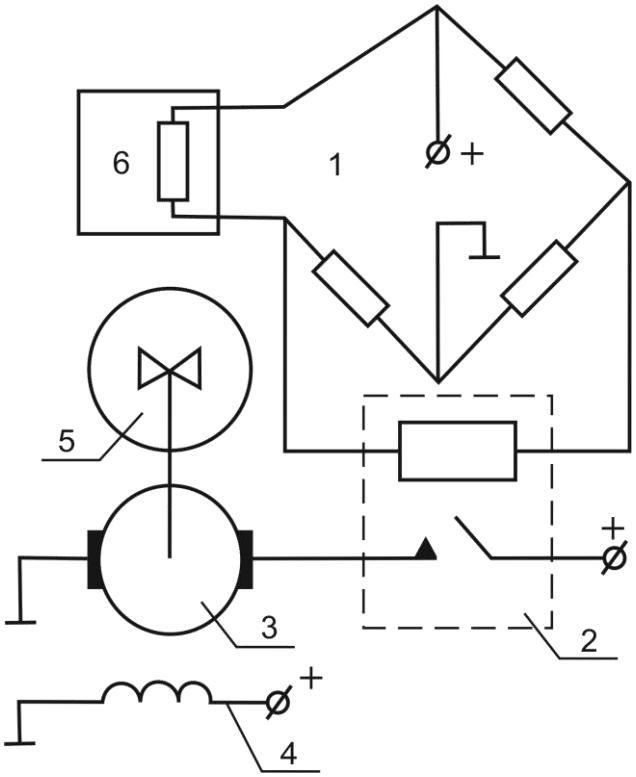

Fig. 3.10. **Schematic diagram of the automatic control system**

The static characteristic of relay 2 with the bridge circuit 1 is shown in Figure 3.11.

When the coolant reaches the temperature $T_0 + \Delta T^*$, the current in the winding of relay 2 reaches the activation value, and the normally open relay contacts close.

At this point, an electrical signal from the onboard electrical network is supplied to the armature winding of the DC motor 3, which has an excitation winding 4. The armature of the motor, mechanically connected to the fan 5, begins to rotate, and the radiator 6 is blown by air, causing a decrease in the current temperature $T(t)$ of the coolant. When the coolant temperature drops to the value $T_0 - \Delta T^*$, the current in the relay winding decreases, the relay contacts open, and the armature of

the motor 3 with the fan 5 stops. Consequently, the airflow blowing the radiator 6 ceases, and the coolant temperature begins to rise.

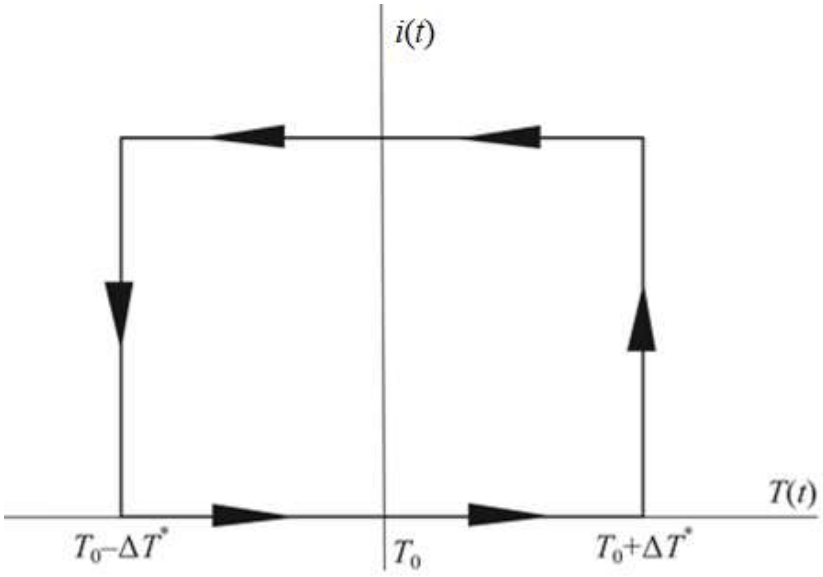

Fig. 3.11. **Static characteristic of the relay with a bridge circuit**

The nonlinear characteristic shown in Figure 3.11 is described by a non-analytical relation:

$$i(t)=\begin{cases} 0 \ \text{ at } \begin{cases} T(t)<T_0-\Delta T^*; \\ T_0-\Delta T^* \le T(t) \le T_0+\Delta T^*;\ \dot{T}(t)>0; \end{cases} \\ i^* \ \text{ at } \begin{cases} T(t)>T_0+\Delta T^*; \\ T_0-\Delta T^* \le T(t) \le T_0+\Delta T^*;\ \dot{T}(t)<0. \end{cases} \end{cases} \tag{3.48}$$

Let us introduce the relative generalized coordinate:

$$\Delta T(t)=T(t)-T_0$$

and assume that it varies according to the equation:

$$\Delta T(t)=A\sin\omega t=A\sin\varphi, \tag{3.49}$$

and the harmonically linearized equation of the nonlinear part of the system under consideration will be written as:

$$i(t)=\frac{a_0}{2}+\left[q(A)+\frac{q_1(A)}{\omega}p\right]\Delta T(t). \tag{3.50}$$

To calculate the harmonic linearization coefficients, consider Figure 3.12.

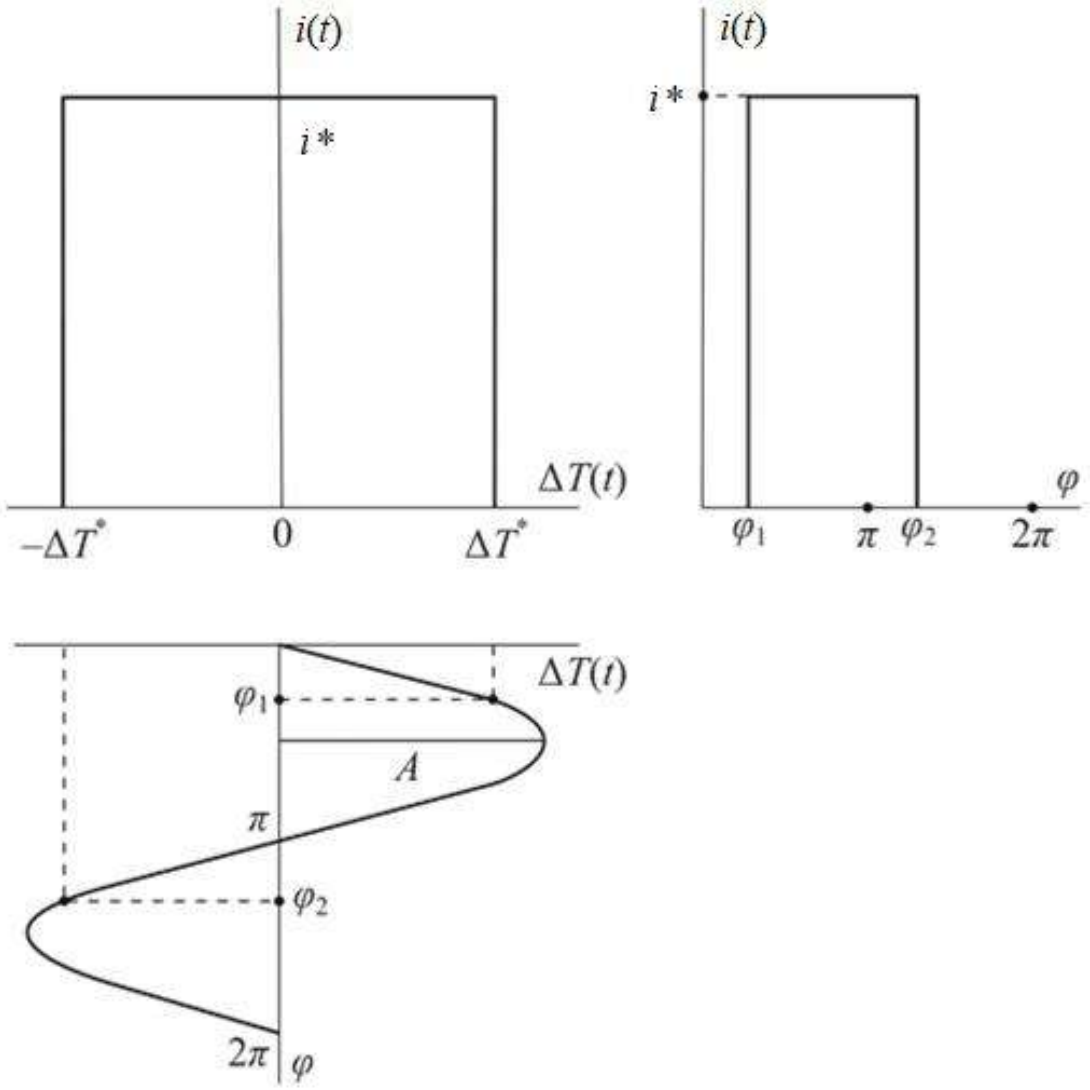

Fig. 3.12. **For the calculation of harmonic linearization coefficients**

The coefficient a_0 is determined according to equation (3.23), by setting $k = 0$ in it:

$$a_0 = \frac{1}{\pi}\int_0^{2\pi} F[A\sin\varphi, A\omega\cos\varphi]d\varphi. \qquad (3.51)$$

According to Fig. 3.12, we write:

$$a_0 = \frac{1}{\pi}\int_{\varphi_1}^{\varphi_2} i_{\ddot{y}}^* d\varphi = \frac{i_{\ddot{y}}^*}{\pi}(\varphi_2 - \varphi_1), \qquad (3.52)$$

where in:

$$\varphi_1 = \arcsin\frac{\Delta T^*}{A}; \tag{3.53}$$

$$\varphi_2 = \pi + \arcsin\frac{\Delta T^*}{A}. \tag{3.54}$$

Substituting equations (3.53) and (3.54) into equation (3.52), we can write:

$$a_0 = i_я^*. \tag{3.55}$$

The coefficient $q(A)$ is calculated using equation (3.26):

$$\begin{gathered} q(A) = \frac{1}{\pi A}\int_{\varphi_1}^{\varphi_2} i^* \sin\varphi d\varphi = \\ = \frac{i^*}{\pi A}(\cos\varphi_1 - \cos\varphi_2) = \frac{2i^*}{\pi A}\sqrt{1-\left(\frac{\Delta T^*}{A}\right)^2}. \end{gathered} \tag{3.56}$$

The coefficient $q_1(A)$ is calculated using equation (3.27):

$$\begin{gathered} q_1(A) = \frac{1}{\pi A}\int_{\varphi_1}^{\varphi_2} i^* \cos\varphi d\varphi = \\ = \frac{i^*}{\pi A}(\sin\varphi_2 - \sin\varphi_1) = -\frac{2i^*\Delta T^*}{\pi A^2}. \end{gathered} \tag{3.57}$$

Substitute equations (3.52), (3.56), and (3.57) into equation (3.50). As a result, we obtain the harmonically linearized equation of the nonlinear part of the system under consideration:

$$i(t) = \frac{i^*}{2} + \frac{2i^*}{\pi A}\left[\sqrt{1-\left(\frac{\Delta T^*}{A}\right)^2} - \frac{\Delta T^*}{A\omega}p\right]\Delta T(t). \tag{3.58}$$

The equation describing the disturbed motion of the linear part of the system has the form:

$$(T_d\,p+1)\Delta T(t) = -k_d i(t) + k_q Q(t), \qquad (3.59)$$

where the gain coefficients k_d and k_q, and the time constant T_d characterize the heating and cooling processes of the coolant, and $Q(t)$ denotes the thermal energy that heats the coolant from the operating engine.

If $i(t) = 0$, then the differential equation

$$(T_d\,p+1)\Delta T(t) = k_q Q(t)$$

describes the process of heating the coolant by the operating diesel engine. When $i(t) = i^*$, the right-hand side of the differential equation (3.59) becomes negative, and this equation describes the cooling process of the fluid.

Let us substitute relation (3.58) into the right-hand side of equation (3.59):

$$\left[T_d\,p+1+k_d\,\frac{2i^*}{\pi A}\left(\sqrt{1-\left(\frac{\Delta T^*}{A}\right)^2}-\frac{\Delta T^*}{A\omega}\,p\right)\right]\Delta T(t) = k_d\,\frac{i^*}{2}+k_q Q(t). \qquad (3.60)$$

The following characteristic equation corresponds to equation (3.60):

$$T_d\,s+1+k_d\,\frac{2i^*}{\pi A}\left(\sqrt{1-\left(\frac{\Delta T^*}{A}\right)^2}-\frac{\Delta T^*}{A\omega}\,s\right)=0. \qquad (3.61)$$

In the characteristic equation (3.61), we perform the substitution $s = j \cdot \omega$

$$j\omega T_d+1+k_d\,\frac{2i^*}{\pi A}\left(\sqrt{1-\left(\frac{\Delta T^*}{A}\right)^2}-j\,\frac{\Delta T^*}{A}\right)=0. \qquad (3.62)$$

Let us represent relation (3.62) in the form (3.33):

$$-\frac{1}{1+j\omega T_d}=\frac{\pi A}{2k_d i^*\left(\sqrt{1-\left(\frac{\Delta T^*}{A}\right)^2}-j\frac{\Delta T^*}{A}\right)}. \qquad (3.63)$$

Consider the left side of (3.63), which we multiply and divide by the complex quantity $1 - j\omega T_d$, which is the conjugate of the denominator of the left side of (3.63).

$$-\frac{1}{1+j\omega T_d}\cdot\frac{1-j\omega T_d}{1-j\omega T_d}=-\frac{1}{1+\omega^2 T_d^2}+j\frac{\omega T_d}{1+\omega^2 T_d^2}. \qquad (3.64)$$

Let us also express the right side of (3.63) as the sum of real and imaginary parts:

$$\frac{\pi A}{2k_d i^*\left(\sqrt{1-\left(\frac{\Delta T^*}{A}\right)^2}-j\frac{\Delta T^*}{A}\right)}\cdot\frac{\sqrt{1-\left(\frac{\Delta T^*}{A}\right)^2}+j\frac{\Delta T^*}{A}}{\sqrt{1-\left(\frac{\Delta T^*}{A}\right)^2}+j\frac{\Delta T^*}{A}}= \qquad (3.65)$$

$$=\frac{\pi}{2k_d i^*}\left(\sqrt{A^2-\left(\Delta T^*\right)^2}+j\Delta T^*\right).$$

The curve described by relation (3.64), as ω varies from zero to infinity in the complex plane (*U*, *V*), is a semicircle of unit diameter. The curve described by relation (3.65), as *A* varies from ΔT^* to infinity, is a straight line parallel to the real axis (see Fig. 3.13).

These curves may not have intersection points when:

$$\frac{\pi\Delta T^*}{2k_d i^*}>0.5,$$

which indicates the absence of periodic motions in the system.

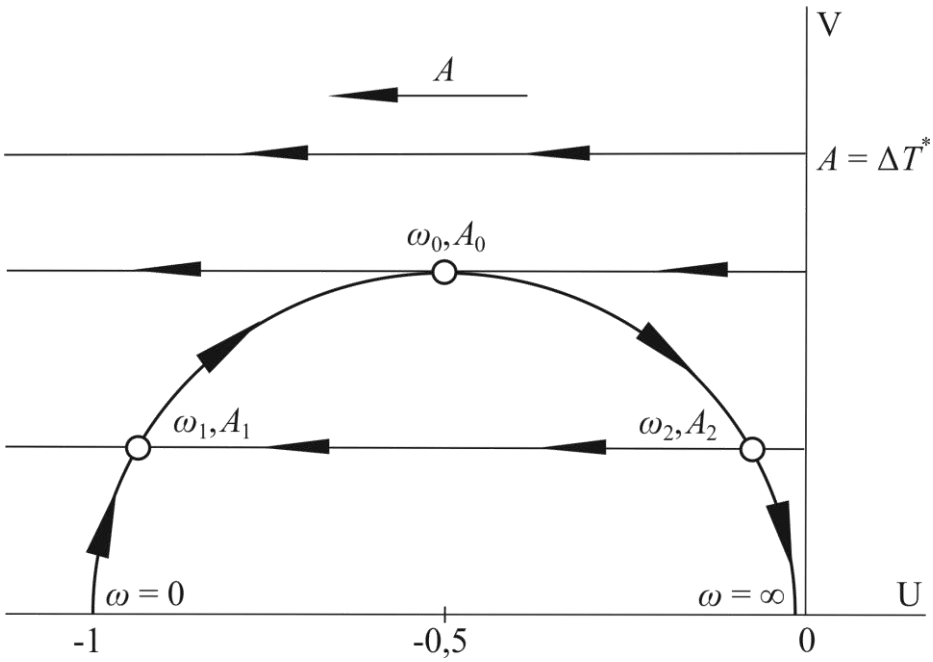

Fig. 3.13. **For the calculation of self-oscillation amplitudes and frequencies**

If the curves have one common point under the condition:

$$\frac{\pi\Delta T^*}{2k_d i^*} = 0.5,$$

then self-oscillations exist with frequency ω_0 and amplitude A_0. If two common points exist under the condition of the inequality:

$$\frac{\pi\Delta T^*}{2k_d i^*} < 0.5,$$

the system has two periodic regimes with frequencies ω_1 and ω_2 and amplitudes A_1 and A_2. However, only one of these regimes is stable. Typically, this is the regime with the smaller amplitude and higher frequency, i.e., ω_2, A_2.

3.5. Oscillations of non-stationary dynamic systems, or parametric oscillations.

In the problems considered above regarding oscillations of linear dynamic systems, the forces acting on the system could be classified into one of three categories:

- Positional forces (or restoring forces), which depend only on the generalized coordinate $q(t)$, for example, the force of a compressed spring.

$$Q(t) = -cq(t);$$

- Dissipative forces, determined by the generalized velocity $\dot{q}(t)$, for example, the force acting on the sprung part of the vehicle body from the shock absorber.

$$Q(t) = -\mu\dot{q}(t);$$

- Forced forces, which are specified functions of time, for example, those determined by the road microprofile.

$$Q(t) = H\sin\omega t.$$

However, there exist forces of a more complex nature, in particular, non-stationary positional forces, which depend both on the generalized coordinate and on time in an explicit form. An example of such a dynamic system is one whose disturbed motion is described by the Mathieu equation:

$$\ddot{q}(t) + 2n\dot{q}(t) + k^2(1-\mu\cos\omega t)q(t) = 0. \qquad (3.66)$$

When $\mu = 0$ the Mathieu equation (3.66) reduces to equation (1.25).

Let us obtain the solution to equation (3.66) by expressing it in the normal Cauchy form:

$$X = \begin{bmatrix} x_1(t) \\ x_2(t) \end{bmatrix} = \begin{bmatrix} q(t) \\ \dot{q}(t) \end{bmatrix};$$

$$\begin{aligned} \dot{x}_1(t) &= x_2(t); \\ \dot{x}_2(t) &= -k^2(1-\mu\cos\omega t)x_1(t) - 2nx_2(t). \end{aligned} \qquad (3.67)$$

In the system (3.67), let us set: $k = 5$; $\omega = 3$ s^{-1}; $\mu = 0{,}5$; $n = 0{,}5$. Let us use the MathLAB software package and integrate the system of differential equations (3.67) using the Runge-Kutta method. The oscillatory processes in the system are shown in Figure 3.14.

Analysis of Figure 3.14 leads to the conclusion that at the beginning of the oscillatory process ($0 < t < 1.5$ s), the oscillatory motion with frequency k dominates, while for $t > 1.5$ s, the motion with frequency ω dominates.

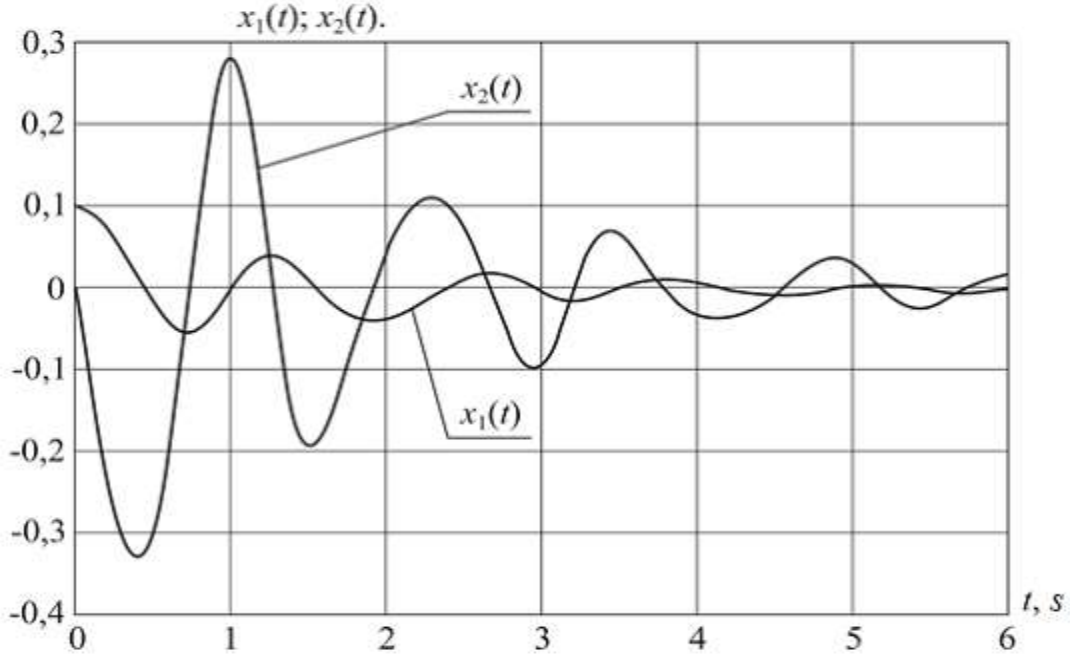

Fig. 3.14. **Solution of the Mathieu equation for** $\omega = 3\ \text{s}^{-1}$

Figures 3.15 and 3.16 show the oscillatory processes in the system (3.67) for $\omega = 4\ \text{s}^{-1}$ and $\omega = 5\ \text{s}^{-1}$, respectively.

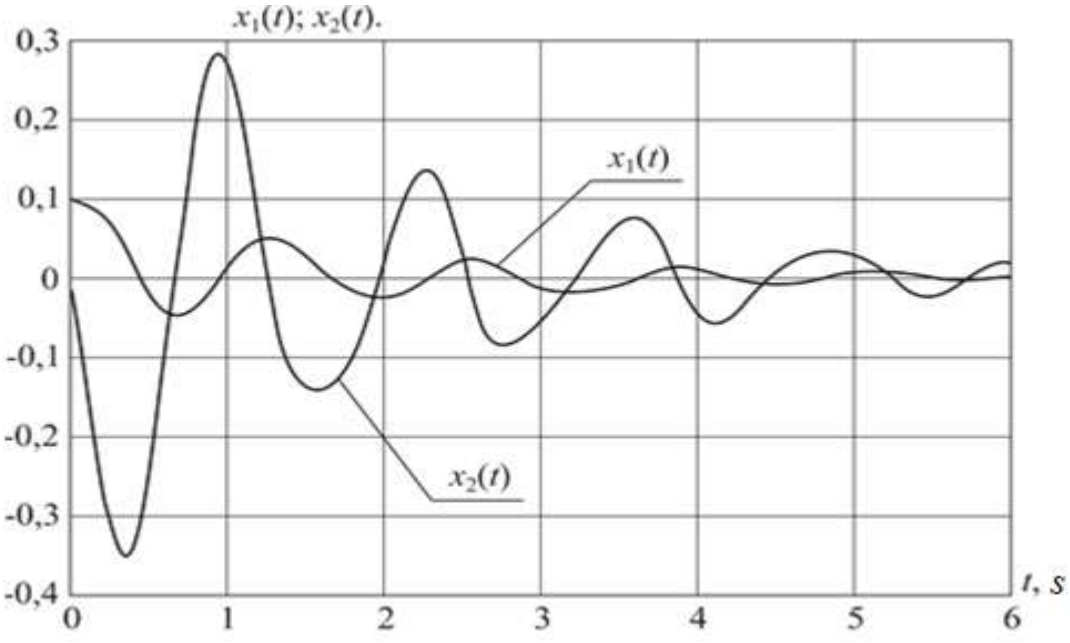

Fig. 3.15. **Solution of the Mathieu equation for** $\omega = 4\,s^{-1}$

Comparison of these figures with Fig. 3.14 proves that as the frequency **ω** approaches the frequency *k*, the amplitude of oscillations in the system (3.67) increases, reaching maximum values when ω = *k*.

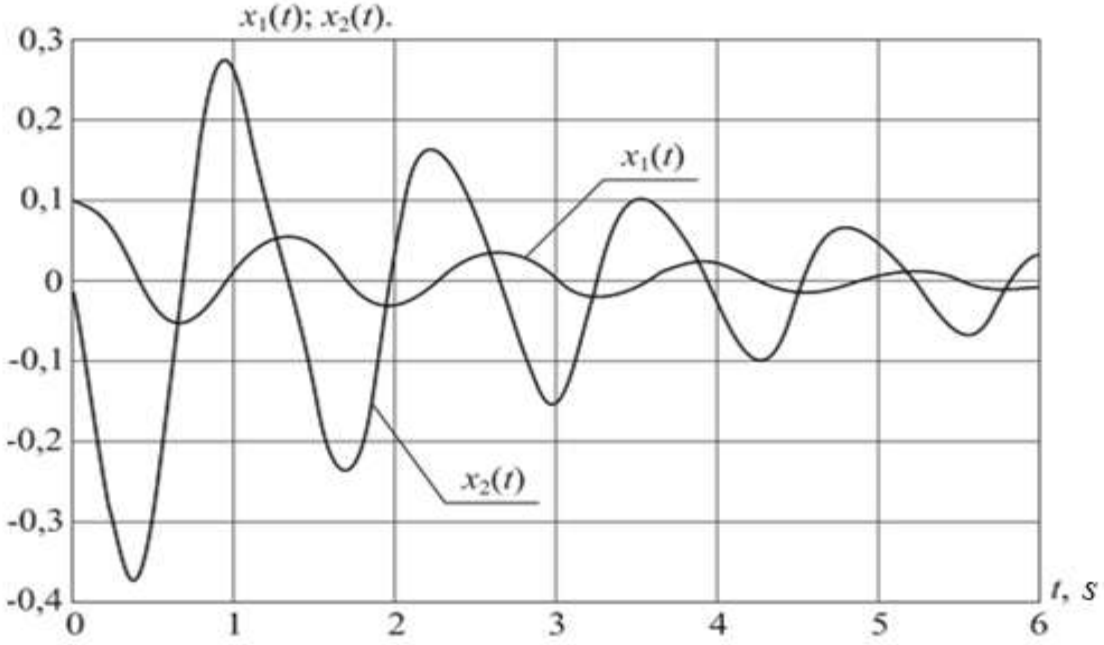

Fig. 3.16. **Solution of the Mathieu equation for** $\omega = 5\,s^{-1}$

A further increase in the frequency ω leads to a decrease in the amplitudes of the oscillatory processes in the system (3.67), as evidenced by the analysis of Figure 3.17 and Figure 3.18.

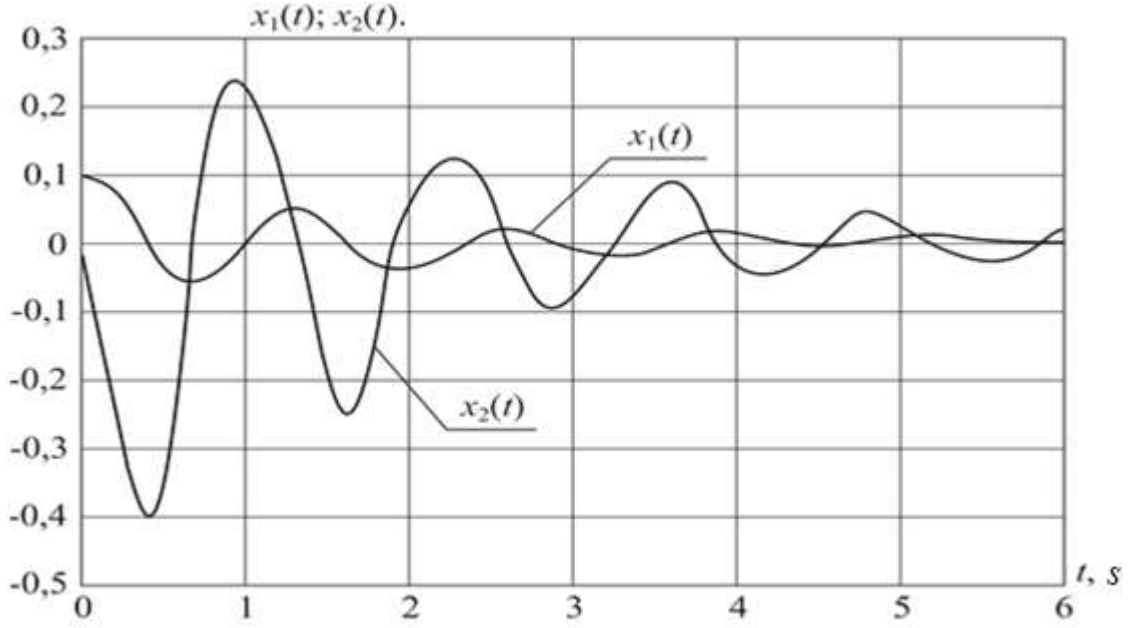

Fig. 3.17. **Solution of the Mathieu equation for** $\omega = 6c^{-1}$

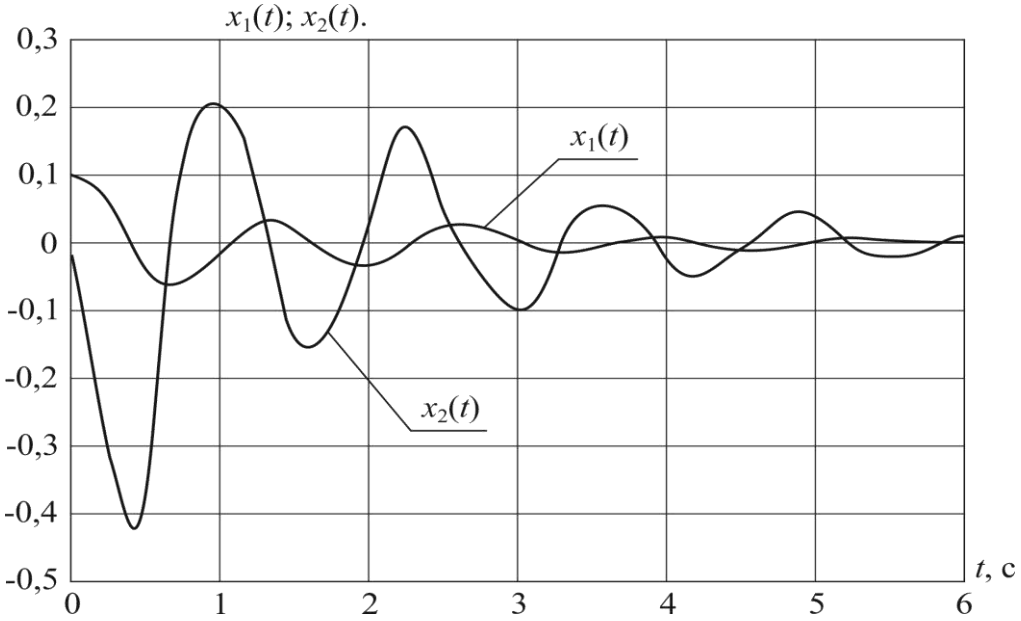

Fig. 3.18. **Solution of the Mathieu equation for** $\omega = 7\,s^{-1}$

Control questions for the chapter 3.

1. Define a nonlinear dynamic system.
2. Define analytical and non-analytical nonlinearities.
3. What do we call the system of the first approximation?
4. Define a dynamic system with nonlinear friction and write the Rayleigh differential equation.
5. Explain the oscillatory processes in a dynamic system described by the Rayleigh equation.
6. Explain the oscillatory processes in a dynamic system described by the Van der Pol equation.
7. Briefly explain the essence of the harmonic linearization of non-analytical nonlinearities.
8. Explain the oscillatory processes in a vehicle suspension system when friction dampers are used.
9. Explain the oscillatory processes in the automatic control system for the coolant temperature of a vehicle engine.
10. Explain the oscillatory processes in a system with periodic coefficients, described by the Mathieu equation.

Chapter 4

TORSIONAL VIBRATIONS OF AUTOMOTIVE ENGINE AND TRANSMISSION SHAFTS.

4.1. Equations of free torsional vibrations of shafts.

Let us consider the torsional vibrations of a multi-mass system, which is a generally accepted model for calculating torsional vibrations of internal combustion engine crankshafts and mechanical transmission shafts. The schematic representation of a crankshaft as a multi-disc system is entirely satisfactory, provided the equivalent moments of inertia of the discs and the stiffnesses of individual shaft sections are determined with sufficient care (Fig. 4.1).

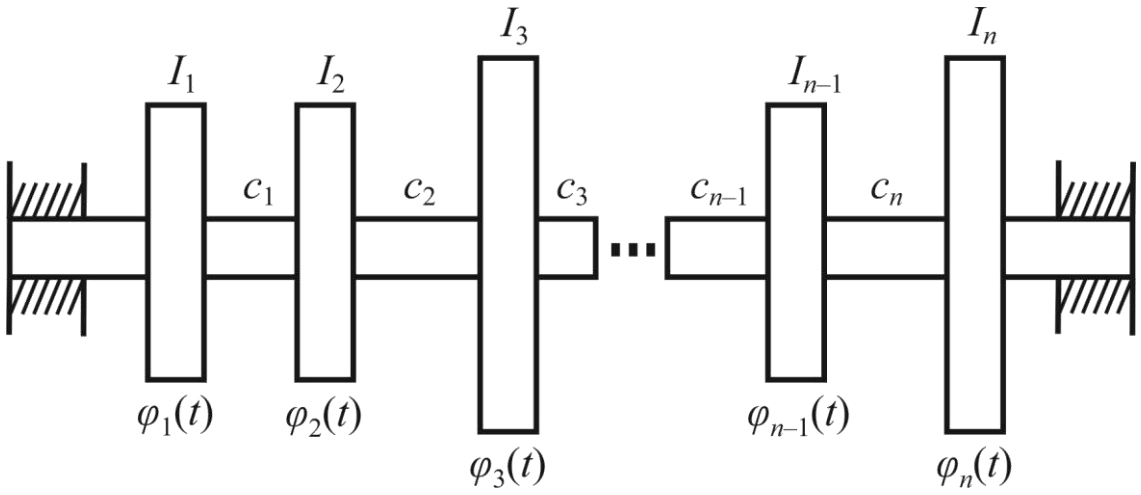

Fig. 4.1. **For the calculation of torsional vibrations of automotive internal combustion engine and transmission shafts**

The state of the system shown in Figure 4.1 is determined by the angles of rotation of each disc, meaning the system has n degrees of freedom. Let us denote: I_1, I_2, …, I_n – moments of inertia of the discs about the shaft axis; c_1, c_2, …, c_n – stiffness coefficients of the inter-disc sections of the shaft; $\varphi_1(t)$, $\varphi_2(t)$, …, $\varphi_n(t)$ – angles of rotation of the discs relative to the shaft axis. The torsional moments acting on the shaft sections depend on the relative twist of two connected discs:

- on the first section

$$c_1[\varphi_2(t) - \varphi_1(t)];$$

- on the second section

$$c_2[\varphi_3(t)-\varphi_2(t)];$$

- …….
- on the last section

$$c_{n-1}[\varphi_n(t)-\varphi_{n-1}(t)].$$

Accordingly, the equations of motion of the system are written as:

$$\begin{aligned}
&I_1\ddot{\varphi}_1(t)-c_1[\varphi_2(t)-\varphi_1(t)]=0;\\
&I_2\ddot{\varphi}_2(t)-c_1[\varphi_1(t)-\varphi_2(t)]-c_2[\varphi_3(t)-\varphi_2(t)]=0;\\
&I_3\ddot{\varphi}_3(t)-c_2[\varphi_2(t)-\varphi_3(t)]-c_3[\varphi_4(t)-\varphi_3(t)]=0;\\
&\vdots\\
&I_{n-1}\ddot{\varphi}_{n-1}(t)-c_{n-2}[\varphi_{n-2}(t)-\varphi_{n-1}(t)]-c_{n-1}[\varphi_n(t)-\varphi_{n-1}(t)]=0;\\
&I_n\ddot{\varphi}_n(t)-c_{n-1}[\varphi_{n-1}(t)-\varphi_n(t)]=0.
\end{aligned} \tag{4.1}$$

The system of differential equations (4.1) represents the mathematical model of free vibrations of a shaft with *n* discs.

Let us sum the left-hand sides of the differential equations (4.1). As a result, we obtain the relation:

$$I_1\ddot{\varphi}_1(t)+I_2\ddot{\varphi}_2(t)+\ldots+I_n\ddot{\varphi}_n(t)=0. \tag{4.2}$$

Relation (4.2) indicates that the total angular momentum of the entire system of discs about the shaft axis remains constant during free torsional vibrations. This moment can be assumed to be zero, and only the vibrations caused by shaft twisting can be considered:

$$\begin{aligned}
&\varphi_1(t)=A_1\sin(kt+\beta);\\
&\varphi_2(t)=A_2\sin(kt+\beta);\\
&\vdots\\
&\varphi_n(t)=A_n\sin(kt+\beta),
\end{aligned} \tag{4.3}$$

where $A_1, A_2, \ldots, A_n$ – amplitudes of torsional vibrations of the discs.

Let us substitute equation (4.3) into the differential equations (4.1) and write them in operator form

$$
\begin{aligned}
&(c_1 - k^2 I_1)A_1 - c_1 A_2 = 0;\\
&-c_1 A_1 + (c_1 + c_2 - k^2 I_2)A_2 - c_2 A_3 = 0;\\
&-c_2 A_2 + (c_2 + c_3 - k^2 I_3)A_3 - c_3 A_4 = 0;\\
&\vdots\\
&-c_{n-1} A_{n-1} + (c_{n-1} - k^2 I_n)A_n = 0.
\end{aligned}
\qquad (4.4)
$$

We will consider relation (4.4) as a system of algebraic equations with $n + 1$ unknowns (n unknown amplitudes and the frequency k). Therefore, it is impossible to determine all unknowns from this system. However, the system (4.4) allows us to compute the frequency k and find the relationships between the amplitudes $A_1, A_2, \ldots, A_n$. The system (4.4) has a trivial solution $A_1 = A_2 = \ldots = A_n = 0$ and admits a non-trivial solution only if the determinant of the system is zero:

$$
\Delta(k^2) = \begin{vmatrix}
(c_1 - k^2 I_1) & -c_1 & 0 & \ldots & 0 & 0\\
-c_1 & (c_1 + c_2 - k^2 I_2) & -c_2 & \ldots & 0 & 0\\
0 & -c_2 & (c_2 + c_3 - k^2 I_3) & \ldots & 0 & 0\\
\ldots & \ldots & \ldots & \ldots & \ldots & \ldots\\
0 & 0 & 0 & \ldots & -c_{n-1} & (c_{n-1} - k^2 I_n)
\end{vmatrix} = 0. \qquad (4.5)
$$

4.2. Frequency equation of free torsional vibrations of shafts.

Expanding the determinant (4.5) and setting it equal to zero, we obtain an equation of the n-th degree with respect to k^2, which is called the frequency equation.

Let us write the frequency equation for different numbers of discs. For $n = 1$, $c_1 = 0$ and in this case $k^2 = 0$. This case corresponds to uniform shaft rotation without deformation, i.e., without torsional vibrations.

For $n = 2$, $c_2 = 0$ the frequency equation takes the form

$$
k^2 - \frac{I_1 + I_2}{I_1 I_2} c_1 = 0. \qquad (4.6)
$$

For $n = 3$, $c_3 = 0$ the frequency equation is written as

$$
k^4 - \left(\frac{I_1 + I_2}{I_1 I_2} c_1 + \frac{I_2 + I_3}{I_2 I_3} c_2 \right) k^2 + \frac{I_1 + I_2 + I_3}{I_1 I_2 I_3} c_1 c_2 = 0. \qquad (4.7)
$$

For $n = 4$, $c_4 = 0$ we have

$$k^6 - \left(\frac{I_1 + I_2}{I_1 I_2} c_1 + \frac{I_2 + I_3}{I_2 I_3} c_2 + \frac{I_3 + I_4}{I_3 I_4} c_3 \right) k^4 + \\ + \left(\frac{I_1 + I_2 + I_3}{I_1 I_2 I_3} c_1 c_2 + \frac{I_1 + I_2}{I_1 I_2} \cdot \frac{I_3 + I_4}{I_3 I_4} c_1 c_3 + \right. \\ \left. + \frac{I_2 + I_3 + I_4}{I_2 I_3 I_4} c_2 c_3 \right) k^2 - \frac{I_1 + I_2 + I_3 + I_4}{I_1 I_2 I_3 I_4} c_1 c_2 c_3 = 0. \quad (4.8)$$

From the system of equations (4.4), it is possible to find not only the frequencies of free torsional vibrations of the shaft but also to sequentially determine the corresponding ratios between the vibration amplitudes associated with each of the shaft's free vibration frequencies.

Let us determine the natural frequencies of torsional vibrations of a cylindrical shaft with four attached discs. The parameters of the dynamic system have the following values:

$$I_1 = 200 \text{ N} \cdot \text{m} \cdot \text{s}^2;$$
$$I_2 = 80 \text{ N} \cdot \text{m} \cdot \text{s}^2;$$
$$I_3 = 50 \text{ N} \cdot \text{m} \cdot \text{s}^2;$$
$$I_4 = 10 \text{ N} \cdot \text{m} \cdot \text{s}^2;$$
$$c_1 = 2 \cdot 10^6 \text{ N} \cdot \text{m};$$
$$c_2 = 1,66 \cdot 10^6 \text{ N} \cdot \text{m};$$
$$c_3 = 2 \cdot 10^6 \text{ N} \cdot \text{m}.$$

To determine the torsional vibration frequencies of the shaft, we will use equation (4.8). Substituting the parameter values of the dynamic system into it, we obtain the following frequency equation:

$$k^6 - 1,4917 \cdot 10^5 k^4 + 5,3917 \cdot 10^9 k^2 - 3,5833 \cdot 10^{13} = 0. \quad (4.9)$$

To calculate the natural frequencies of free vibrations of the shaft, we will use the MathLAB software package (see Appendix 1). As a result, we have:

$$k_1^2 = 8556,25 \ s^{-2};$$
$$k_2^2 = 42849 \ s^{-2};$$
$$k_3^2 = 97781,29 \ s^{-2}.$$

4.3. Normal modes of torsional vibrations of shafts.

From the main system of equations (4.4), it is possible to find not only the natural frequencies of free vibrations of the shaft but also the corresponding relationships between the amplitudes. If the first natural frequency k_1^2, found from the frequency equation (4.8), is substituted into the system (4.4), then all amplitudes of torsional vibrations of the discs can be sequentially expressed in terms of the amplitude A_1. For example, from the first equation of (4.4), we can write:

$$c_1 A_2 = (c_1 - k_1^2 I_1) A_1,$$

or

$$A_2 = \left(1 - \frac{k_1^2 I_1}{c_1}\right) A_1. \qquad (4.10)$$

Let us write the second equation of (4.4) in the form:

$$c_2 A_3 = -c_1 A_1 + \left(c_1 + c_2 - k_1^2 I_2\right) A_2,$$

or

$$A_3 = -\frac{c_1}{c_2} A_1 + \left(1 + \frac{c_1}{c_2} - \frac{k_1^2 I_2}{c_2}\right) A_2. \qquad (4.11)$$

Substitute equation (4.10) for A_2 into the right-hand side. As a result, we obtain:

$$A_3 = \left[1 - \frac{k_1^2}{c_1 c_2}\left(I_1 c_2 + I_2 c_1 - I_1 c_1 + k_1^2 I_1 I_2\right)\right] A_1. \qquad (4.12)$$

And, finally, let us write the last equation of (4.4) in the form:

$$c_3 A_3 = \left(c_3 - k_1^2 I_4\right) A_4, \qquad (4.13)$$

substitute relation (4.12) for A_3 into the left-hand side of (4.13).

As a result, we obtain:

$$A_4 = \frac{c_3 \cdot A_3}{c_3 - k_1^2 I_4} = \frac{c_3 A_1 \left(1 - \frac{k_1^2}{c_1 c_2} \left(I_1 c_2 + I_2 c_1 - I_1 c_1 + k_1^2 I_1 I_2 \right) \right)}{c_3 - k_1^2 I_4}. \quad (4.14)$$

If we conventionally assume $A_1 = 1$, then the equations

$$\bar{A}_2 = 1 - \frac{k_1^2 I_1}{c_1};$$

$$\bar{A}_3 = 1 - \frac{k_1^2}{c_1 c_2} \left(I_1 c_2 + I_2 c_1 - I_1 c_1 + k_1^2 I_1 I_2 \right); \quad (4.15)$$

$$\bar{A}_4 = \frac{c_3}{c_3 - k_1^2 I_4} \left[1 - \frac{k_1^2}{c_1 c_2} \left(I_1 c_2 + I_2 c_1 - I_1 c_1 + k_1^2 I_1 I_2 \right) \right]$$

determine the relative amplitudes of free torsional vibrations of the shaft with four discs, corresponding to the first natural frequency of torsional vibrations.

To obtain the relative amplitudes of free vibrations of the shaft corresponding to the second natural frequency, the value k_1^2 in equation (4.15) should be replaced with k_2^2. Similarly, to obtain the relative amplitudes corresponding to the third natural frequency, k_1^2 in equation (4.15) should be replaced with k_3^2.

4.4. Forced torsional vibrations of shafts.

Forced vibrations of crankshafts are an inevitable consequence of the variability of the active moments acting on the crank throws. These moments are periodic in nature and are caused, firstly, by gas pressure in the cylinders and, secondly, by the inertia forces of the engine's moving parts. Let us consider the most general case where variable moments act on individual discs of the equivalent system. The time-averaged values of these moments cause a constant deformation of the crankshaft over time. Therefore, to analyze forced vibrations, the average values of the moments should be excluded from consideration, and only the influence of the variable parts of each moment should be analyzed. These parts will be called disturbing moments and denoted as

$$
\begin{aligned}
M_1(t) &= M_1 \sin \omega t; \\
M_2(t) &= M_2 \sin \omega t; \\
&\vdots \\
M_n(t) &= M_n \sin \omega t,
\end{aligned}
\tag{4.16}
$$

where M_1, M_2, …, M_n – amplitudes of the disturbing moments on each of the discs of the equivalent system; ω – frequency of the disturbing moments.

The equations of forced oscillations will differ from the equations of free oscillations (4.1) by the presence of disturbing moments

$$
\begin{aligned}
I_1\ddot{\varphi}_1(t) - c_1[\varphi_2(t) - \varphi_1(t)] &= M_1 \sin \omega t; \\
I_2\ddot{\varphi}_2(t) - c_1[\varphi_1(t) - \varphi_2(t)] - c_2[\varphi_3(t) - \varphi_2(t)] &= M_2 \sin \omega t; \\
I_3\ddot{\varphi}_3(t) - c_2[\varphi_2(t) - \varphi_3(t)] - c_3[\varphi_4(t) - \varphi_3(t)] &= M_3 \sin \omega t; \\
I_4\ddot{\varphi}_4(t) - c_3[\varphi_3(t) - \varphi_4(t)] &= M_4 \sin \omega t.
\end{aligned}
\tag{4.17}
$$

The system of differential equations (4.17) describes the forced vibrations of the crankshaft of a four-cylinder engine.

Under sinusoidal disturbances, the steady-state vibrations will occur at the disturbance frequency ω

$$
\begin{aligned}
\varphi_1(t) &= A_1 \sin \omega t; \\
\varphi_2(t) &= A_2 \sin \omega t; \\
\varphi_3(t) &= A_3 \sin \omega t; \\
\varphi_4(t) &= A_4 \sin \omega t.
\end{aligned}
\tag{4.18}
$$

Let us substitute relations (4.16) and (4.18) into equations (4.17) and obtain a system of algebraic equations:

$$
\begin{aligned}
-A_1 I_1 \omega^2 - c_1(A_2 - A_1) &= M_1; \\
-A_2 I_2 \omega^2 - c_1(A_1 - A_2) - c_2(A_3 - A_2) &= M_2; \\
-A_3 I_3 \omega^2 - c_2(A_2 - A_3) - c_3(A_4 - A_3) &= M_3; \\
-A_4 I_4 \omega^2 - c_3(A_3 - A_4) &= M_4.
\end{aligned}
\tag{4.19}
$$

Let us write the system (4.19) in the form of equation (4.20).

$$\begin{aligned} A_1(c_1 - I_1\omega^2) - A_2c_1 &= M_1; \\ -A_1c_1 + A_2(c_1 + c_2 - I_2\omega^2) - A_3c_2 &= M_2; \\ -A_2c_2 + A_3(c_2 + c_3 - I_3\omega^2) - A_4c_3 &= M_3; \\ -A_3c_3 + A_4(c_3 - I_4\omega^2) &= M_4. \end{aligned} \tag{4.20}$$

The determinant of the system of algebraic equations (4.20) is written as:

$$D = \begin{vmatrix} c_1 - I_1\omega^2 & -c_1 & 0 & 0 \\ -c_1 & c_1 + c_2 - I_2\omega^2 & -c_2 & 0 \\ 0 & -c_2 & c_2 + c_3 - I_3\omega^2 & -c_3 \\ 0 & 0 & -c_3 & c_3 - I_4\omega^2 \end{vmatrix}. \tag{4.21}$$

Let us introduce two four-dimensional vectors:

$$A = \begin{bmatrix} A_1 \\ A_2 \\ A_3 \\ A_4 \end{bmatrix}; \; M = \begin{bmatrix} M_1 \\ M_2 \\ M_3 \\ M_4 \end{bmatrix}.$$

Then we write the system (4.20) in vector-matrix form:

$$DA = M, \tag{4.22}$$

and the solution of the system (4.22) is obtained in the form:

$$A = D^{-1}M. \tag{4.23}$$

To obtain the values of the unknown amplitudes of forced vibrations of the crankshaft, it is also advisable to use the MathLAB software package. If the frequency ω of the disturbing moments (4.16) approaches any of the natural frequencies k_1, k_2, …, k_n of the crankshaft, the phenomenon of resonance occurs in the oscillatory system. The frequencies at which resonant torsional vibrations occur are called critical frequencies.

To prevent resonant vibrations, the parameters of the crankshaft must be selected such that its rotational speed is sufficiently far from the critical frequency.

The values of the critical frequencies can be obtained when $D = 0$, which is a consequence of considering relation (4.23).

Let us consider a two-cylinder automotive engine, the equivalent scheme of which is shown in Fig. 4.2.

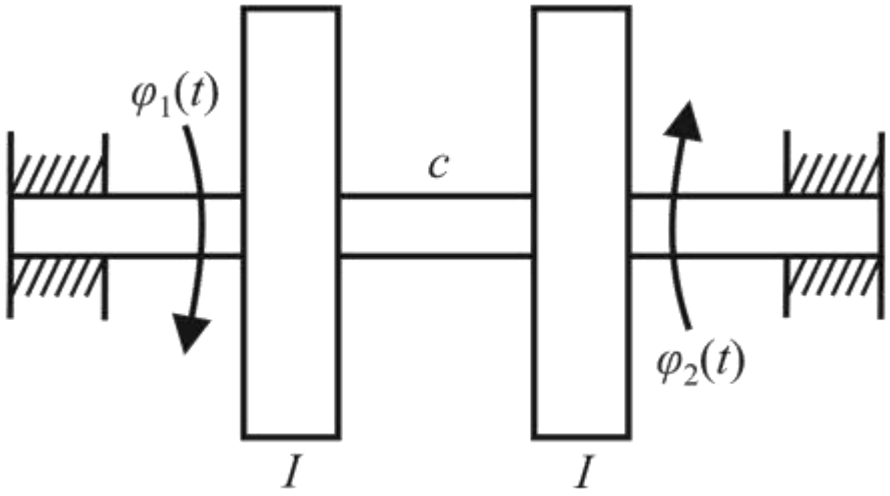

Fig. 4.2. **Equivalent Scheme of the Crankshaft of a Two-Cylinder Internal Combustion Engine**

The determinant of the system of algebraic equations for the amplitudes of torsional vibrations A_1 and A_2 takes the following form:

$$D = \begin{vmatrix} c - I\omega^2 & -c \\ -c & c - I\omega^2 \end{vmatrix} = \left(c - I\omega^2\right)^2 - c^2 = \\ = -2cI\omega^2 + I^2\omega^4 = I\omega^2\left(I\omega^2 - 2c\right). \tag{4.24}$$

We set the determinant (4.24) to zero and obtain the value of the critical frequency of torsional vibrations:

$$(\omega^*)^2 = \frac{2c}{I};\ \omega^* = \sqrt{\frac{2c}{I}}. \tag{4.25}$$

Resonant torsional vibrations in the equivalent scheme shown in Fig. 4.2 will be absent if the values of the critical frequency (4.25) do not fall within the engine's operating frequency range (ω_{min} … ω_{max}).

Let us proceed to consider a three-cylinder internal combustion engine, the equivalent scheme of which is shown in Fig. 4.3.

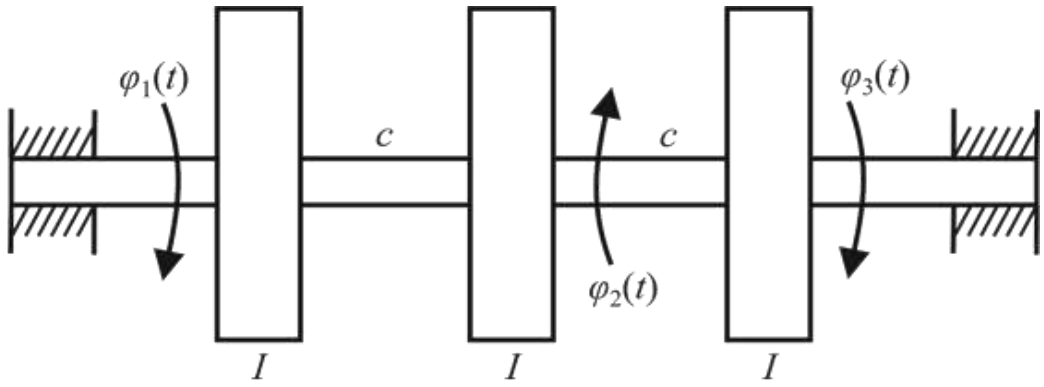

Fig. 4.3. **Equivalent Scheme of the Crankshaft of a Three-Cylinder Internal Combustion Engine**

The determinant of the system of algebraic equations for the torsional vibration amplitudes A_1, A_2 and A_3 has the following form:

$$D = \begin{vmatrix} c - I\omega^2 & -c & 0 \\ -c & 2c - I\omega^2 & -c \\ 0 & -c & c - I\omega^2 \end{vmatrix} = -I\omega^2(I^2\omega^4 - 4cI\omega^2 + 3c^2). \quad (4.26)$$

We set the determinant (4.26) to zero and obtain a biquadratic equation for determining the critical frequencies of torsional vibrations of the equivalent scheme shown in Fig. 4.3:

$$I^2\omega^4 - 4cI\omega^2 + 3c^2 = 0. \quad (4.27)$$

Let us divide both sides of the biquadratic equation (4.27) by I^2. As a result, we obtain:

$$\omega^4 - 4\frac{c}{I}\omega^2 + 3\frac{c^2}{I^2} = 0. \quad (4.28)$$

The solution of the biquadratic equation (4.28) determines the values of the critical frequencies of torsional vibrations of the crankshaft of a three-cylinder internal combustion engine.

$$\omega_1^* = \sqrt{\frac{3c}{I}};\ \omega_2^* = \sqrt{\frac{c}{I}}.$$

And finally, let us expand the determinant (4.21), which corresponds to a four-cylinder internal combustion engine:

$$D = \omega^2 \left(\omega^6 - 6\frac{c}{I}\omega^4 + 10\frac{c^2}{I^2}\omega^2 - 4\frac{c^3}{I^3} \right). \qquad (4.29)$$

Unfortunately, there are no analytical dependencies for calculating the roots of a 6th-order polynomial.

$$\omega^6 - 6\frac{c}{I}\omega^4 + 10\frac{c^2}{I^2}\omega^2 - 4\frac{c^3}{I^3} = 0. \qquad (4.30)$$

To calculate the roots of the polynomial (4.30), we will use the MathLAB software package (see Appendix 1).

Control questions for the chapter 4.

1. Explain the equivalent scheme used in developing the mathematical model of free vibrations of an engine crankshaft.
2. Write down the mathematical model of free vibrations of a four-cylinder engine crankshaft.
3. Write down the mathematical model of forced vibrations of a four-cylinder engine crankshaft.

Chapter 5

VIBRATIONS OF DISCRETE-CONTINUOUS DYNAMIC SYSTEMS

5.1. Free vibrations of an elastic gun barrel on a military vehicle chassis.

Discrete-continuous dynamic systems are complex technical objects comprising a combination of a discrete part with lumped parameters and a continuous part with distributed parameters, which interact with each other. The mathematical model of the disturbed motion of a discrete-continuous dynamic system consists of a set of ordinary differential equations and partial differential equations. Examples of such systems include various classes of rockets with liquid-propellant engines, spacecraft with elastic solar panel elements, various classes of aircraft with elastic wings, self-propelled artillery units with gun barrel lengths exceeding 40 calibers, and refueler trucks with tank volumes exceeding 20 m^3.

Let us consider a 120 mm caliber wheeled self-propelled artillery gun, the calculation scheme of which is shown in Figure 5.1.

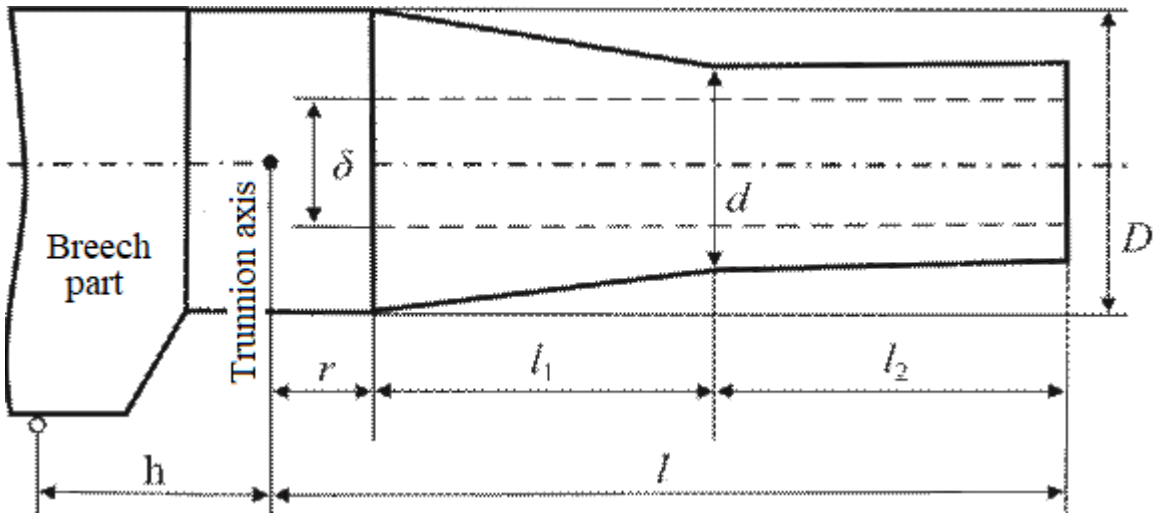

Fig. 5.1. **Calculation Schematic of the Self-Propelled Artillery Gun:** δ = 120 mm; d = 172 mm; D = 252 mm; r = 250 mm; l_1 = 2180 mm; l_2 = 2400 mm; l = 4830 mm.

We will consider the gun as a combination of a rigid body (the breech part) and an elastic element (the barrel). Let us introduce the following coordinate systems: $0X_0Y_0Z_0$ – an inertial coordinate system

with its origin 0 located on the trunnion axis, where the axes $0X_0$ and $0Y_0$ form the firing plane; $0X_1Y_1Z_1$ – a coordinate system attached to the breech part (Fig. 5.2).

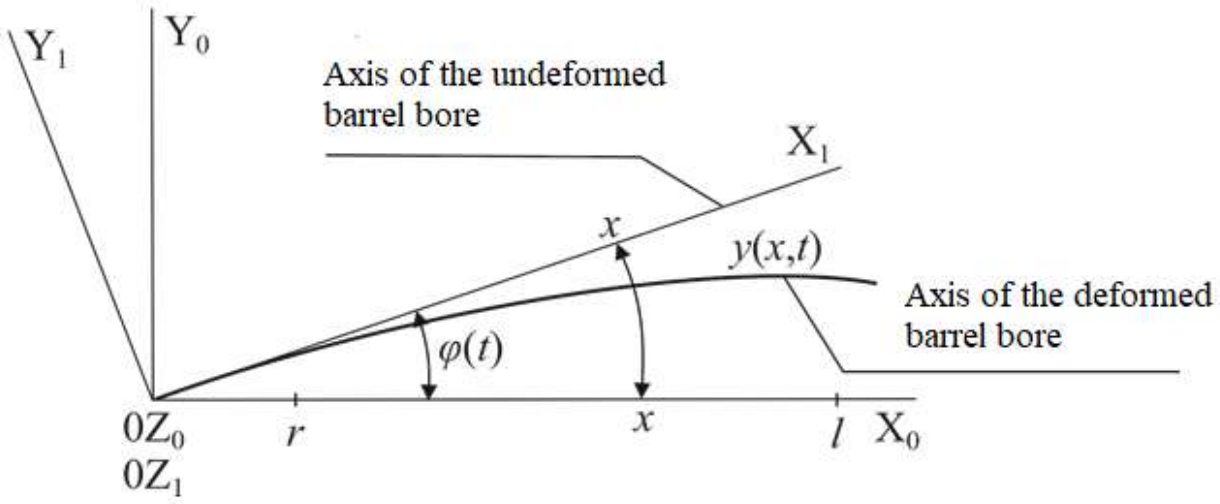

Fig. 5.2. **Coordinate Systems**

The $0X_0$ axis coincides with the line of sight, and the $0X_1$ axis is directed along the axis of the undeformed barrel bore. The distance $0r$ is equal to the length of the segment from the gun's trunnion axis to the connection point of the barrel and the breech part, and the distance $0l$ is equal to the length of the segment from the trunnion axis to the muzzle. Therefore, the length of the deformable gun barrel is $l-r$. The $0Z_0$ and $0Z_1$ axes are perpendicular to the firing plane.

Let us denote by x the current distance from the gun's trunnion axis to any point on the barrel. Then, $y(x,t)$ represents the current deviation of this point from the $0X_1$ axis.

Let us consider the mathematical model of the free vibrations of the gun barrel using Hamilton's principle. The kinetic and potential energy of the elastic gun barrel are determined by the relations:

$$\mathrm{K} = \frac{1}{2}\left\{ I_n\left[\frac{d\varphi(t)}{dt}\right]^2 + \int_r^l m(x)v^2(x,t)dx \right\}; \qquad (5.1)$$

$$\Pi = \frac{1}{2}\int_r^l EI(x)\left[\frac{\partial^2 y(x,t)}{\partial x^2}\right]^2 dx, \qquad (5.2)$$

where $\varphi(t)$ – the angle of rotation of the coordinate system associated with the gun relative to the inertial system; $v(x,t)$ – the current velocity of point X on the barrel, which is determined by the equation:

$$v(x,t) = (x+r)\frac{d\varphi(t)}{dt} - \frac{\partial y(x,t)}{\partial t}; \tag{5.3}$$

$m(x)$– linear mass density of the barrel; $EI(x)$ – bending stiffness of the barrel; I_n – moment of inertia of the undeformable gun about the trunnion axis.

According to Hamilton's principle, consider the kinetic potential, which is equal to

$$\mathcal{L} = \mathrm{K} - \Pi, \tag{5.4}$$

and also introduce the quantity S, called the Hamiltonian action over the time interval (0, T), defined by the equation:

$$S = \int_{\mathrm{o}}^{\mathrm{T}} \mathcal{L} dt. \tag{5.5}$$

Taking into account equations (5.1) – (5.4), let us compute the variation of the quantity (5.5), considering the boundary conditions:

$$y(x,t)\big|_{x=r} = 0; \tag{5.6}$$

$$\left.\frac{\partial y(x,t)}{\partial x}\right|_{x=r} = 0; \tag{5.7}$$

$$EI(x)\left.\frac{\partial^2 y(x,t)}{\partial x^2}\right|_{x=l} = 0; \tag{5.8}$$

$$\frac{\partial}{\partial x}\left[EI(x)\frac{\partial^2 y(x,t)}{\partial x^2}\right]_{x=l} = 0 \tag{5.9}$$

and set this variation to zero. As a result, we obtain:

$$I_n \frac{d^2\varphi(t)}{dt^2} - \int_r^l m_1(x)\frac{\partial^2 y(x,t)}{\partial t^2} dx = 0; \tag{5.10}$$

$$m_1(x)\frac{d^2\varphi(t)}{dt^2}+m(x)\frac{\partial^2 y(x,t)}{\partial t^2}+$$
$$+\frac{\partial^2}{\partial x^2}EI(x)\frac{\partial^2 y(x,t)}{\partial x^2}=-m(x)g, \tag{5.11}$$

where the quantity $m_1(x)$ is determined by the equation:

$$m_1(x)=m(x)(x-r). \tag{5.13}$$

Taking into account the internal damping of the gun barrel material, the mathematical model of the free vibrations of the gun barrel is written in its final form as:

$$I_n\frac{d^2\varphi(t)}{dt^2}-\int_r^l m_1(x)\frac{\partial^2 y(x,t)}{dt^2}dx=0; \tag{5.14}$$

$$m_1(x)\frac{d^2\varphi(t)}{dt^2}+m(x)\frac{\partial^2 y(x,t)}{\partial t^2}+\frac{\partial^2}{\partial x^2}EI(x)\frac{\partial^2 y(x,t)}{\partial x^2}+$$
$$+\zeta\frac{\partial^2}{\partial x^2}EI(x)\frac{\partial^3 y(x,t)}{\partial x^2\partial t}=-m(x)g, \tag{5.15}$$

where ζ is the coefficient of internal damping.

In accordance with the works, we represent the function $y(x,t)$ in the form (Fourier method):

$$y(x,t)=\sum_{i=1}^{n}\gamma_i(x)T_i(t), \tag{5.16}$$

where n is the number of considered modes of elastic vibrations of the barrel.

Let us substitute (5.16) into equations (5.14) and (5.15):

$$I_n\ddot{\varphi}(t)-\sum_{i=1}^{n}\ddot{T}_i(t)\int_r^l m_1(x)\gamma_i(x)dx=0; \tag{5.17}$$

$$m_1(x)\ddot{\varphi}(t)+m(x)\sum_{i=1}^{n}\gamma_i(x)\ddot{T}_i(t)+E\frac{\partial^2}{\partial x^2}\left[I(x)\sum_{i=1}^{n}\ddot{\gamma}_i(x)T_i(t)\right]+$$
$$+\zeta E\frac{\partial^2}{\partial x^2}\left[I(x)\sum_{i=1}^{n}\ddot{\gamma}_i(x)\dot{T}_i(t)\right]=-m(x)g. \qquad (5.18)$$

Let us multiply both sides of equation (5.18) by $\gamma_j(x)$, $(j=\overline{1,n})$ and integrate within the limits from *r* to *l*:

$$\ddot{\varphi}(t)\int_r^l m_1(x)\gamma_j(x)dx+\sum_{i=1}^{n}\ddot{T}_i(t)\int_r^l m(x)\gamma_i(x)\gamma_j(x)dx+$$
$$+E\sum_{i=1}^{n}T_i(t)\int_r^l\frac{\partial^2}{\partial x^2}\left[I(x)\ddot{\gamma}_i(x)\gamma_j(x)\right]dx+ \qquad (5.19)$$
$$+\zeta E\sum_{i=1}^{n}\dot{T}_i(t)\frac{\partial^2}{\partial x^2}\int_r^l\frac{\partial^2}{\partial x^2}\left[I(x)\ddot{\gamma}_i(x)\gamma_j(x)\right]dx=-\int_r^l m(x)g\gamma_j(x)dx.$$

Let us write the orthogonality conditions for the natural modes of elastic vibrations of the barrel:

$$\int_r^l m_1(x)\gamma_j(x)dx=a_j,\ (y=\overline{1,n});$$
$$E\int_r^l\frac{\partial^2}{\partial x^2}\left[I(x)\ddot{\gamma}_i(x)\gamma_j(x)\right]dx=\begin{cases}0 \text{ at } i\neq j\\ b_j \text{ at } i=j\end{cases};$$
$$\int_r^l m(x)\gamma_i(x)\gamma_j(x)dx=\begin{cases}0 \text{ at } i\neq j\\ c_j \text{ at } i=j\end{cases}; \qquad (5.20)$$
$$\int_r^l m(x)\gamma_j(x)dx=k_j;\ (j=\overline{1,n}).$$

In relations (5.20), we can set:

$$\gamma_i(x) = \sin\frac{i\pi}{2(l-r)}x;\ (i=\overline{1,n}). \qquad (5.21)$$

Taking into account relations (5.19) and (5.20), the system (5.17), (5.18) is written in the form:

$$I_n\ddot{\varphi}(t) - \sum_{i=1}^{n} a_i\ddot{T}_i(t) = 0; \qquad (5.22)$$

$$a_i\ddot{\varphi}(t) + c_i\ddot{T}_i(t) + \zeta b_i\dot{T}_i(t) + b_iT_i(t) = -k_ig;\ (i=\overline{1,n}).$$

For a 120 mm caliber gun, the calculation scheme of which is shown in Fig. 5.1, the coefficients of the mathematical model (5.21), taking into account the first three modes of elastic vibrations of the barrel, are given in Table 5.1. In this case, the value of the moment of inertia I_n is I_n = 736,9 N·m·s^2, and the value of the internal friction coefficient ζ is ζ = 0,0082 s.

Table 5.1 – **Coefficients of the mathematical model of free vibrations of an elastic gun barrel**

Mode Number	a_i , N·s^2	b_i , N·m^{-1}	c_i , N·m^{-1}·s^2	k_i , N·m^{-1}·s^2
1	$9{,}721\cdot10^2$	$2{,}213\cdot10^5$	$2{,}152\cdot10^3$	$3{,}612\cdot10^2$
2	$7{,}999\cdot10^2$	$3{,}194\cdot10^6$	$1{,}941\cdot10^3$	$3{,}994\cdot10^2$
3	$6{,}340\cdot10^2$	$1{,}736\cdot10^7$	$2{,}144\cdot10^3$	$2{,}2860\cdot10^2$

We will assume the gun is locked (secured), and the angle $\varphi(t)$ is set to $\varphi(t) = \varphi_0$. In this case, equations (5.22) are written as:

$$c_i\ddot{T}_i(t) + \zeta b_i\dot{T}_i(t) + b_iT_i(t) = -k_ig;\ (i=\overline{1,n}). \qquad (5.23)$$

Let us assume that:

$$T_i(t) = T_{i0} + \Delta T_i(t), \qquad (5.24)$$

where T_{i0}, $(i=\overline{1,n})$ are the static components caused by the static deflection of the barrel; $\Delta T_i(t)$, $(i=\overline{1,n})$ – dynamic components.

Then each of the equations (5.23) splits into two equations:

$$b_i T_{i0} = -k_i g; \tag{5.25}$$

$$c_i \Delta\ddot{T}_i(t) + \zeta b_i \Delta\dot{T}_i(t) + b_i \Delta T_i(t) = 0; \ (i = \overline{1,n}). \tag{5.26}$$

Taking into account relations (5.16), (5.21), and (5.25), we obtain the equation for calculating the static deflection of the barrel:

$$y(x) = -g\sum_{i=1}^{n}\gamma_i(x)T_{i0} = -g\sum_{i=1}^{n}\frac{k_i}{b_i}\sin\frac{i\pi}{2(l-r)}x. \tag{5.26}$$

The static deflection of the barrel at the muzzle can be calculated by substituting the expression $x = l - r$ into equation (5.26):

$$y(l-r) = -g\sum_{i=1}^{n}\frac{k_i}{b_i}. \tag{5.27}$$

Let us proceed to consider the free vibrations of the gun. For this purpose, we move from the system (5.22) to the system:

$$\begin{gathered} I_n\ddot{\varphi}(t) - \sum_{i=1}^{n} a_i \Delta\ddot{T}_i(t) = 0; \\ a_i\ddot{\varphi}(t) + c_i\Delta\ddot{T}_i(t) + \zeta b_i\Delta\dot{T}_i(t) + b_i\Delta T(t) = 0; \\ (i = \overline{1,n}). \end{gathered} \tag{5.28}$$

Each of the equations (5.26) describes the free vibrations of the *i*-th partial oscillator. Therefore, the method described above for transitioning from the mathematical model (5.14), (5.15) in partial derivatives to the mathematical model (5.28) in ordinary differential equations has been named the method of partial oscillators. This method was first applied by B.I. Rabinovich and G.S. Narimanov in developing the mathematical model of the disturbed motion of the two-stage intercontinental ballistic missile R-16 with four tanks filled with liquid fuel and oxidizer.

Let us solve the system (5.28) with respect to the highest derivatives, considering only the first mode of elastic vibrations of the gun:

$$\begin{aligned} I_n\ddot{\varphi}(t) - a_1\Delta\ddot{T}_1(t) = 0; \\ a_1\ddot{\varphi}(t) + c_1\Delta\ddot{T}_1(t) = -\zeta b_1\Delta\dot{T}_1(t) - b_1\Delta T_1(t); \end{aligned} \tag{5.29}$$

Let us introduce a second-order vector:

$$Y(t) = \begin{bmatrix} \varphi(t) \\ \Delta T_1(t) \end{bmatrix},$$

and write equation (5.29) in vector-matrix form:

$$A\ddot{Y}(t) = B\dot{Y}(t) + CY(t), \tag{5.30}$$

where matrices *A*, *B*, and *C* are equal to:

$$A = \begin{bmatrix} I_n & -a_1 \\ a_1 & c_1 \end{bmatrix};\ B = \begin{bmatrix} 0 & 0 \\ 0 & -\zeta b_1 \end{bmatrix};\ C = \begin{bmatrix} 0 & 0 \\ 0 & -b_1 \end{bmatrix}$$

From equation (5.30), we obtain:

$$\ddot{Y}(t) = A^{-1}B\dot{Y}(t) + A^{-1}CY(t). \tag{5.31}$$

The inverse matrix A^{-1} equal to:

$$A^{-1} = \begin{bmatrix} \dfrac{c_1}{I_n c_1 + a_1^2} & +\dfrac{a_1}{I_n c_1 + a_1^2} \\ -\dfrac{a_1}{I_n c_1 + a_1^2} & \dfrac{I_n}{I_n c_1 + a_1^2} \end{bmatrix}.$$

Let's perform a check by multiplying the matrices A and A^{-1}.

$$\begin{bmatrix} I_n & -a_1 \\ a_1 & c_1 \end{bmatrix} \begin{bmatrix} \dfrac{c_1}{I_n c_1 + a_1^2} & +\dfrac{a_1}{I_n c_1 + a_1^2} \\ -\dfrac{a_1}{I_n c_1 + a_1^2} & \dfrac{I_n}{I_n c_1 + a_1^2} \end{bmatrix} = \begin{bmatrix} 1 & 0 \\ 0 & 1 \end{bmatrix} = E.$$

The product of matrices A and A^{-1} equals the identity matrix, meaning the matrix A^{-1} has been computed correctly.

Let's find the matrices $A^{-1}B$ and $A^{-1}C$

$$\frac{1}{I_n c_1 + a_1^2}\begin{bmatrix} c_1 & a_1 \\ -a_1 & I_n \end{bmatrix}\begin{bmatrix} 0 & 0 \\ 0 & -\zeta b_1 \end{bmatrix} = \frac{1}{I_n c_1^2 + a_1^2}\begin{bmatrix} 0 & -a_1\zeta b_1 \\ 0 & -I_n\zeta b_1 \end{bmatrix};$$

$$\frac{1}{I_n c_1 + a_1^2}\begin{bmatrix} c_1 & a_1 \\ -a_1 & I_n \end{bmatrix}\begin{bmatrix} 0 & 0 \\ 0 & -b_1 \end{bmatrix} = \frac{1}{I_n c_1 + a_1^2}\begin{bmatrix} 0 & -a_1 b_1 \\ 0 & -I_n b_1 \end{bmatrix}.$$

As a result, the vector-matrix equation (5.31) can be written in scalar form:

$$\begin{aligned} \ddot{\varphi}(t) &= \frac{1}{I_n c_1 + a_1^2}\left[-a_1\zeta b_1\Delta\dot{T}_1(t) - a_1 b_1\Delta T_1(t)\right]; \\ \Delta\ddot{T}(t) &= \frac{1}{I_n c_1 + a_1^2}\left[-I_n\zeta b_1\Delta\dot{T}_1(t) - I_n b_1\Delta T_1(t)\right]. \end{aligned} \tag{5.32}$$

The differential equations (5.32) represent the mathematical model of the free vibrations of the elastic gun barrel.

Let us introduce the notation:

$$a_{\varphi\text{т}} = -\frac{a_1 b_1}{I_n c_1 + a_1^2};\ a_{\text{тт}} = -\frac{I_n b_1}{I_n c_1 + a_1^2},$$

and write the system (5.32) as:

$$\begin{aligned} \ddot{\varphi}(t) &= a_{\varphi t}\left[\zeta\Delta\dot{T}_1(t) + \Delta T_1(t)\right]; \\ \Delta\ddot{T}(t) &= a_{tt}\left[\zeta\Delta\dot{T}_1(t) + \Delta T_1(t)\right]. \end{aligned} \tag{5.33}$$

Let us introduce a fourth-order state vector for the elastic gun:

$$X(t) = \begin{bmatrix} x_1(t) \\ x_2(t) \\ x_3(t) \\ x_4(t) \end{bmatrix} = \begin{bmatrix} \varphi(t) \\ \dot{\varphi}(t) \\ \Delta T_1(t) \\ \Delta\dot{T}_1(t) \end{bmatrix}$$

and write the system (5.33) in the normal Cauchy form:

$$
\begin{aligned}
\dot{x}_1(t) &= x_2(t);\\
\dot{x}_2(t) &= a_{\varphi t} x_3(t) + a_{\varphi t}\zeta x_4(t);\\
\dot{x}_3(t) &= x_4(t);\\
\dot{x}_4(t) &= a_{tt} x_3(t) + a_{tt}\zeta x_4(t).
\end{aligned}
\qquad (5.34)
$$

Let us use the MathLAB software package and obtain the solution to the system of differential equations (5.34) under the initial conditions: $x_1(0) = 0$; $x_2(0) = 0$; $x_3(0) = 0{,}16\cdot10^{-1}$ m; $x_4(0) = 0$.

Using the data from Table 5.1, we calculate the values of the coefficients $a_{\varphi t}$ and a_{tt}, which are:

$$a_{\varphi t} = -0{,}848\cdot10^{2}\ \text{m}^{-1}\cdot\text{s}^{-2};$$

$$a_{tt} = -0{,}643\cdot10^{2}\ \text{s}^{-2}.$$

Figure 5.3 shows the oscillatory processes described by the system of differential equations (5.34), representing the free vibrations of the elastic barrel of a 120 mm caliber tank gun.

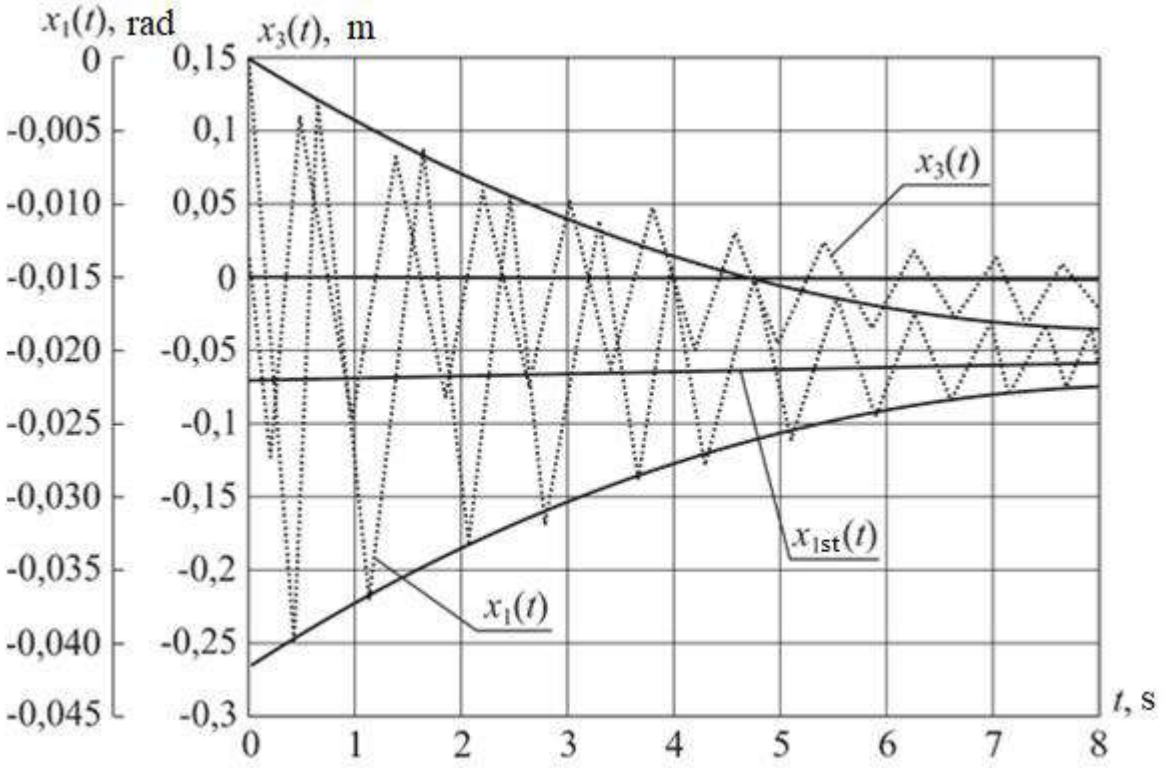

Fig. 5.3. **Free vibrations of a tank gun balanced relative to the trunnion axis**

Analysis of the oscillatory processes leads to the following conclusions:

- The oscillatory process $x_3(t) = \Delta T_1(t)$ is damped due to the internal friction of the barrel material;
- The oscillatory process $x_3(t)$ is independent of the solutions of the first two differential equations in the system (5.34), because the third and fourth differential equations (5.34) constitute an independent dynamic subsystem;
- The overall oscillatory process $x_1(t)$ is not damped but has a static error $x_{1st}(t)$;
- Only the transient component of the process $x_1(t)$, which is the sum of transient and steady-state components, is damped

$$x_1(t) = x_{1\,per}(t) + x_{1st}(t);$$

- The oscillatory process $x_3(t)$ acts as a disturbing process for the process $x_1(t)$.

5.2. Forced vibrations of an elastic gun on a military vehicle chassis.

The gun mounted on the chassis of a military vehicle is subjected to forced vibrations from the sprung part of the chassis. Due to the friction in the gun's trunnion axis, an excitation force acts upon it.

$$M_3(t) = m_c \operatorname{sign}\left[\dot{\varphi}_o(t) - \dot{\varphi}(t)\right] + \mu\left[\dot{\varphi}_o(t) - \dot{\varphi}(t)\right], \qquad (5.35)$$

where $\dot{\varphi}(t)$ – angular velocity of the gun's rotation about the trunnion axis; $\dot{\varphi}_o(t)$ – angular velocity of the turret (with the gun) rotation in the firing plane; m_c – dry friction moment in the trunnion axis; μ – coefficient of viscous friction in the trunnion axis.

Figure 5.4 shows the following coordinate systems: $O_kX_kY_kZ_k$ – a coordinate system attached to the sprung part of the vehicle body; $O_oX_oY_oZ_o$ – a coordinate system attached to the turret, which rotates in the horizontal plane and houses the gun; $O_hX_hY_h$ – a coordinate system attached to the gun, where the O_hX_h axis coincides with the axis of the undeformed barrel, and the O_hY_h axis coincides with the trunnion axis.

The current angle of the turret's rotation relative to the sprung part of the body is $\alpha(t)$, the current velocity of the pitch oscillations of the body is $\dot{\varphi}_k(t)$, and the current velocity of the roll oscillations of the body is $\dot{\theta}_k(t)$.

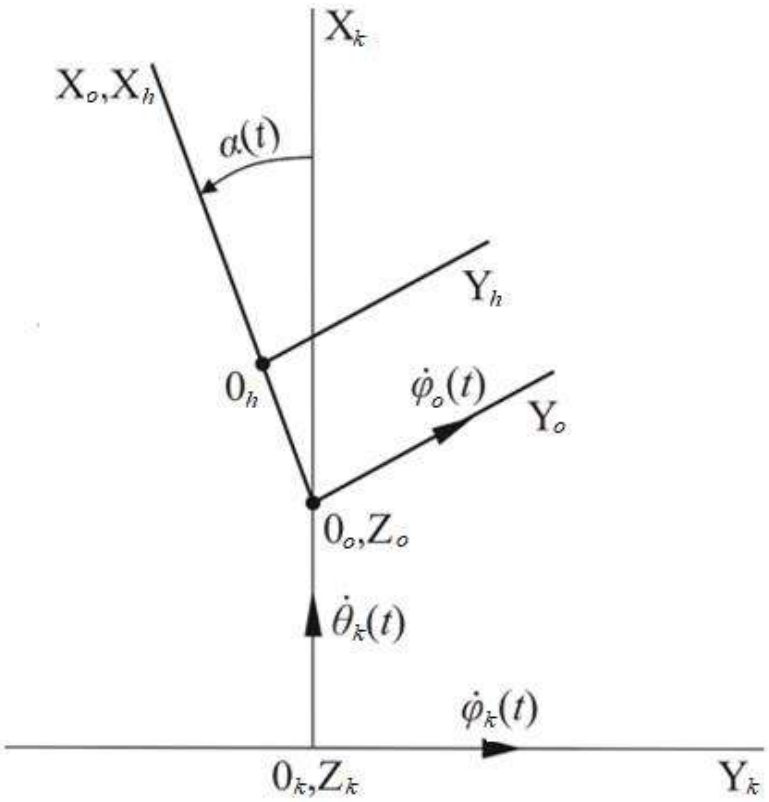

Fig. 5.4. **Coordinate Systems Associated with the Hull, Turret, and Gun**

Then, from the examination of Figure 5.4, the relation for the angular velocity of the pitch oscillations of the turret can be written as:

$$\dot{\varphi}_o(t) = \dot{\varphi}_k(t)\cos\alpha(t) + \dot{\theta}_k(t)\sin\alpha(t). \qquad (5.36)$$

Substituting relation (5.36) into equation (5.35) allows us to obtain the value of the disturbing moment acting on the gun. Additionally, a distributed force acts on the gun barrel, determined by the equation:

$$F(x,t) = m(x)\left[\ddot{z}_k(t) - g\right], \qquad (5.37)$$

where $\ddot{z}_k(t)$ – vertical acceleration of the center of gravity of the sprung part of the vehicle body.

As a result, the mathematical model of the forced vibrations of the elastic tank gun is written as:

$$I_n\ddot{\varphi}(t) - \sum_{i=1}^{n} a_i\Delta\ddot{T}_i(t) = M_3(t);$$

$$a_i\ddot{\varphi}(t) + c_i\Delta\ddot{T}_i(t) + \zeta b_i\Delta\dot{T}_i(t) + b_i\Delta T_i(t) = k_i\ddot{z}_k(t); \qquad (5.38)$$

$$\left(i = \overline{1,n}\right).$$

The current values $\ddot{z}_k(t)$, $\dot{\varphi}_k(t)$ and $\dot{\theta}_k(t)$ are determined by the mathematical model (2.11). If we add to the mathematical model (5.38) of order 2(n+1) the system of differential equations (2.11) of the 6th order, as well as the system of differential equations (2.10) of the fourth order, and take into account relations (5.35) and (5.36), we obtain a system of differential equations of order 2(n+6). This system describes the random oscillatory processes of the gun barrel mounted on the chassis of a military vehicle moving on a random surface.[1]

5.3. The refueling truck as a discrete-continuous system. Forced oscillations of the free surface of the transported liquid and their influence on the vehicle's directional stability.

Supplying liquid fuel to military units is carried out by refueling trucks under extremely difficult conditions on damaged roads, where emergency braking often leads to the vehicle losing stability due to compromised wheel-road adhesion. The world's best refueling truck models are equipped with brake control systems consisting of at least two parallel functioning automatic control systems: an Anti-lock Braking System (ABS), which prevents wheel lock-up during hard braking, and a Vehicle Stability Control (VSC) system. The VSC system works in conjunction with the ABS, allowing for more effective distribution of braking forces across the wheels and enhancing vehicle controllability and stability during braking.

ABS and VSC systems are installed on all vehicles manufactured in the European Union, Great Britain, the USA, Japan, and South Korea. However, the use of such systems is most effective on refueling trucks due to the influence of liquid fuel sloshing in the tank on the vehicle's motion stability. Let us evaluate this influence using the example of the domestic refueling truck KrAZ-63221 with a single-section suitcase-type tank of 20 m^3 volume, length a = 6 m, width b = 2,4 m , and height H = 1,4 m. The wheel track is B = 2 m , the curb weight is 10700 kg , and when the tank is half-filled with fuel, the vehicle's mass is M = 20000 kg,

[1] The complete solution to the problem of random forced vibrations of a tank gun is provided in the article: Aleksandrov, E. E., Aleksandrova, T. E. (2015). Parametric synthesis of digital stabilization system of tank gun. *International Scientific Technical Journal Problems of Control and Informatics*, 6, 5-20.

with a moment of inertia about its vertical axis of I = 14,8·10^4 kg·m^2. The distance between the centers of gravity of the vehicle and the tank is $\Delta L = 1$ m. When moving on a dirt road, the refueler can reach a speed of $V_0 = 18$ m/s.

A mathematical model of the vehicle's disturbed motion during braking with "solidified" fuel has been developed. This model has the following form:

$$\dot{v}(t) = -\frac{1}{M}\left\{2k_{\text{g}}\, p_0 + Gf_0\right] + F_x(t);$$

$$\ddot{\psi}(t) = -\frac{Bk_{\text{g}}}{2I}\Delta p(t) - \frac{2H_m M}{I} v(t)\dot{\psi}(t)\, f_0 + \frac{1}{I} M_{\psi}(t); \qquad (5.39)$$

$$\dot{y}(t) = -v(t)\psi(t),$$

where k_{g} – braking efficiency coefficient; p_0 – brake fluid pressure at the outlet of the main brake cylinder; f_0 – average value of the motion resistance coefficient; $\Delta p(t)$ – difference in brake fluid pressure between the right and left side brake lines of the vehicle; $v(t)$ – current speed of the vehicle during braking; $\psi(t)$ – current yaw angle of the vehicle body during braking; $y(t)$ – lateral displacement of the vehicle's center of gravity during braking; H_m – distance from the vehicle's running surface to its center of gravity; $F_x(t)$, $M_\psi(t)$ – disturbing force and moment caused by deviations of the motion resistance coefficients on the vehicle's sides from their average value.

$$f_r(t) = f_0 + \Delta f_r(t);$$

$$f_l(t) = f_0 + \Delta f_l(t),$$

and are determined by the equations:

$$F_x(t) = \frac{G}{2M}\left[\Delta f_r(t) + \Delta f_l(t)\right];$$

$$M_{\psi}(t) = \frac{H_m M}{I} v_x(t)\dot{\psi}(t)\left[\Delta f_r(t) - \Delta f_l(t)\right]. \qquad (5.40)$$

A mathematical model of the disturbed motion of a refueling truck, taking into account the oscillations of the free fuel surface in the tank, has been developed. The model was obtained using the method of partial oscillators and has the following form:

$$\dot{v}(t) = -\frac{1}{M}\left[2k_{\text{g}}\, p_0 + Gf_0\right] - \frac{1}{M}\sum_{k=1}^{n} m_k \ddot{x}_k(t) + F_x(t);$$

$$\ddot{\psi}(t) = -\frac{Bk_{\text{g}}}{2I}\Delta p(t) - \frac{2H_m M}{I} v(t)\dot{\psi}(t)\, f_0 +$$

$$+\frac{f_0}{I}\sum_{l=1}^{m} m_l \left\{\left[\Delta L - \left(H_n + h_l\right)\right]\ddot{y}_l(t) - g y_l(t)\right\} + M_{\psi}(t); \qquad (5.41)$$

$$\dot{y}(t) = -v(t)\psi(t);$$

$$\ddot{x}_k(t) + \varepsilon_k \dot{x}_k(t) + \omega_k^2 x_k(t) = -\dot{v}(t);\ \left(k = \overline{1,n}\right);$$

$$\ddot{y}_l(t) + \varepsilon_l \dot{y}_l(t) + \omega_l^2 y_l(t) = -v(t)\dot{\psi}(t) - \Delta L\ddot{\psi}(t);\ \left(l = \overline{1,m}\right).$$

where ΔL – distance between the vehicle's center of gravity and the vertical axis of the tank; H_n – distance from the road surface to the bottom of the tank; g – acceleration due to gravity, h_l – distance from the bottom of the tank to the center of gravity of the l-th partial oscillator.

$$h_l = h - \frac{th\left(\lambda_l^y \frac{h}{2}\right)}{\lambda_l^y};\ \left(l = \overline{1,m}\right),$$

The following notations are used in the mathematical model (5.41): $x_k(t),\ (k = \overline{1,n})$ – longitudinal displacements of the centers of gravity of the partial oscillators relative to the vertical axis of the tank, describing n modes of longitudinal fuel oscillations in the tank; $y_l(t),\ (l = \overline{1,m})$ – lateral displacements of the centers of gravity of the partial oscillators relative to the vertical axis of the tank, describing the first m modes of

lateral fuel oscillations in the tank; m_k, $(k=\overline{1,n})$; m_l, $(l=\overline{1,m})$ – masses of the partial oscillators, determined by the relations:

$$m_k = m\frac{2th\left(\lambda_k^x h\right)}{\pi^2\lambda_k^x h\left(k-0{,}5\right)^2};\ \left(k=\overline{1,n}\right);$$

$$m_l = m\frac{2th\left(\lambda_l^y h\right)}{\pi^2\lambda_l^y h\left(l-0{,}5\right)^2};\ \left(l=\overline{1,m}\right),$$

where m is the mass of the liquid in the tank; h is the liquid level in the tank in the absence of oscillations; λ_k^x, $(k=\overline{1,n})$; λ_l^y, $(l=\overline{1,m})$ is the wave numbers of the longitudinal and transverse liquid oscillations, where:

$$\lambda_k^x = \left(1+n_x\right)\frac{\pi\left(2k-1\right)}{a};\ \left(k=\overline{1,n}\right);$$

$$\lambda_l^y = \left(1+n_y\right)\frac{\pi\left(2l-1\right)}{b};\ \left(l=\overline{1,m}\right),$$

where n_x is the number of transverse baffles in the tank; n_y is the number of longitudinal baffles; a, b are the length and width of the suitcase-type tank, respectively; ε_k, $(k=\overline{1,n})$; ε_l, $(l=\overline{1,m})$ is the damping coefficients of the partial oscillators

$$\varepsilon_k = \omega_k\frac{\Delta f}{\pi};\ \left(k=\overline{1,n}\right);$$

$$\varepsilon_l = \omega_l\frac{\Delta f}{\pi};\ \left(l=\overline{1,m}\right),$$

where Δf – is the logarithmic decrement of fuel oscillation damping; ω_k, $(k=\overline{1,n})$; ω_l, $(l=\overline{1,m})$ – are the natural frequencies of the partial oscillators, determined by the equations:

$$\omega_k = \sqrt{g\lambda_k^x th\left(\lambda_k^x h\right)};\ \left(k=\overline{1,n}\right);$$

$$\omega_l = \sqrt{g\lambda_l^y th\left(\lambda_l^y h\right)};\ \left(l=\overline{1,m}\right),$$

Let us consider the emergency braking mode of the KrAZ-63221 refueling truck with f_0 = 0,09; p_0 = 1 MPa, initial speed $v(0)$ = 18 m·s^{-1}, braking intensity coefficient k_g = 0,02 m^2, and a half-filled tank ($M = 20 \cdot 10^3$ kg; $I = 14{,}8 \cdot 10^4$ kg·m^2). Figure 5.5 shows the braking processes (current speed $v(t)$ and current acceleration $w(t)$ of the vehicle's center of gravity) when using a tank without transverse baffles, while Fig. 5.6 shows the same processes when using a tank with one transverse baffle.

The graphs in these figures reflect a noticeable negative influence of longitudinal free surface fuel oscillations on the smoothness of the refueling truck's motion and indicate the possibility of reducing longitudinal fuel oscillations by using transverse baffles.

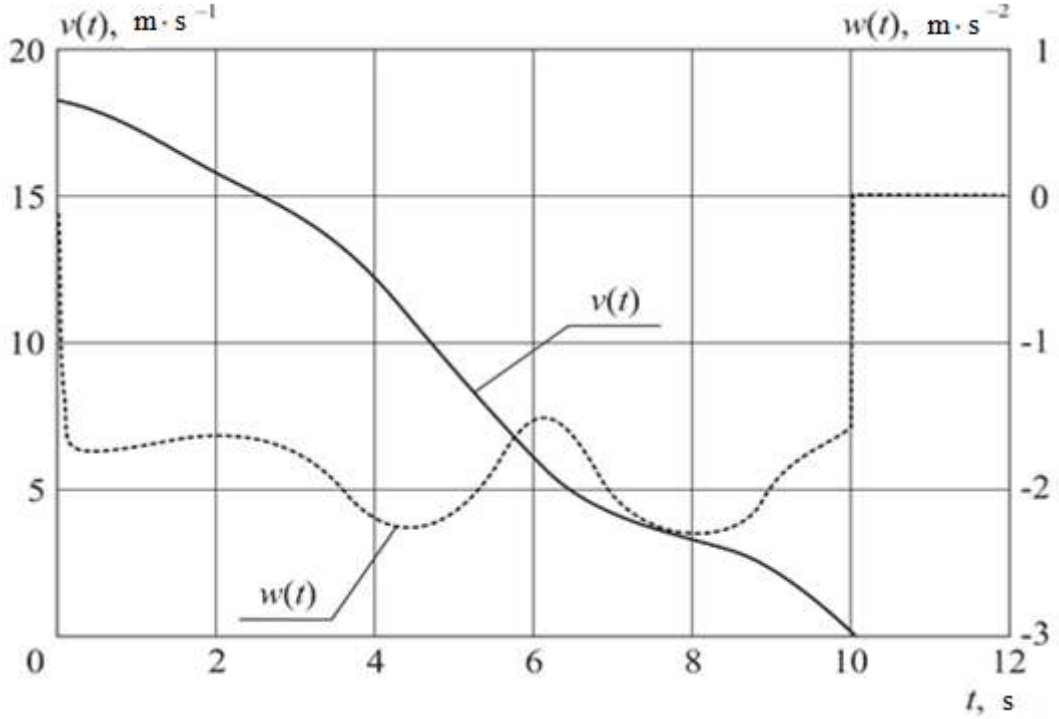

Fig. 5.5. **Braking processes of the refueling truck with a tank without transverse baffles**

Figure 5.7 shows the dependencies of the first three natural frequencies of free longitudinal and transverse fuel oscillations on the liquid level in the tank. Analysis of Figure 5.7 leads to the conclusion that the natural frequencies of fuel oscillations in the tank significantly depend on the fill level and increase as this level rises.

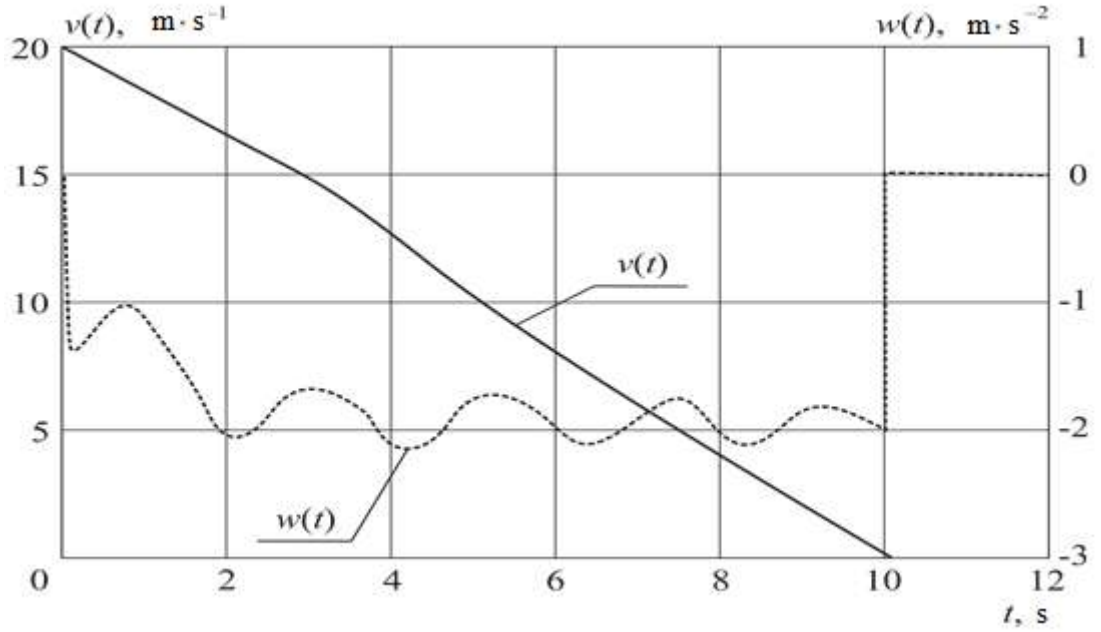

Fig. 5.6. **Braking processes of the refueling truck with a tank having one transverse baffle**

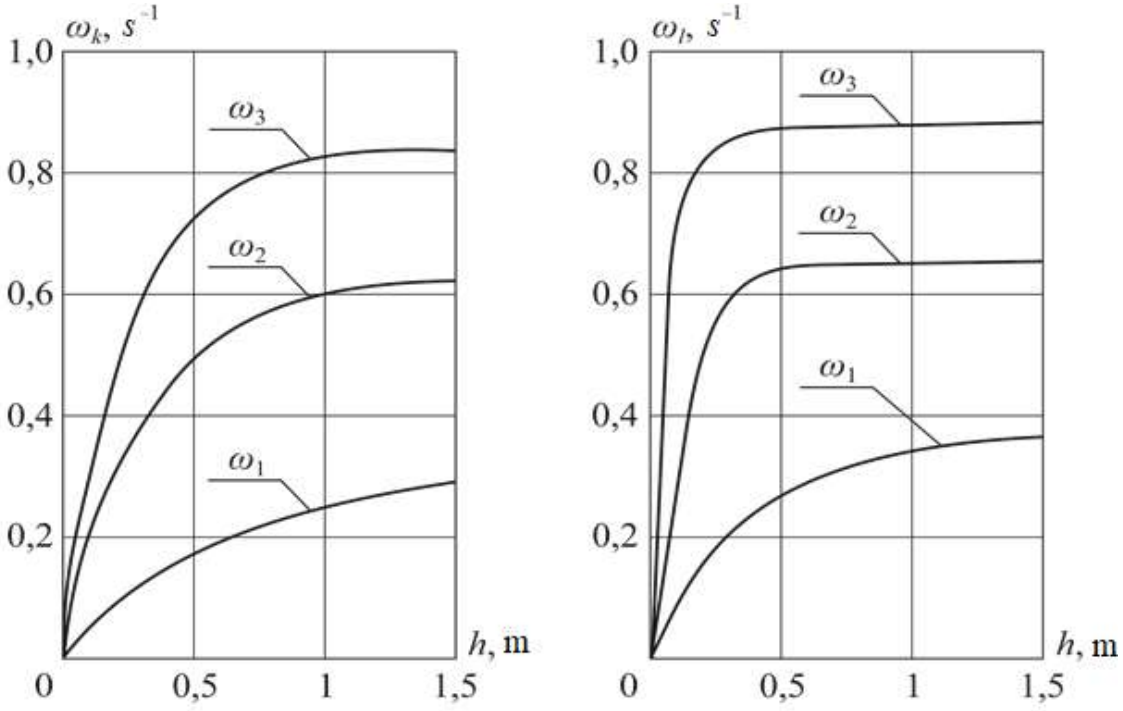

Fig. 5.7. **Dependence of the natural frequencies of the oscillators on the fuel level in the tank**

However, if the tank is more than half full, the frequency growth slows down, especially for the second and third oscillation modes.

Figure 5.8 shows the dependencies of the relative total partial mass on the fuel level in the tank and the number of oscillators taken into account.

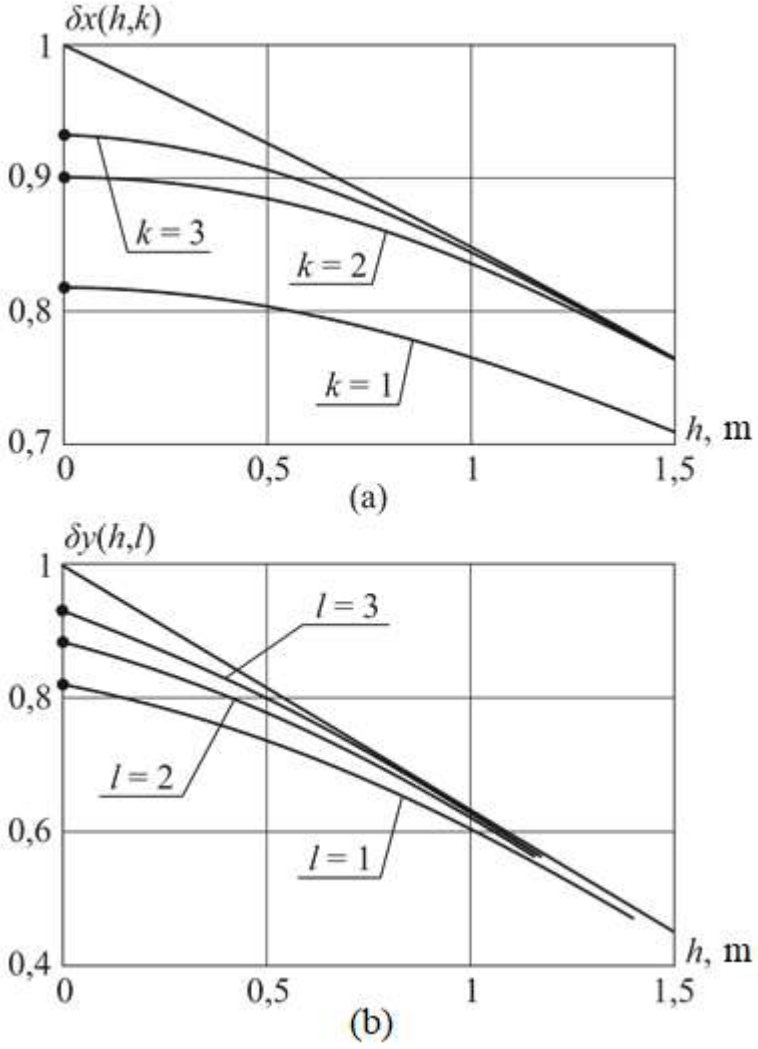

Fig. 5.8. **Relative mass of liquid moving in partial layers:**
(a – during longitudinal oscillations; b – during transverse oscillations)

$$\delta x(h,k) = \frac{1}{m(h)} \sum_{i=1}^{k} m_i(h);$$

$$\delta y(h,l) = \frac{1}{m(h)} \sum_{j=1}^{l} m_j(h).$$

As a result of the comparative analysis of the graphs in Figure 5.8, it can be concluded that when considering longitudinal fuel oscillations in the tank, it is advisable to account for the first three oscillation modes, i.e., set $n = 3$ in equations (5.41). When considering transverse oscillations, it is sufficient to account for only the first mode, i.e., set $m = 1$ in the system (5.41).

It should be noted that longitudinal fuel oscillations in the tank only affect the smoothness of motion of the refueling truck. Typically,

modern refueling truck tanks are equipped with 2–3 transverse semi-transparent baffles, which also serve as tank stiffening ribs. Therefore, when solving problems of analysis and synthesis of directional stability systems for refueling trucks, longitudinal fuel oscillations in the tank are generally neglected, and only the first mode of transverse oscillations is considered in the mathematical model of the disturbed fuel motion.

Clearly, if the tank is completely filled, the free fuel surface is absent, and low-frequency fuel oscillations are not observed. A rule followed by marine tanker crews is known: every tank and container during transport must be either completely full or completely empty. Unfortunately, military refueling trucks cannot adhere to this rule. Therefore, the only way to enhance their stability is to equip such vehicles with Vehicle Stability Control (VSC) systems.

Control questions for the chapter 5.

1. What dynamic systems are called discrete-continuous?
2. What is the essence of Hamilton's principle?
3. What is the cause of forced vibrations of an elastic gun mounted on a military vehicle chassis?
4. How does the mathematical model of the disturbed motion of a refueling truck with "solidified" fuel differ from the disturbed motion of a vehicle with liquid fuel?
5. What does the mathematical model of the disturbed motion of a refueling truck with a completely filled tank look like?
6. What is the essence of the method of partial oscillators?

Chapter 6
STABILITY OF LINEAR DYNAMIC SYSTEMS.

6.1. Definition of dynamic system stability according to Lyapunov.

A dynamic system is understood as an object of any physical nature or a physical process whose behavior is described by a system of differential equations (ordinary or partial derivatives), called the mathematical model of the object or process. The state of the mathematical model at any time t can be represented as an element $X(t)$ of the set of possible states G_x, which can be considered as the state space of the dynamic system. For most problems in the theory of dynamic systems, the state space is a Euclidean metric space, where the distance between two of its elements $X_1 \in G_x$ and $X_2 \in G_x$ in the form of a real function $\rho(X_1, X_2)$ satisfies three axioms:

1. $\rho(X_1, X_2) = 0$ at $X_1 = X_2$;
2. axiom of symmetry: $\rho(X_1, X_2) = \rho(X_2, X_1)$;
3. axiom of the triangle: $\rho(X_1, X_3) \le \rho(X_1, X_2) + \rho(X_2, X_3)$.

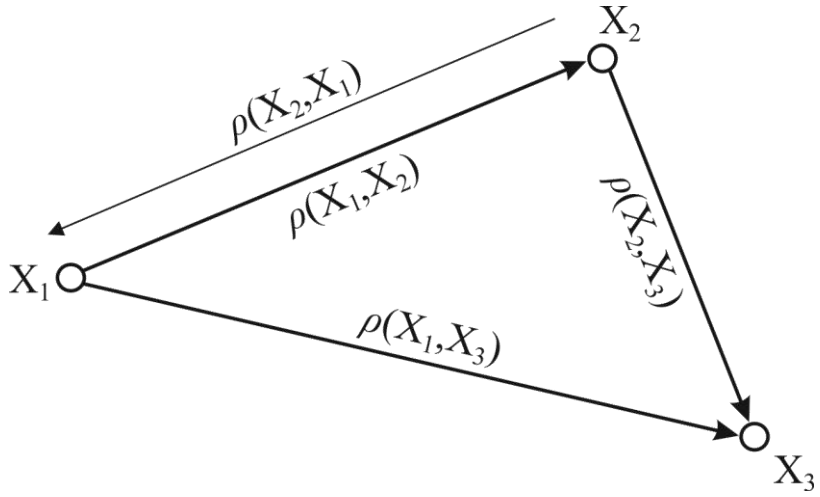

Fig. 6.1. **On the axioms of a metric space**

The elements of the metric Euclidean state space R^n are n-dimensional vectors:

$$X(t) = \left[x_1(t)\ x_2(t)\ \ldots\ x_n(t) \right]^{\mathrm{T}}, \qquad (6.1)$$

and the distance ρ is defined as the Euclidean norm of the difference between vectors $X_1(t)$ and $X_2(t)$

$$\rho\left[X_1(t), X_2(t)\right] = \left\{\left[x_{11}(t) - x_{12}(t)\right]^2 + \left[x_{21}(t) - x_{22}(t)\right]^2 + \right.$$

$$\left. + \ldots + \left[x_{n1}(t) - x_{n2}(t)\right]^2\right\}^{1/2} = \qquad (6.2)$$

$$= \left\langle\left[X_1(t) - X_2(t)\right], \left[X_1(t) - X_2(t)\right]\right\rangle^{1/2}.$$

The distance (6.2) satisfies the three axioms mentioned above. For $n = 3$, the Euclidean space is the real three-dimensional space.

The vector differential equation describing the disturbed motion of a dynamic system relative to a state of stable equilibrium has the form:

$$\dot{X}(t) = \Phi\left[X(t), \alpha\right];\ X(t) \in R^n;\ \alpha \in R^s, \qquad (6.3)$$

where α is an s-dimensional vector of the variable parameters of the dynamic system; $\Phi[X(t), \alpha]$ is an n-dimensional vector function of the components of the n-dimensional state vector $X(t)$ and the s-dimensional vector of variable parameters α. When developing the mathematical model (6.3), it is usually assumed that in the state of stable equilibrium, $X(t) = 0$.

Along with the concept of a dynamic system, we will use the concept of a **dynamic process**. If the behavior of a dynamic system is described by equation (6.3), then a dynamic process represents the solution of the differential equation (6.3) for a given initial condition $X(0)$ and a given vector of variable parameters $\alpha \in G_\alpha \in R^s$. The state vector of the dynamic process will be denoted as $X(t,\alpha)$. The endpoint of the vector $X(t,\alpha)$, called the **representative point**, describes a **phase trajectory** in the space R^n as time t changes.

The **stability of a dynamic system** is understood as the property of the system to return to the steady-state equilibrium regime after being displaced from it due to an external disturbance.

The concept of disturbed-undisturbed motion of the dynamic system (6.3) was formulated by A.M. Lyapunov. It states that at time $t = 0$, the dynamic system (6.3) instantaneously transitions from the state of stable equilibrium $X = 0$ to the point $X(0)$ and then moves on its own, without the influence of external disturbances. The definition of stability for the dynamic system (6.3) according to Lyapunov is as follows: the

state of stable equilibrium $X = 0$ of the dynamic system (6.3) is stable if, for any small positive number $\varepsilon > 0$, one can find a second positive number $r(\varepsilon) > 0$, which depends on ε, such that over time the inequality $\| X(t,\alpha) \| \le \varepsilon$ holds, provided the initial condition vector is chosen according to the inequality $\| X(0) \| \le r(\varepsilon)$.

The notation $\| X(t,\alpha) \|$ denotes the norm of the vector $X(t,\alpha)$

$$\left\| X(t,\alpha) \right\| = \rho\left[X(t,\alpha) \right] = \sqrt{\sum_{i=1}^{n} x_i^2(t,\alpha)}. \qquad (6.4)$$

Figure 6.2 shows the dependence of the norm of the state vector $X(t,\alpha)$ on time for stable and unstable dynamic systems.

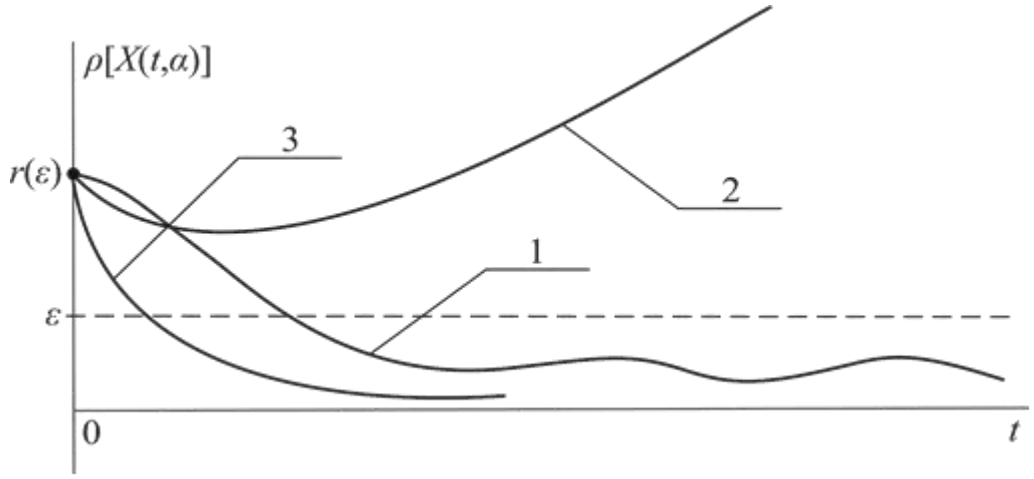

Fig. 6.2. **Dependence of the state vector norm on current time for stable (1) and unstable (2) dynamic systems**

The state of stable equilibrium of the dynamic system (6.3) is called **asymptotically stable** if for any $\varepsilon > 0$, one can choose a value $r(\varepsilon) > 0$ such that:

$$\lim_{t \to \infty} \left\| X(t,\alpha) \right\| = 0,$$

how does curve 3 in Figure 6.2 behave.

6.2. Stability of linear dynamic systems.

The disturbed motion of a linear dynamic system is described by the vector-matrix differential equation (3.8). It is known that the solution of the linear differential equation (3.8) is written in the form:

$$X(t) = X_{st}(t) + X_{per}(t), \tag{6.5}$$

where $X_{st}(t)$ is the steady-state component, representing a particular solution of the differential equation (3.8) for a given vector of external disturbances $F(t)$; $X_{per}(t)$ is the **transient component**, representing the general solution of the homogeneous differential equation:

$$\dot{X}(t) = A(\alpha)X(t). \tag{6.6}$$

A dynamic system is **stable** if the norm of the vector $X_{per}(t)$ decays over time:

$$\lim_{t\to\infty} \rho\left[X_{per}(t) \right] = \lim_{t\to\infty} \left\| X_{per}(t) \right\| = 0.$$

If the vector transient process diverges over time:

$$\lim_{t\to\infty} \rho\left[X_{per}(t) \right] = \infty,$$

then the dynamic system (3.8) is unstable.

Dynamic systems in which the vector transient process neither diverges nor decays over time are called neutral or on the stability boundary.

The solutions of the homogeneous differential equation (6.6) can be written in the form:

$$\begin{aligned}
&x_{per1}(t) = c_{11}e^{s_1 t} + c_{12}e^{s_2 t} + \ldots + c_{1n}e^{s_n t};\\
&x_{per2}(t) = c_{21}e^{s_1 t} + c_{22}e^{s_2 t} + \ldots + c_{2n}e^{s_n t};\\
&\vdots\\
&x_{per_n}(t) = c_{n1}e^{s_1 t} + c_{n2}e^{s_2 t} + \ldots + c_{nn}e^{s_n t},
\end{aligned} \tag{6.7}$$

where the constants c_{ij}, $(i, j = \overline{1,n})$ are determined by the initial conditions of the system (6.6), and the quantities s_1, s_2, …, s_n are the roots of the characteristic equation:

$$\det\left[A(\alpha) - Es \right] = 0. \tag{6.8}$$

The roots of the characteristic equation (6.8) are determined solely by the elements of matrix A and do not depend on the vector function $F(t)$. Thus, the stability of a linear dynamic system is entirely its internal property and does not depend on the external disturbances acting on the system.

The roots of the characteristic equation (6.8) can be real and complex conjugate. Let us consider these cases.

Assume one of the roots, for example s_k, is real and negative: $s_k = -\alpha_k$. Then the k-th term in the solutions (6.7), determined by this root, is:

$$c_{ik} e^{-\alpha_k t}, \ \left(i = \overline{1,n}\right).$$

Obviously, as $t \to \infty$, this term will decay. If the root s_k is positive, $s_k = \alpha_k$, then it corresponds to the k-th term in the solutions (6.7), which has the form:

$$c_{ik} e^{\alpha_k t}, \ \left(i = \overline{1,n}\right)$$

and diverges over time.

Assume the k-th and k+1 roots of the characteristic equation are complex conjugates with a negative real part:

$$s_{k,k+1} = -\alpha_k \pm j\beta_k.$$

Then the term in the solutions (6.7) corresponding to these roots has the form:

$$\begin{aligned} & c_{ik} e^{(-\alpha_k + j\beta_k)t} + c_{ik+1} e^{(-\alpha_k - j\beta_k)t} = \\ & = c_{ik} e^{-\alpha_k t} e^{j\beta_k t} + c_{ik+1} e^{-\alpha_k t} e^{-j\beta_k t} = \\ & = A_{ik} e^{-\alpha_k t} \sin\left(\beta_k t + \psi_k\right), \ \left(i = \overline{1,n}\right), \end{aligned} \qquad (6.9)$$

where

$$A_{ik} = \sqrt{c_{ik}^2 + c_{ik+1}^2}; \ \psi_k = \operatorname{arctg} \frac{c_{ik+1}}{c_{ik}}.$$

The term (6.9) represents a damped sinusoid. If the complex conjugate roots have a positive real part:

$$s_{k,k+1} = \alpha_k \pm j\beta_k,$$

the term in the solutions (6.7) corresponding to these roots is:

$$A_{ik} e^{\alpha_k t} \sin\left(\beta_k t + \psi_k\right)$$

and represents a diverging sinusoid.

Assume the k-th root of the characteristic equation is a real zero: $\alpha_k = 0$. Then the term in the solutions (6.7) corresponding to this root is written as:

$$c_{ik} e^{0 \cdot t} = c_{ik},$$

that is, it neither diverges nor decays.

And finally, assume that the k and k+1 roots of the characteristic equation (6.8) are purely imaginary:

$$s_{k,k+1} = \pm j\beta_k.$$

Then the term in the solutions (6.7) corresponding to these roots has the form:

$$A_k \sin\left(\beta_k t + \psi_k\right),$$

that is, it represents a sinusoid that neither decays nor diverges but has a constant amplitude.

Thus, the linear dynamic system (3.8) is stable if all roots of its characteristic equation (6.8) have negative real parts.

If at least one root of the characteristic equation (6.8) has a positive real part, then the dynamic system is unstable. If the characteristic equation of the dynamic system has no roots with a positive real part but has at least one root with a zero real part, then such a dynamic system is neutral, or on the stability boundary.

The direct method for investigating the stability of a linear dynamic system involves finding the roots of its characteristic equation. However, this approach is very labor-intensive, especially when the degree of the characteristic equation is higher than three. In such cases, it is very

important to find criteria that allow conclusions about the stability of the dynamic system without directly determining the roots of its characteristic equation. These criteria are called **stability criteria**.

Let us consider the stability of free vibrations of an elastic tank gun, the mathematical model of which has the form (5.34).

Consider the characteristic equation of the system of linear differential equations (5.34):

$$\det\begin{bmatrix} -s & 1 & 0 & 0 \\ 0 & -s & \alpha_{\varphi t} & \alpha_{\varphi t}\zeta \\ 0 & 0 & -s & 1 \\ 0 & 0 & \alpha_{tt} & \alpha_{tt}\zeta - s \end{bmatrix} = s^2\left(s^2 - \alpha_{tt}\zeta s - \alpha_{tt}\right) = 0.$$

The characteristic equation of system (5.34) has two zero roots; therefore, the system (5.34) is not stable. At best, it is neutral, meaning it lies on the stability boundary, as evidenced by the transient process curves shown in Figure 5.3.

The third and fourth equations of (5.34) represent a separate oscillatory subsystem model, whose processes do not depend on the first two equations of system (5.34), since the right-hand sides of these equations do not contain solutions from the first two equations of (5.34). However, changes in the components $x_3(t)$ and $x_4(t)$ influence the solutions of the first two equations of the system, as evidenced by the process $x_1(t)$ in Figure 5.3.

6.3. Algebraic stability criteria.

All stability criteria for linear dynamic systems are divided into two groups: algebraic stability criteria and frequency stability criteria. Among the algebraic stability criteria, the Routh-Hurwitz stability criterion is the most widely used.

Let us expand the determinant on the left side of the characteristic equation of the dynamic system (6.8) and write the characteristic equation in the form of an n-th order polynomial:

$$D(s) = a_0 s^n + a_1 s^{n-1} + a_2 s^{n-2} + \ldots + a_{n-1} s + a_n = 0. \qquad (6.10)$$

For the characteristic equation (6.10), we construct a square matrix of size $n \times n$, called the **Hurwitz matrix**, according to the following rule. The first row of the Hurwitz matrix is filled with the coefficients of the characteristic equation (6.10) having odd indices, and any missing elements in the first row are filled with zeros. The second row is filled with the coefficients having even indices, and any missing elements in the second row are also filled with zeros. The third row is the first row shifted one element to the right, and the fourth row is the second row shifted one element to the right. When applying this rule, the last element of the last row is the coefficient a_n of the characteristic equation. For the characteristic equation (6.10), the Hurwitz matrix takes the form:

$$\Gamma = \begin{bmatrix} a_1 & a_3 & a_5 & \dots & 0 \\ a_0 & a_2 & a_4 & \dots & 0 \\ 0 & a_1 & a_3 & \dots & 0 \\ 0 & a_0 & a_2 & \dots & 0 \\ \dots & \dots & \dots & \dots & \dots \\ 0 & 0 & 0 & \dots & a_n \end{bmatrix}. \qquad (6.11)$$

The **Routh-Hurwitz criterion** is formulated as follows: a dynamic system with the characteristic equation (6.10) is stable if, given $a_0 > 0$, all leading principal minors of the Hurwitz matrix are positive.

The leading principal minors of the Hurwitz matrix (6.11) are called the Hurwitz determinants and are written as:

$$\Delta_1 = a_1;$$

$$\Delta_2 = \begin{vmatrix} a_1 & a_3 \\ a_0 & a_2 \end{vmatrix};$$

$$\Delta_3 = \begin{vmatrix} a_1 & a_3 & a_5 \\ a_0 & a_2 & a_4 \\ 0 & a_1 & a_3 \end{vmatrix};$$

$$\vdots$$

$$\Delta_n = \det \Gamma.$$

As an example, let us consider the stability of a vehicle suspension system whose characteristic equation has the form (2.5).

Let us calculate the coefficients of the characteristic equation (2.5) using equations (1.13) and (1.20):

$$m+s=\frac{6\mu}{M_n}+\frac{2\mu\sum_{i=1}^{3}l_{ai}^2}{I_y}=2\mu\left(\frac{3}{M_n}+\frac{\sum_{i=1}^{3}l_{ai}^2}{I_y}\right);$$

$$a+d+ms-qr=\frac{6c}{M_n}+\frac{12\mu^2\sum_{i=1}^{3}l_{ai}^2}{M_nI_y}+\frac{2c\sum_{i=1}^{3}l_{pi}^2}{I_y}-\frac{4\mu^2\left(\sum_{i=1}^{3}l_{ai}\right)^2}{M_nI_y};$$

$$md+as-br-fq=\frac{12c\mu\sum_{i=1}^{3}l_{pi}^2}{M_nI_y}+\frac{6c}{M_n}\cdot\frac{2\mu\sum_{i=1}^{3}l_{ai}^2}{I_y}-\frac{2c\sum_{i=1}^{3}l_{pi}}{M_n}\cdot\frac{2\mu\sum_{i=1}^{3}l_{ai}}{I_y}-$$

$$-\frac{2c\sum_{i=1}^{3}l_{pi}}{I_y}\cdot\frac{2\mu\sum_{i=1}^{3}l_{ai}}{M_n}=\frac{24c\mu}{M_nI_y}\sum_{i=1}^{3}l_{ai}^2-\frac{8c\mu}{M_nI_y}\sum_{i=1}^{3}l_{pi}\cdot\sum_{i=1}^{3}l_{ai}=$$

$$=c\mu\frac{8}{M_nI_y}\left[3\sum_{i=1}^{3}l_{ai}^2-\left(\sum_{i=1}^{3}l_{pi}\right)\left(\sum_{i=1}^{3}l_{ai}\right)\right];$$

$$ad-fb=\frac{c^2 12\sum_{i=1}^{3}l_{pi}^2}{M_nI_y}-\frac{c^4 4\left(\sum_{i=1}^{3}l_{pi}\right)^2}{M_nI_y}=$$

$$=c^2\left[\frac{12}{M_nI_y}\sum_{i=1}^{3}l_{pi}^2-\frac{4}{M_nI_y}\left(\sum_{i=1}^{3}l_{pi}\right)^2\right]=$$

$$=c^2\frac{4}{M_nI_y}\left[3\sum_{i=1}^{3}l_{pi}^2-\left(\sum_{i=1}^{3}l_{pi}\right)^2\right].$$

Let us introduce the notation:

$$a_1 = 2\left(\frac{3}{M_n} + \frac{\sum_{i=1}^{3} l_{ai}^2}{I_y}\right);$$

$$a_{21} = \frac{6}{M_n} + \frac{2\sum_{i=1}^{3} l_{pi}^2}{I_y};$$

$$a_{22} = \frac{12\sum_{i=1}^{3} l_{ai}^2}{M_n I_y} - \frac{4\left(\sum_{i=1}^{3} l_{ai}\right)^2}{M_n I_y}; \qquad (6.12)$$

$$a_3 = \frac{8}{M_n I_y}\left[3\sum_{i=1}^{3} l_{ai}^2 - \sum_{i=1}^{3}\left(\sum_{i=1}^{3} l_{pi}\right)\left(\sum_{i=1}^{3} l_{ai}\right)\right];$$

$$a_4 = \frac{4}{M_n I_y}\left[3\sum_{i=1}^{3} l_{pi}^2 - \left(\sum_{i=1}^{3} l_{pi}\right)^2\right].$$

As a result, the characteristic equation (2.5) takes the form:

$$D(s) = s^4 + \mu a_1 s^3 + c a_{21} s^2 + \mu^2 a_{22} s^2 + c\mu a_3 s + c^2 a_4 = 0. \qquad (6.13)$$

Let the parameters of the suspension system be equal to: $M_n = 2\cdot10^4$ N·m^{-1}·s^2 (kg); $I_y = 2\cdot10^5$ N·m·s^2 (kg·m^2); $c = 0{,}33\cdot10^6$ N·m^{-1}; $\mu = 0{,}51\cdot10^5$ N·m^{-1}·c; $l_{p1} = 2$ m; $l_{p2} = -0{,}66$ m; $l_{p3} = -1{,}34$ m; $l_{a1} = 2{,}5$ m; $l_{a2} = -0{,}16$ m; $l_{a3} = -0{,}84$ m.

Using equation (6.12), let us evaluate the values of the coefficients of the characteristic equation (6.13): $a_1 = 3{,}7\cdot10^{-4}$; $a_{21} = 3\cdot10^{-4}$; $a_{22} = 20{,}87\cdot10^{-9}$; $a_3 = 20{,}871$; $a_4 = 18{,}69\cdot10^{-9}$; $\mu a_1 = 18{,}27$; $ca_{21} = 10^2$; $\mu^2 a_{22} = 54{,}26$; $c\mu a_3 = 350{,}6$; $c^2 a_4 = 2020$.

Let's form the Hurwitz matrix:

$$\Gamma = \begin{bmatrix} 18,27 & 350,6 & 0 & 0 \\ 1 & 154,26 & 2020 & 0 \\ 0 & 18,27 & 350,6 & 0 \\ 0 & 1 & 154,26 & 2020 \end{bmatrix} \qquad (6.14)$$

and calculate the leading principal minors of the matrix (6.14):

$$\Delta_1 = 18,27 > 0;$$

$$\Delta_2 = \begin{vmatrix} 18,27 & 350,6 \\ 1 & 154,26 \end{vmatrix} =$$
$$= 2818,33 - 350,6 = 2467,730 > 0;$$

$$\Delta_3 = \begin{vmatrix} 18,27 & 350,6 & 0 \\ 1 & 154,26 & 2020 \\ 0 & 18,27 & 350,6 \end{vmatrix} =$$
$$= 988106,568 - 122920,360 - 674261,658 =$$
$$= 190924,550 > 0;$$

$$\Delta_4 = 2020 \cdot \Delta_3 = 385667591 > 0.$$

All leading principal minors of the Hurwitz matrix (6.14) are positive; therefore, the vehicle suspension dynamic system with the selected values of the variable parameters *c* and μ is stable.

6.4. Frequency stability criteria.

Among the frequency stability criteria, the Mikhailov stability criterion is the most widely used. In the characteristic equation (6.10), we perform the substitution $s = j\omega$. As a result, we obtain the characteristic vector:

$$D(j\omega) = \sum_{i=0}^{n} a_i (j\omega)^{n-i} = \sum_{i=0}^{n} a_{n-i} (j\omega)^i. \qquad (6.15)$$

Let us represent the characteristic vector (6.15) as the sum of real and imaginary parts:

$$X(\omega) = \sum_{i=0}^{\lfloor n/2 \rfloor} (-1)^i a_{n-2i}\omega^{2i} = a_n - a_{n-2}\omega^2 + a_{n-4}\omega^4 - \dots ; \quad (6.16)$$

$$Y(\omega) = \sum_{i=0}^{\lfloor (n-1)/2 \rfloor} (-1)^i a_{n-1-2i}\omega^{2i+1} = a_{n-1}\omega - a_{n-3}\omega^3 + a_{n-5}\omega^5 - \dots . (6.17)$$

The hodograph of the characteristic vector (6.15) represents a curve described by the endpoint of the vector as ω varies from zero to infinity in the complex plane (X, Y) and is constructed using relations (6.16) and (6.17) (Fig. 6.3).

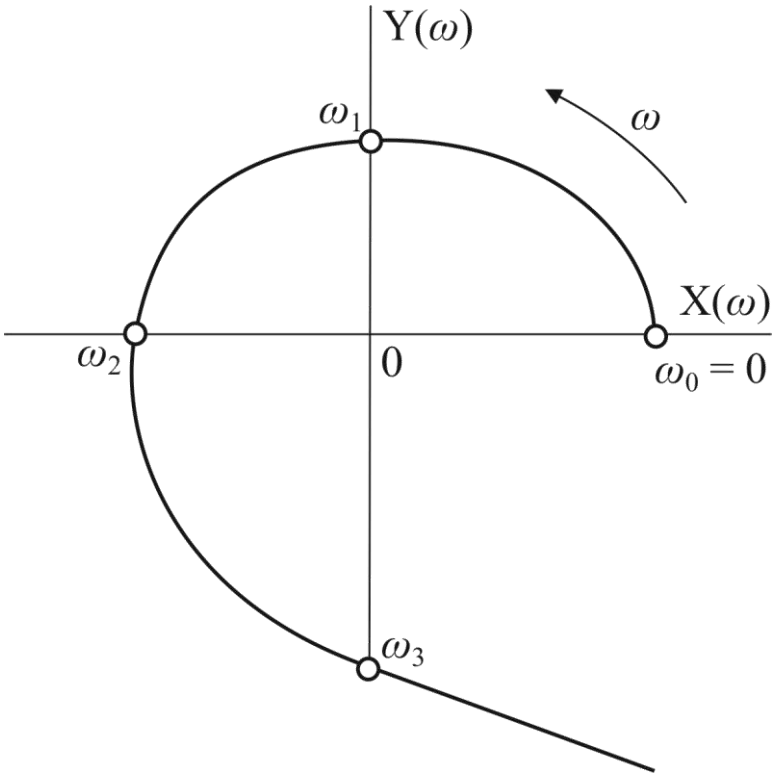

Fig. 6.3. **Hodograph of the characteristic vector**

In the characteristic polynomial (6.10), the coefficient values are: $a_0 = 1$; $a_1 = 18{,}27$; $a_2 = 154{,}26$; $a_3 = 350{,}6$; $a_4 = 2020$. Then the characteristic polynomial of the system under consideration takes the form:

$$D(s) = s^4 + 18{,}27s^3 + 154{,}26s^2 + 350{,}6s + 2020. \quad (6.18)$$

In (6.18), we perform the substitution $s = j\omega$ and obtain the characteristic vector:

$$D(j\omega) = \omega^4 - j18,27\omega^3 - 154,26\omega^2 + j350,6\omega + 2020. \quad (6.19)$$

Let us separate the real and imaginary parts in (6.19):

$$X(\omega) = \omega^4 - 154,26\omega^2 + 2020; \quad (6.20)$$

$$Y(\omega) = -18,27\omega^3 + 350,6\omega. \quad (6.21)$$

Let us find the frequencies ω_1, ω_2 and ω_3 corresponding to the points where the hodograph of the characteristic vector intersects the axes of the complex plane (X,Y). At the points corresponding to frequencies ω_1 and ω_3, the value of $X(\omega)$ is zero. Therefore, the values of frequencies $\boldsymbol{\omega_1}$ and $\boldsymbol{\omega_3}$ should be found by solving the biquadratic equation:

$$\omega_{1,3}^4 - 154,26\omega_{1,3}^2 + 2020 = 0, \quad (6.22)$$

from which:

$$\omega_{1,3}^2 = 77,13 \pm \sqrt{5949,036 - 2020} =$$

$$= 77,13 \pm \sqrt{3929,036} =$$

$$= 77,13 \pm 62,682;$$

$$\omega_1^2 = 14,448;\ \omega_3^2 = 139,812.$$

At the point corresponding to frequency ω_2, the value of $Y(\omega)$ is zero. Therefore, the value of frequency ω_2 is found from the equation:

$$-18,27\omega_2^2 + 350,6 = 0;$$

$$\omega_2^2 = 19,189.$$

The hodograph of the characteristic vector (6.19) passes sequentially through four quadrants of the complex plane (X, Y) if the frequencies ω_1, ω_2 and ω_3 satisfy the inequality:

$$\omega_1 < \omega_2 < \omega_3,$$

or

$$\omega_1^2 < \omega_2^2 < \omega_3^2. \qquad (6.23)$$

The obtained frequency values corresponding to the points where the hodograph of the characteristic vector intersects the axes of the complex plane satisfy the inequalities (6.23), meaning the considered suspension system is stable.

6.5. Constructing stability regions of linear dynamic systems in the plane of variable parameters.

Let us consider the characteristic equation (6.13), in which the variable parameters of the suspension system are identified: the spring stiffness coefficient (c) and the damper damping coefficient (μ)

$$D(s,c,\mu) = s^4 + \mu a_1 s^3 + c a_{21} s^2 + \mu^2 a_{22} s^2 + c\mu a_3 s + c^2 a_4 = 0. \quad (6.24)$$

In (6.24), we perform the substitution $s = j\omega$, separate the real and imaginary parts in the resulting expression, and set them equal to zero:

$$\omega^4 - j\mu a_1 \omega^3 - c a_{21}\omega^2 - \mu^2 a_{22}\omega^2 + jc\mu a_3 \omega + c^2 a_4 = \\ = X(\omega,c,\mu) + jY(\omega,c,\mu) = 0,$$

where

$$X(\omega,c,\mu) = \omega^4 - c a_{21}\omega^2 - \mu^2 a_{22}\omega^2 + c^2 a_4 = 0; \qquad (6.25)$$

$$Y(\omega,c,\mu) = -\mu a_1 \omega^3 + c\mu a_3 \omega = 0. \qquad (6.26)$$

From equation (6.26), we have:

$$-a_1\omega^2 + c a_3 = 0,$$

from which:

$$c = \frac{a_1}{a_3}\omega^2. \qquad (6.27)$$

Let us substitute equation (6.27) into equation (6.25):

$$\omega^4 - \frac{a_1}{a_3} a_{21}\omega^4 - \mu^2 a_{22}\omega^2 + \frac{a_1^2}{a_3^2} a_4\omega^4 = 0. \qquad (6.28)$$

From equation (6.28), we obtain:

$$\mu^2 = \frac{1}{a_{22}}\left\{1 - \frac{a_1 a_{21}}{a_3} + \frac{a_1^2 a_4}{a_3^2}\right\}\omega^2,$$

or

$$\mu = \omega\sqrt{\frac{1}{a_{22}} - \frac{a_1 a_{21}}{a_3 a_{22}} + \frac{a_1^2 a_4}{a_3^2 a_{22}}}. \qquad (6.29)$$

Using equations (6.27) and (6.29), we will construct the stability boundary in the plane of the suspension system's variable parameters (c,μ) as ω varies from zero to infinity (Fig. 6.4).

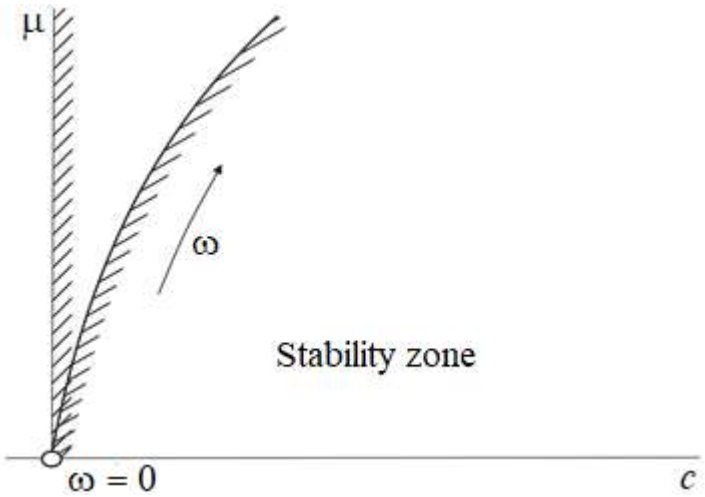

Fig. 6.4. **Stability zone of the vehicle suspension system**

To determine the stability zone of the vehicle suspension system, we will use the hatching rule, which is formulated as follows: if we move along the stability boundary in the direction of increasing ω and calculate the determinant:

$$\Delta = \begin{vmatrix} \dfrac{\partial X(\omega, c, \mu)}{\partial c} & \dfrac{\partial X(\omega, c, \mu)}{\partial \mu} \\ \dfrac{\partial Y(\omega, c, \mu)}{\partial c} & \dfrac{\partial Y(\omega, c, \mu)}{\partial \mu} \end{vmatrix}, \qquad (6.30)$$

then the stability boundary should be hatched on the left if the determinant (6.30) is positive, and on the right if it is negative. In this case, the hatching is directed towards the interior of the stability zone.

Using dependencies (6.25) and (6.26), let us compute the determinant (6.30):

$$\Delta = \begin{vmatrix} -a_{21}\omega^2 + 2ca_4 & -2\mu a_{22}\omega^2 \\ \mu a_3 \omega & 0 \end{vmatrix} = 2\mu^2 a_3 a_{22}\omega^3. \qquad (6.31)$$

The determinant (6.31) is positive for any value of ω, so the stability boundary should be hatched on the left.

Control questions for the chapter 6

1. Define a dynamic system.
2. Explain what we call the state vector of a dynamic system.
3. Define the norm of the state vector of a dynamic system.
4. Define the stability of a dynamic system according to Lyapunov.
5. How do external disturbances acting on a system affect its stability?
6. Write the mathematical model of the disturbed motion of a linear dynamic system.
7. Write the characteristic equation of a linear dynamic system.
8. How are the roots of the characteristic equation located for stable, unstable, and neutral dynamic systems?
9. Formulate the Routh-Hurwitz stability criterion.
10. Formulate the Mikhailov stability criterion.
11. What do we call the hodograph of the characteristic vector?
12. Formulate the hatching rule.

Chapter 7

STABILITY OF NONLINEAR DYNAMIC SYSTEMS.

7.1. Lyapunov's theorems on stability in the first approximation.

The mathematical model of the disturbed motion of a dynamic system in vector-matrix form is written as (3.2):

$$\dot{X} = \Phi[X(t)] + F(t). \tag{7.1}$$

If the vector function $\Phi[X(t)]$ is an analytic function of the components of the state vector $X(t)$, then it can be represented as a Taylor series in the vicinity of the stable equilibrium state $X(t) = 0$

$$\begin{aligned}\Phi[X(t)] = \Phi[0] + \left(\frac{\partial \Phi[X(t)]}{\partial X(t)}\right)_0 X(t) + \\ + \frac{1}{2!}\left(\frac{\partial^2 \Phi[X(t)]}{\partial X(t)\partial X(t)}\right)_0 X(t)X^{\mathrm{T}}(t) + \dots .\end{aligned} \tag{7.2}$$

If in the state of stable equilibrium $X(t) = 0$, then $\Phi[0] = 0$. Discarding the nonlinear terms of the expansion in equation (7.2), we obtain the linearized differential equation:

$$\dot{X}(t) = AX(t) + F(t), \tag{7.3}$$

where the elements of matrix A are determined by formulas (3.7). The dynamic system whose disturbed motion is described by the linear differential equation (7.3) will be called the system of the first approximation relative to the nonlinear system (7.1).

As indicated earlier, the stability of a dynamic system relative to a state of stable equilibrium is an internal property of the system and does not depend on external disturbances acting on the system. Therefore, in what follows, we will consider the mathematical model of a nonlinear dynamic system in the form:

$$\dot{X}(t) = \Phi[X(t)], \tag{7.4}$$

and the corresponding mathematical model of the first approximation system in the form:

$$\dot{X}(t) = AX(t). \tag{7.5}$$

Let us write the characteristic equation of the first approximation system (7.5):

$$\det\left[A - Es\right] = 0. \tag{7.6}$$

The foundation for studying the stability of nonlinear dynamic systems described by equations of the type (7.4) is based on Lyapunov's theorems on stability in the first approximation.

Theorem 1. If all roots of the characteristic equation (7.6) of the first approximation system (7.5) have negative real parts, then the nonlinear system (7.4) is stable, regardless of the terms discarded when formulating the first approximation equation.

Theorem 2. If among the roots of the characteristic equation (7.6) of the first approximation system (7.5) there is at least one root with a positive real part, then the nonlinear system (7.4) is unstable, regardless of the terms discarded when formulating the first approximation equation.

Theorem 3. If the characteristic equation (7.6) of the first approximation system (7.5) has no roots with a positive real part but has at least one root with a zero real part, then no conclusion can be drawn about the stability of the nonlinear system (7.4) based on the first approximation equation (7.5); in this case, the nonlinear system (7.4) can be either stable or unstable.

As an example, consider an oscillatory system with friction described by the Rayleigh equation (3.10). Let us write the differential equation (3.10) in the normal Cauchy form. The state vector of the dynamic system (3.10) has the form:

$$X(t) = \begin{bmatrix} x_1(t) \\ x_2(t) \end{bmatrix} = \begin{bmatrix} q(t) \\ \dot{q}(t) \end{bmatrix}.$$

As a result, we obtain:

$$\begin{aligned} \dot{x}_1(t) &= x_2(t); \\ \dot{x}_2(t) &= a_1 x_2(t) - a_3 x_2^3(t) - c x_1(t). \end{aligned} \tag{7.7}$$

The first approximation system relative to the nonlinear system of equations (7.7) is written as:

$$\begin{aligned} \dot{x}_1(t) &= x_2(t); \\ \dot{x}_2(t) &= -cx_1(t) + a_1 x_2(t). \end{aligned} \tag{7.8}$$

Let us write the characteristic equation of the first approximation system (7.8):

$$\begin{vmatrix} -s & 1 \\ -c & a_1 - s \end{vmatrix} = s^2 - a_1 s + c = 0. \tag{7.9}$$

The roots of the characteristic equation (7.9) are:

$$s_{1,2} = \frac{a_1}{2} \pm \sqrt{\frac{a_1^2}{4} - c}.$$

Both roots of the characteristic equation (7.9) of the first approximation system (7.8) have positive real parts. In this case, the state of stable equilibrium of the system (7.7) is unstable.

Suppose the disturbed motion of a dynamic system is described by the differential equations:

$$\begin{aligned} \dot{x}_1(t) &= x_2(t) + \alpha x_1^3(t); \\ \dot{x}_2(t) &= -x_1(t) + \alpha x_2^3(t). \end{aligned} \tag{7.10}$$

The first approximation system corresponding to the nonlinear system (7.10) is written as:

$$\begin{aligned} \dot{x}_1(t) &= x_2(t); \\ \dot{x}_2(t) &= -x_1(t). \end{aligned} \tag{7.11}$$

The characteristic equation of the first approximation system (7.11) has the form:

$$D(s) = \begin{vmatrix} -s & 1 \\ -1 & -s \end{vmatrix} = s^2 + 1 = 0. \tag{7.12}$$

The roots of the characteristic equation (7.12) are purely imaginary with a zero real part.

$$s_{1,2} = \pm j.$$

Thus, it is impossible to draw a conclusion about the stability of the nonlinear dynamic system (7.10) based on the analysis of its first approximation (7.11).

7.2. Theorems of the second or direct method of Lyapunov.

The general theory of stability of dynamic systems, authored by A. Lyapunov, is based on the use of special functions called Lyapunov functions.

Consider a function $V[x_1(t),x_2(t),\ldots,x_n(t)]$, whose arguments are the components of the state vector $X(t)$ of the dynamic system. The function $V[x_1(t),x_2(t),\ldots,x_n(t)]$ is a sign-definite function of its arguments if it equals zero only at one point in the phase space R^n: $x_1 = x_2 = x_3 = \ldots = x_n = 0$, and at all other points of the phase space, it has the same sign..

An example of a positive-definite function in a two-dimensional phase space is the function:

$$V\left[x_1(t), x_2(t)\right] = x_1^2(t) + x_2^2(t). \qquad (7.13)$$

The function (7.13) equals zero only at the point $x_1 = x_2 = 0$, and at all other points of the two-dimensional phase space, it has a positive value (Fig. 7.1).

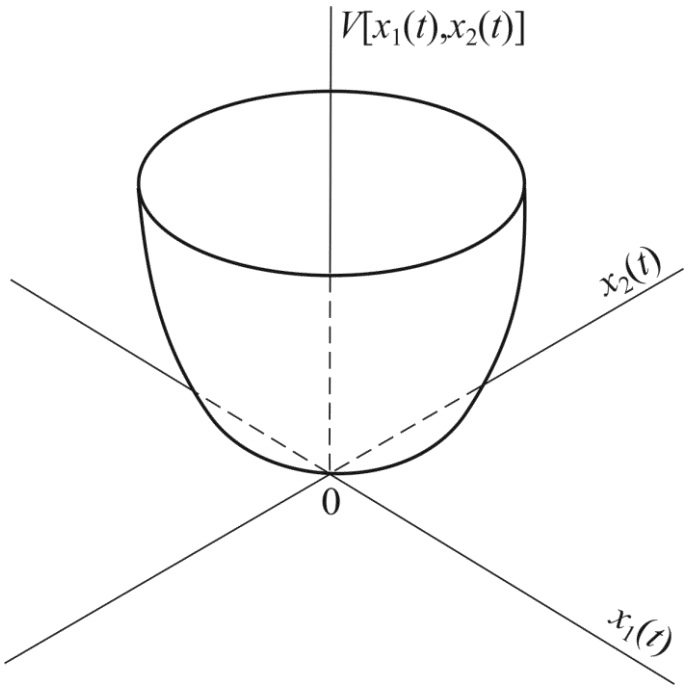

Fig. 7.1. **Example of a positive-definite function**

The function $V[x_1(t),x_2(t),\ldots,x_n(t)]$ is a sign-constant function of its arguments if it equals zero not only at the point $x_1 = x_2 = x_3 = \ldots = x_n = 0$, but also at some other points of the n-dimensional phase space, and at all other points it has the same sign.

An example of a positive sign-constant function in a two-dimensional phase space is the function:

$$V\left[x_1(t), x_2(t)\right] = \left[x_1(t) + x_2(t)\right]^2. \qquad (7.14)$$

The function (7.14) equals zero not only at the point $x_1 = x_2 = 0$, but also everywhere where $x_1 = -x_2$, and at all other points of the two-dimensional phase space, it has a positive value (Fig. 7.2).

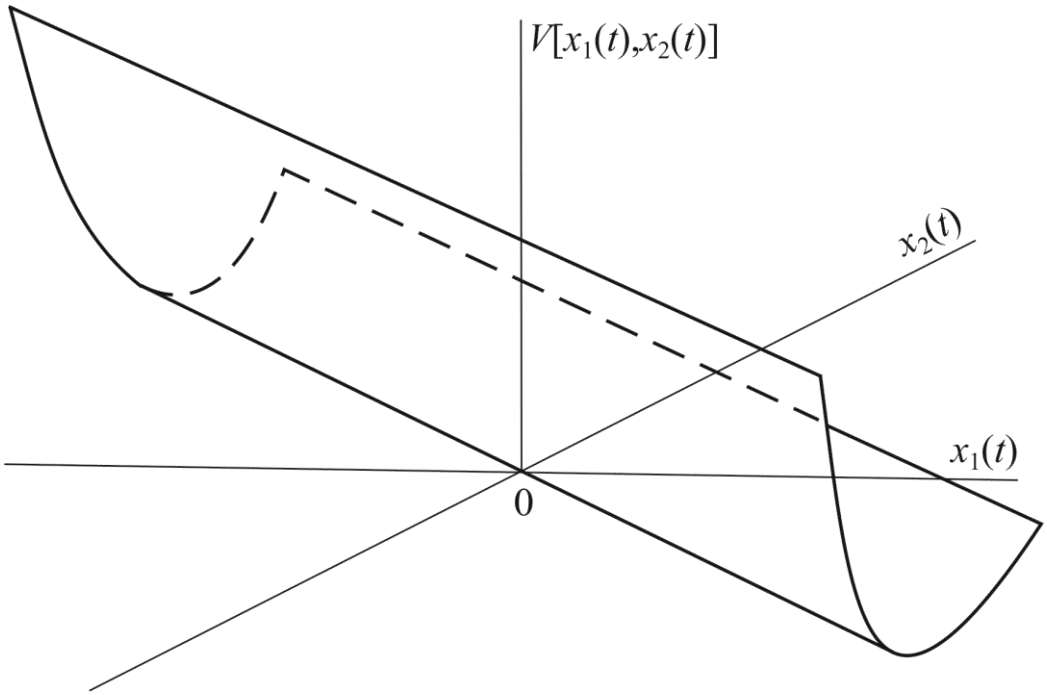

Fig. 7.2. **Example of a positive sign-constant function**

Theorems of A. Lyapunov on the Stability of Motion of Dynamic Systems, which form the basis of the second, or direct, method of Lyapunov, are formulated as follows.

***Theorem* 1.** If the differential equation of the disturbed motion of a dynamic system (7.4) is such that one can specify a sign-definite function $V[X(t)]$ for which the total time derivative of this function, computed in accordance with equation (7.4), is a sign-constant function of the opposite sign to $V[X(t)]$, or is identically zero, then the disturbed motion of the dynamic system is stable.

Theorem 2. If the differential equation of the disturbed motion of a dynamic system (7.4) is such that one can specify a sign-definite function $V[X(t)]$ for which the total time derivative of this function, computed in accordance with equation (7.4), is a sign-definite function of the opposite sign to $V[X(t)]$, then the disturbed motion of the dynamic system is asymptotically stable.

The total time derivative of the function $V[X(t)]$, computed in accordance with equation (7.4), is equal to:

$$W\left[X(t)\right] = \frac{dV\left[X(t)\right]}{dt} = \left\langle \frac{\partial V\left[X(t)\right]}{\partial X(t)}, \frac{\partial X(t)}{\partial t} \right\rangle =$$

$$= \sum_{i=1}^{n} \frac{\partial V\left[X(t)\right]}{\partial x_i(t)} \cdot \frac{\partial x_i(t)}{\partial t} = \sum_{i=1}^{n} \frac{\partial V\left[X(t)\right]}{\partial x_i(t)} \cdot \dot{x}_i(t) = \qquad (7.15)$$

$$= \sum_{i=1}^{n} \frac{\partial V\left[X(t)\right]}{\partial x_i(t)} \cdot \varphi_i\left[X(t)\right].$$

As an example, let us consider the stability of the dynamic system (7.10). We choose a positive definite Lyapunov function for system (7.10) in the form of (7.13).

Let us compute the total time derivative of function (7.13) in accordance with equations (7.10), using formula (7.15):

$$\frac{dV\left[X(t)\right]}{dt} = \frac{\partial V\left[X(t)\right]}{\partial x_1(t)} \dot{x}_1(t) + \frac{\partial V\left[X(t)\right]}{\partial x_2(t)} \dot{x}_2(t) =$$

$$= 2x_1(t)\left[x_2(t) + \alpha x_1^3(t) \right] + 2x_2(t)\left[-x_1(t) + \alpha x_2^3(t) \right] = \qquad (7.16)$$

$$= 2\alpha\left[x_1^4(t) + x_2^4(t) \right].$$

When $\alpha < 0$ the total time derivative of the positive definite Lyapunov function (7.13) is a negative definite function. Therefore, for $\alpha < 0$ the dynamic system (7.10) is asymptotically stable.

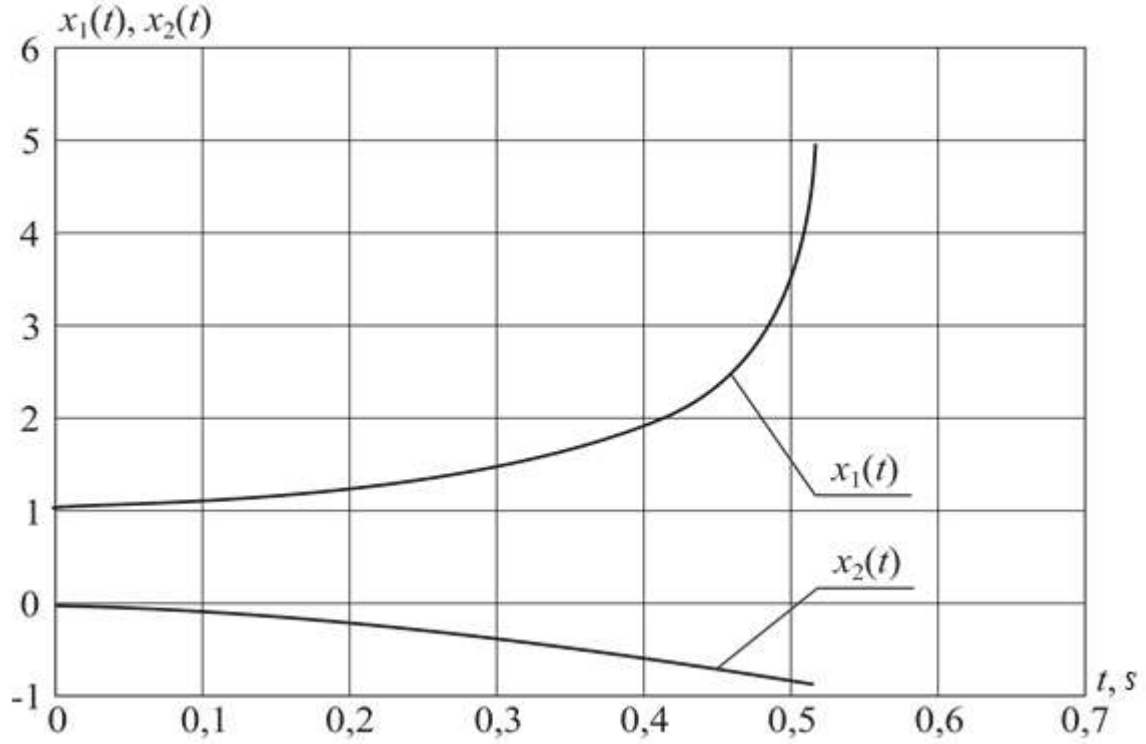

Fig. 7.3.a. **Solution of the system of differential equations (7.10), where α = 1**

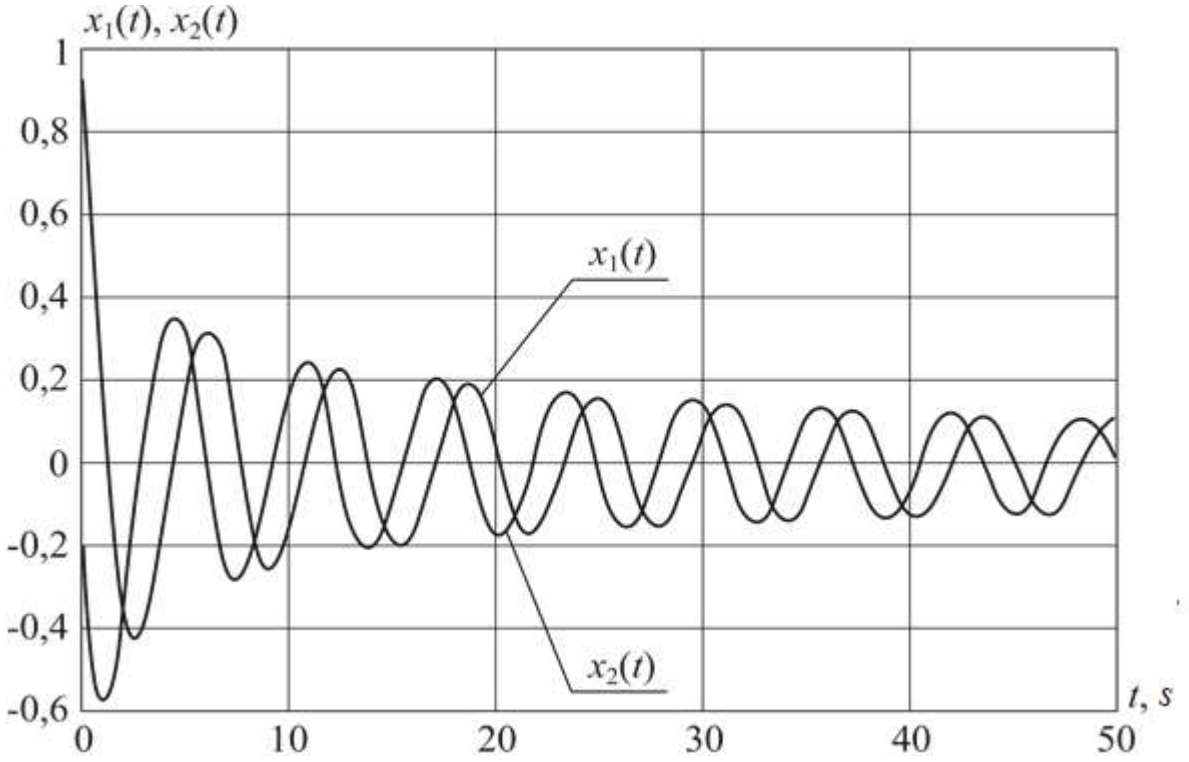

Fig. 7.3.b. **Solution of the system of differential equations (7.10), where α = –1**

Figure 7.3 shows the solutions of the system of differential equations (7.10) under the initial conditions $x_1(0) = 1$; $x_2(0) = 0$. Variant *a* corresponds to α = +1, and variant *b* corresponds to α = –1.

7.3. Lyapunov's theorem on the instability of motion of dynamic systems.

Lyapunov's theorem on the instability of the state of stable equilibrium of a dynamic system is formulated as follows.

Theorem. If the equation of the disturbed motion of a dynamic system (7.4) relative to the state of stable equilibrium $x_1 = x_2 = \ldots = x_n = 0$ is such that one can specify a sign-definite function $V[x_1(t),x_2(t),\ldots,x_n(t)]$, whose total time derivative computed in accordance with equation (7.4), $\dot{V}[x_1(t),x_2(t),\ldots,x_n(t)]$ has the same sign as $V[x_1(t),x_2(t),\ldots,x_n(t)]$, then the state of stable equilibrium is unstable; that is, the motion of the dynamic system in the vicinity of the stable equilibrium state is unstable.

As an example, consider a dynamic system whose disturbed motion in the vicinity of the stable equilibrium $x_1 = x_2 = 0$ is described by the differential equations:

$$\begin{aligned} \frac{dx_1(t)}{dt} &= 3x_2(t) + 4x_1^3(t) + x_1^5(t); \\ \frac{dx_2(t)}{dt} &= -5x_1(t) + 3x_2^5(t). \end{aligned} \tag{7.17}$$

Let us choose the Lyapunov function $V[x_1(t),x_2(t)]$ in the form:

$$V\left[x_1(t), x_2(t)\right] = 5x_1^2(t) + 3x_2^2(t). \tag{7.18}$$

Let us compute the total time derivative of the positive definite function (7.18) in accordance with equations (7.17):

$$\begin{aligned} \frac{dV\left[x_1(t), x_2(t)\right]}{dt} &= \frac{\partial V\left[x_1(t), x_2(t)\right]}{\partial x_1(t)} \cdot \left[3x_2(t) + 4x_1^3(t) + x_1^5(t)\right] + \\ &+ \frac{\partial V\left[x_1(t), x_2(t)\right]}{\partial x_2(t)} \cdot \left[-5x_1(t) + 3x_2^5(t)\right] = \\ &= 10x_1(t)\left[3x_2(t) + 4x_1^3(t) + x_1^5(t)\right] + 6x_2(t)\left[-5x_1(t) + 3x_2^5(t)\right] = \\ &= 30x_1(t)x_2(t) + 40x_1^4(t) + 10x_1^6(t) - \\ &-30x_2(t)x_1(t) + 18x_2^6(t) = 40x_1^4(t) + 10x_1^6(t) + 18x_2^6(t). \end{aligned} \tag{7.19}$$

For any $x_1(t)$ and $x_2(t)$ the functions $V[x_1(t),x_2(t)]$ and $\dot{V}[x_1(t),x_2(t)]$ are positive-definite, meaning they have the same sign. Therefore, the state of stable equilibrium $x_1 = x_2 = 0$ is unstable, and the motion of the dynamic system in the vicinity of this equilibrium state is unstable.

Figure 7.4 shows the solutions of the system of differential equations (7.17) under the initial conditions $x_1(0) = 1$; $x_2(0) = 0$, which confirm the instability of the system (7.17).

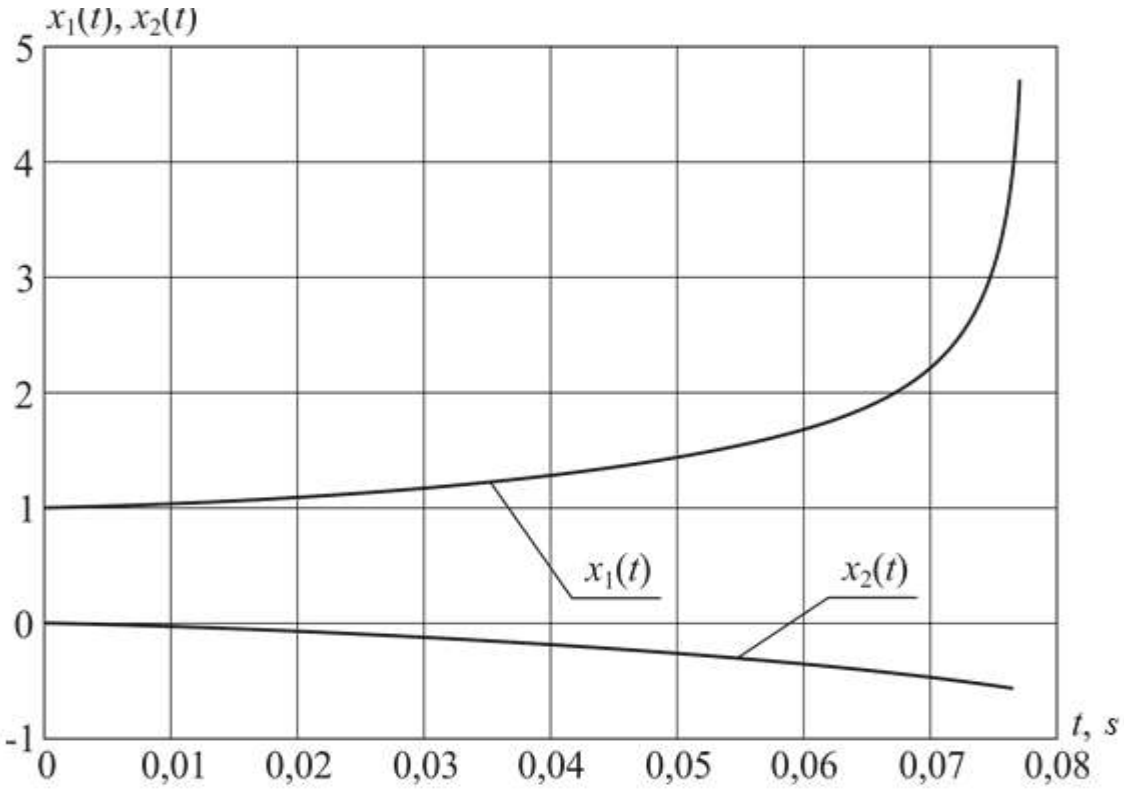

Fig. 7.4. **Solution of the system of differential equations (7.17)**

Control questions for the chapter 7.

1. What do we call the first approximation of a dynamic system?
2. Write the formula for the characteristic equation of the first approximation system.
3. What can be said about the stability of a nonlinear dynamic system if the real parts of all roots of the characteristic equation of its first approximation system have negative values?
4. What can be said about the stability of a nonlinear dynamic system if among the roots of the characteristic equation of its first approximation system there is one root with a positive real part?

5. What can be said about the stability of a nonlinear dynamic system if among the roots of the characteristic equation of its first approximation system there is one root with a zero real part, while all other roots have negative real parts?
6. Define a sign-definite function of its arguments.
7. Define a sign-constant function of its arguments.
8. Formulate Lyapunov's theorem on the stability of motion of dynamic systems.
9. Formulate Lyapunov's theorem on the asymptotic stability of motion of dynamic systems.
10. Formulate Lyapunov's theorem on the instability of motion of dynamic systems.

APPENDIX 1

METHODOLOGICAL GUIDELINES FOR COMPLETING CALCULATION-GRAPHIC WORK NO. 1.

Topic of calculation-graphic work (CGW) No. 1: "Selection of the crankshaft design parameters for an automotive diesel engine according to the requirement of absence of resonance phenomena."

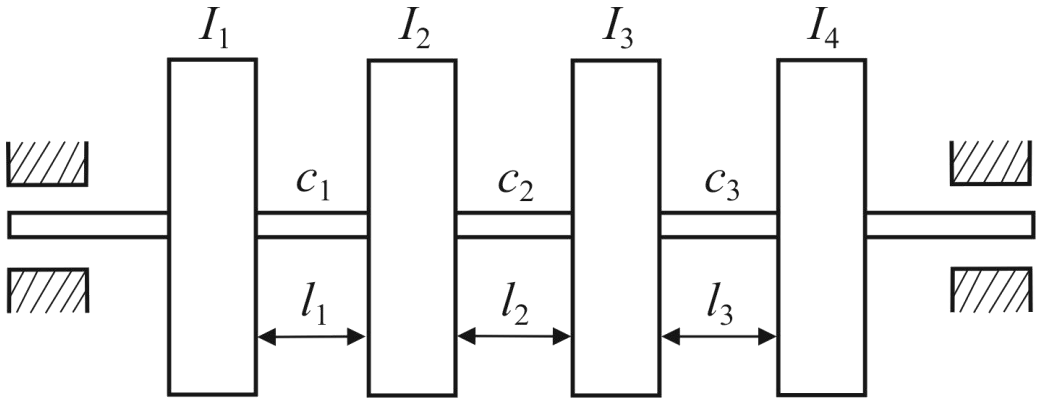

Fig. A.1. **Equivalent scheme of an automotive engine crankshaft**

Input data for CGW No. 1. Let us consider the torsional vibrations of a multi-mass system, the calculation scheme of which is shown in Figure A1. This scheme is generally accepted, though not flawless, for calculating torsional vibrations of internal combustion engine crankshafts (both gasoline and diesel). The reduction of a real crankshaft to a straight shaft scheme is based on the following assumptions:

- The polar moment of inertia of a disc about the shaft axis must equal the polar moment of inertia of the crank throw, taking into account the associated mass of the connecting rod and piston;
- The torsional stiffness of the shaft section between discs must equal the torsional stiffness of the corresponding part of the crankshaft.

These assumptions cannot fully ensure the complete equivalence of the substitute scheme and the real crankshaft. This is because the reduced polar moment of inertia of the crank throw and connecting rod assembly changes during the crankshaft rotation due to the piston's motion in the cylinder. Therefore, replacing the crank and connecting rod with a disc of constant moment of inertia is not strictly rigorous. Despite its shortcomings, the substitute scheme is satisfactory. Numerous experiments confirm the acceptability of the substitute scheme, provided

the equivalent moments of inertia and stiffnesses are determined with sufficient care.

In the adopted substitute scheme in Figure A1, we will take the values of the moments of inertia and stiffnesses as equal to:

$$I_1 = I_2 = I_3 = I_4 = I; \tag{A.1}$$

$$\begin{aligned} c_1 = c_2 = c_3 = c, \\ l_1 = l_2 = l_3 = l, \end{aligned} \tag{A.2}$$

where I = 80 N·m·s^2; $c = 2 \cdot 10^6$ N·m; l = 0,25 m.

Sequence for completing CGW No. 1. The frequency equation, according to formula (4.5), is written as:

$$\Delta(k^2) = \begin{vmatrix} c_1 - k^2 I_1 & -c_1 & 0 & 0 \\ -c_1 & c_1 + c_2 - k^2 I_2 & -c_2 & 0 \\ 0 & -c_2 & c_2 + c_3 - k^2 I_3 & -c_3 \\ 0 & 0 & -c_3 & c_3 - k^2 I_4 \end{vmatrix} = 0. \tag{A.3}$$

Taking into account relations (A.1) and (A.2), the frequency equation (A.3) reduces to the form:

$$\Delta(k^2) = \begin{vmatrix} c - k^2 I & -c & 0 & 0 \\ -c & 2c - k^2 I & -c & 0 \\ 0 & -c & 2c - k^2 I & -c \\ 0 & 0 & -c & c - k^2 I \end{vmatrix} = 0. \tag{A.4}$$

Let us sum all the rows of the determinant (A.4) and place the corresponding sums into the first row:

$$\Delta(k^2) = \begin{vmatrix} -k^2 I & -k^2 I & -k^2 I & -k^2 I \\ -c & 2c - k^2 I & -c & 0 \\ 0 & -c & 2c - k^2 I & -c \\ 0 & 0 & -c & c - k^2 I \end{vmatrix} = 0. \tag{A.5}$$

All elements of the first row of the determinant (A.5) are identical; therefore, let us reduce the determinant (A.5) to the form:

$$\Delta(k^2) = -k^2 \begin{vmatrix} I & I & I & I \\ -c & 2c - k^2 I & -c & 0 \\ 0 & -c & 2c - k^2 I & -c \\ 0 & 0 & -c & c - k^2 I \end{vmatrix} = 0. \qquad \text{(A.6)}$$

Expanding the determinant (A.6), we obtain the frequency equation (A.6) in the form:

$$\Delta(k^2) = k^2 \left[k^6 - \frac{6c}{I} k^4 + \frac{10c^2}{I^2} k^2 - \frac{4c^3}{I^3} \right] = 0. \qquad \text{(A.7)}$$

The resulting equation has one root $k^2 = 0$, which corresponds to the uniform rotation of the crankshaft without deformation, i.e., without torsional vibrations. The other roots correspond to the frequencies k_1, k_2 and k_3 of the natural torsional vibrations. To find them, it is necessary to solve the algebraic equation:

$$k^6 - \frac{6c}{I} k^4 + \frac{10c^2}{I^2} k^2 - \frac{4c^3}{I^3} = 0. \qquad \text{(A.8)}$$

For the crankshaft parameters $I = 80$ N·m·s^2 and $c = 2 \cdot 10^6$ N·m, the roots of equation (A.8) are: $k_1 = 125$ s^{-1}; $k_2 = 231$ s^{-1}; $k_3 = 303$ s^{-1}. The operating frequency range of the automotive diesel engine is: $\omega_{min} = 50$ s^{-1}; $\omega_{max} = 280$ s^{-1}.

For the selected operating frequency range of the internal combustion engine crankshaft, the stiffness value $c = 2 \cdot 10^6$ N·m of the shaft segments between the discs does not protect the engine from resonant regimes. Indeed, the natural frequencies of torsional vibrations of the shaft $k_1 = 125$ s^{-1} and $k_2 = 231$ s^{-1} fall within the selected operating frequency range of the crankshaft.

The stiffness of the part of the crankshaft between the discs is determined by the equation:

$$c = \frac{GI_p}{l}, \qquad \text{(A.9)}$$

where l – is the length of the part of the crankshaft between the discs; G – is the shear modulus, whose average value for steel is

$G = 8{,}3 \cdot 10^{10}$ N·m^{-2}; I_p – is the polar geometric moment of inertia of the cross-section of the crankshaft part between the discs, determined by the equation:

$$I_p = \frac{\pi D^4}{32}, \tag{A.10}$$

where D – the diameter of the cross-sectional circle.

Let us substitute (A.10) into (A.9). As a result, we have:

$$c = \frac{G\pi D^4}{32l}. \tag{A.11}$$

Analysis of equation (A.11) leads to the conclusion that the stiffness value of the crankshaft part between the discs depends, firstly, on the diameter D and, secondly, on the length l. Moreover, the dependence on the diameter D is proportional to the fourth power of D, meaning this dependence is very strong.

Designing an internal combustion engine of the required power involves selecting the moment of inertia I for the equivalent scheme and the distance l between the discs. Therefore, it is undesirable to change these quantities when implementing anti-resonance measures. That is, the only variable parameter is the choice of the diameter D, for which the roots of the frequency equation (A.8) lie outside the range (ω_{min}, ω_{max}) of the operating frequencies of the internal combustion engine crankshaft.

The frequency equation (A.8), taking into account equation (A.11), is written as:

$$k^6 - \frac{6G\pi D^4}{32lI}k^4 + \frac{10G^2\pi^2 D^8}{1024l^2I^2}k^2 - \frac{4G^3\pi^3 D^{12}}{32768l^3I^3} = 0,$$

or

$$k^6 - \frac{G\pi D^4}{5{,}33lI}k^4 + \frac{G^2\pi^2 D^8}{102{,}4l^2I^2}k^2 - \frac{G^3\pi^3 D^{12}}{8192l^3I^3} = 0. \tag{A.12}$$

For the selected stiffness value of the crankshaft parts between the discs, we will find its diameter D using equation (A.9):

$$I_p = \frac{cl}{G} = \frac{2 \cdot 10^6 \text{ N} \cdot \text{m} \times 0{,}25 \text{ m}}{8{,}3 \cdot 10^{10} \text{ N} \cdot \text{m}^{-2}} = \frac{0{,}5 \cdot 10^6}{8{,}3 \cdot 10^{10}} \text{m}^4 = 0{,}6 \cdot 10^{-5} \text{ m}^4.$$

According to formula (A.10), we have:

$$D = \sqrt[4]{\frac{32I_p}{3{,}14}} = \sqrt[4]{\frac{32 \times 0{,}06 \cdot 10^{-4}}{3{,}14}} =$$
$$= \sqrt[4]{0{,}611 \cdot 10^{-4}} = \sqrt{0{,}78 \cdot 10^{-2}} =$$
$$= 0{,}088 \text{ m}.$$

We will vary the diameter of the crankshaft part between the discs and evaluate the natural frequencies of the crankshaft vibrations. The results will be placed in Table A.1.

Table A.1 – **Dependence of the natural frequencies of crankshaft vibrations on the variable parameter *D*.**

D, m	k_1, s^{-1}	k_2, s^{-1}	k_3, s^{-1}
0,08	99	182	239
0,088	125	231	303
0,1	155	285	374
0,11	187	345	452
0,14	303	558	723
0,15	348	641	840

Analysis of the data presented in Table A.1 proves that for $D \geq 0{,}14$ m, all roots of the frequency equation (A.12) leave the range of operating frequencies of the internal combustion engine crankshaft (Fig. A2).

In Figure A2, the operating frequency range of the internal combustion engine ($\omega_{min} = 50$ s^{-1} – $\omega_{max} = 280$ s^{-1}) is shaded. The roots of the frequency equation (A.12) leave the shaded zone at $D \geq 0{,}137$ m, therefore, the diameter of the crankshaft part between the discs must satisfy the inequality:

$$D \geq 0{,}14 \text{ m}.$$

Thus, when $D \geq 0{,}14$ m, resonance phenomena do not occur in the designed internal combustion engine.

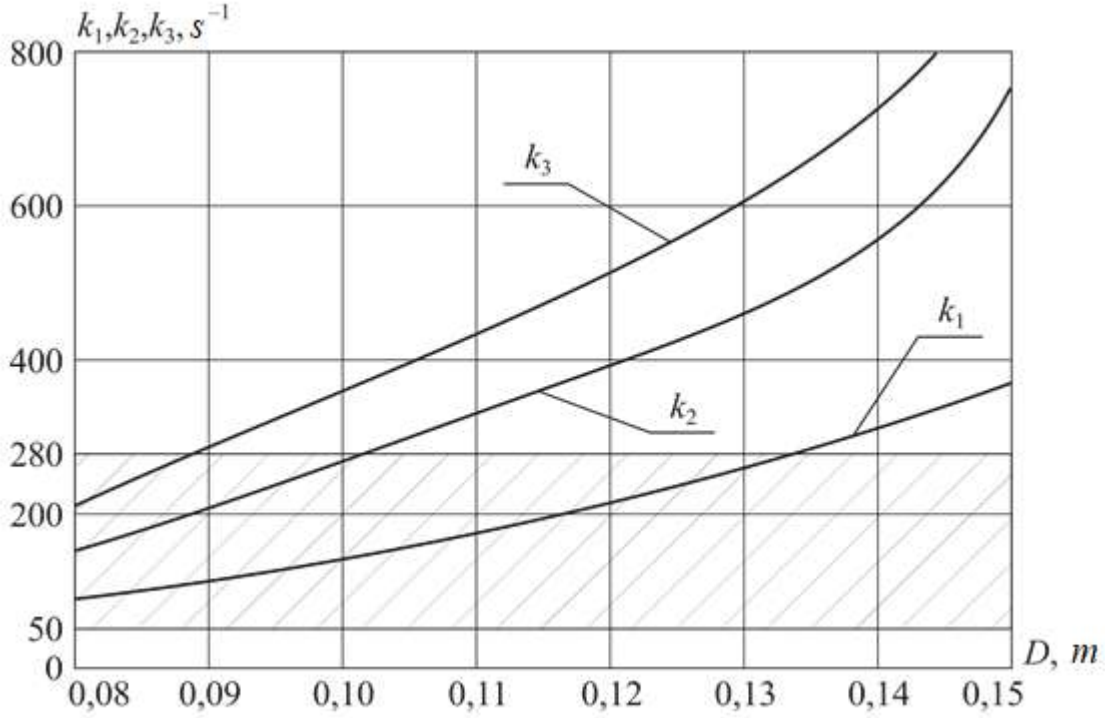

Fig. A2. **Dependence of the roots of the frequency equation on the diameter of the crankshaft parts between the discs**

Object of Study. Resonance phenomena in a four-cylinder, four-stroke automotive internal combustion engine are associated with the torsional vibrations of the crankshaft:

a) Operating frequency range of the ICE: $(50 \div 280)$ s^{-1};

b) Moment of inertia of the crank throw, taking into account the associated mass of the connecting rod and piston: $I = (50 + n \cdot 5)$ $N \cdot m \cdot s^2$, where n – is the number according to the academic group list;

c) Length of the crankshaft part between the crank throws: $(0{,}20 + n \cdot 0{,}01)$ m;

d) Shear modulus value for the crankshaft material: $G = 8{,}3 \cdot 10^{10}$ $N \cdot m^{-2}$;

e) Diameter of the crankshaft part is varied from $D_{min} = 0{,}05$ m to the value at which all roots of the frequency equation (A.12) leave the operating frequency range of the ICE, with a step of $\Delta D = 0{,}01$ m;

f) Fill in Table A.1 and construct Fig. A2;

g) Draw general conclusions.

APPENDIX 2

METHODOLOGICAL GUIDELINES FOR COMPLETING CALCULATION-GRAPHIC WORK NO. 2.

Topic of calculation-graphic work No. 2: "Constructing stability regions of the vehicle directional stability system in the plane of the electronic control unit's variable parameters."

Input data for CGW No. 2. Let us consider the angular oscillations of a vehicle body equipped with a Vehicle Stability Control (VSC) system, described by the second equation of (5.39):

$$\ddot{\psi}(t) = -\frac{BK_g}{2I}\Delta p(t) - \frac{2H_m M}{I} v(t)\dot{\psi}(t) f_0 + \frac{1}{I} M_\psi(t). \qquad \text{(A.13)}$$

The difference in brake fluid pressure between the brake lines of the right and left sides of the vehicle.

$$\Delta p(t) = p_r(t) - p_l(t)$$

is generated by the actuator of the VSC system, the schematic diagram of which is shown in Figure A3.

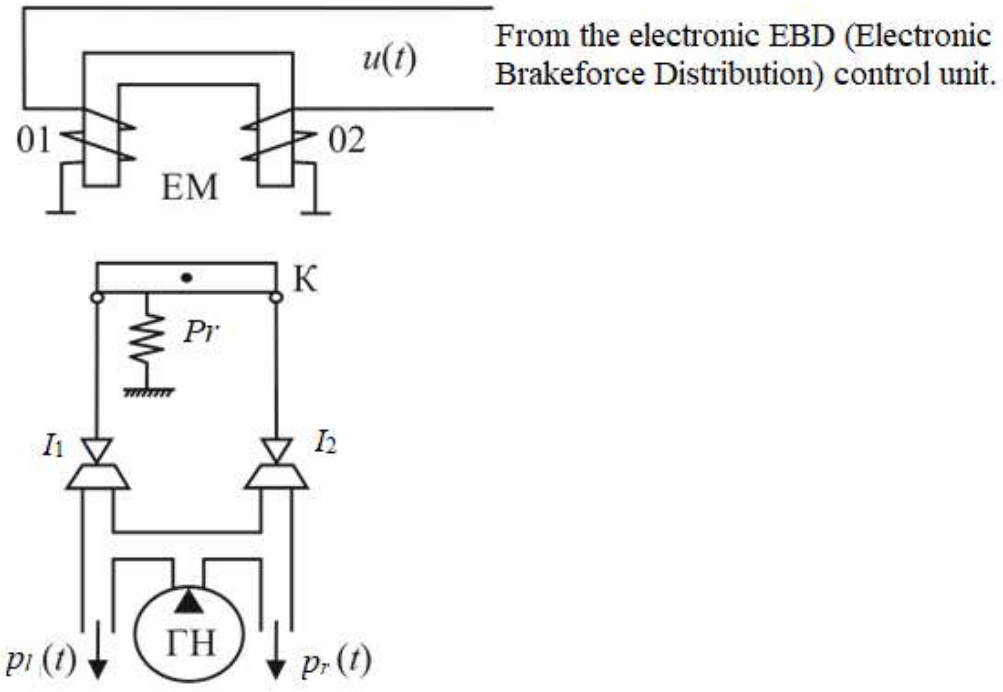

Fig. A3. **Schematic diagram of the VSC system actuator**

The Electronic Brakeforce Distribution (EBD) control unit, based on the output signals from the sensors, generates a control signal in the form of:

$$u(t) = k_1\psi(t) + k_2\dot{\psi}(t), \qquad \text{(A.14)}$$

where k_1 and k_2 – are the variable parameters of the EBD. The signal $|u(t)|$ is applied to the winding 01, if $u(t) < 0$, , or to the winding 02, if $u(t) \geq 0$, This causes the rocker arm K to rotate by a negative angle $\gamma(t)$ (clockwise) in the first case, or by a positive angle $\gamma(t)$ (counterclockwise) in the second case. In this case, the disturbed motion of the rocker arm K is described by the differential equation:

$$I_k\ddot{\gamma}(t) + f_k\dot{\gamma}(t) + c_k\gamma(t) = k_{\text{EM}}u(t), \qquad \text{(A.15)}$$

and the difference in brake fluid pressure between the brake lines of the right and left sides of the vehicle is proportional to the rocker arm's rotation angle $\gamma(t)$

$$\Delta p(t) = k_p\gamma(t). \qquad \text{(A.16)}$$

The following notations are used in the differential equation (A.15): I_k – moment of inertia of the rocker arm K about its axis of rotation; f_k – coefficient of viscous friction in the rotation axis; c_k – stiffness coefficient of the spring *Pr*, , which fixes the rocker arm in the neutral state when $u(t) = 0$; k_{EM} – gain coefficient of the electromagnet EM.

Taking into account relations (A.14) and (A.16), the differential equation (A.15) takes the following form:

$$\Delta\ddot{p}(t) = -\frac{f_k}{I_k}\Delta\dot{p}(t) - \frac{c_k}{I_k}\Delta p(t) + \frac{k_{\text{EM}}k_p}{I_k}\left[k_1\psi(t) + k_2\dot{\psi}(t)\right]. \qquad \text{(A.17)}$$

The differential equations (A.13) and (A.17) together represent the mathematical model of the closed-loop vehicle directional stability system.

Sequence for completing the CGW. In the mathematical model (A.13), (A.17), let us introduce the notation:

$$\frac{BK_{\text{g}}}{2I} = a_{\psi p};\ \frac{2H_mM}{I}f_0 = a'_{\psi\psi};\ \frac{f_k}{I_k} = a'_{pp};\ \frac{c_k}{I_k} = a_{pp};\ \frac{k_{\text{EM}}k_p}{I_k} = k.$$

As a result, the mathematical model (A.13), (A.17) takes the following form:

$$\begin{aligned}\ddot{\psi}(t) &= -a_{\psi p}\Delta p(t) - a'_{\psi\psi}v(t)\dot{\psi}(t);\\ \Delta\ddot{p}(t) &= -a_{pp}\Delta p(t) - a'_{pp}\Delta\dot{p}(t) + kk_1\psi(t) + kk_2\dot{\psi}(t).\end{aligned} \qquad \text{(A.18)}$$

Let us reduce the system of differential equations (A.18) to the normal Cauchy form. To do this, consider the system's state vector:

$$X(t) = \begin{bmatrix} x_1(t)\\ x_2(t)\\ x_3(t)\\ x_4(t)\end{bmatrix} = \begin{bmatrix} \psi(t)\\ \dot{\psi}(t)\\ \Delta p(t)\\ \Delta\dot{p}(t)\end{bmatrix}.$$

As a result, we have:

$$\begin{aligned}\dot{x}_1(t) &= x_2(t);\\ \dot{x}_2(t) &= -a'_{\psi\psi}v(t)x_2(t) - a_{\psi p}x_3(t);\\ \dot{x}_3(t) &= x_4(t);\\ \dot{x}_4(t) &= kk_1x_1(t) + kk_2x_2(t) - a_{pp}x_3(t) - a'_{pp}x_4(t).\end{aligned} \qquad \text{(A.19)}$$

The mathematical model (A.19) is non-stationary because the coefficient $-\alpha'_{\psi\psi}v(t)$ depends on the current time. To study such a system, we will use the "frozen" coefficients method. We will assume that the vehicle's speed values at time instances t_0, t_1, t_2, …, t_n are constant and construct stability regions for each of these moments $t_k \in [0,\tau]$, $(k = \overline{0,n})$ in the plane of variable parameters (k_1, k_2). Let us introduce the notation $v_k = v(t_k)$ and write the system of differential equations (A.19) in the form:

$$\begin{aligned}\dot{x}_1(t) &= x_2(t);\\ \dot{x}_2(t) &= -a'_{\psi\psi}v_kx_2(t) - a_{\psi p}x_3(t);\\ \dot{x}_3(t) &= x_4(t);\\ \dot{x}_4(t) &= kk_1x_1(t) + kk_2x_2(t) - a_{pp}x_3(t) - a'_{pp}x_4(t),\\ &\left(k = \overline{0,n}\right).\end{aligned} \qquad \text{(A.20)}$$

The system matrix of (A.20) is equal to:

$$A=\begin{bmatrix} 0 & 1 & 0 & 0 \\ 0 & -a'_{\psi\psi}v_k & -a_{\psi p} & 0 \\ 0 & 0 & 0 & 1 \\ kk_1 & kk_2 & -a_{pp} & -a'_{pp} \end{bmatrix}, \quad \left(k=\overline{0,n}\right).$$

Let us write the characteristic polynomial of the system (A.20) in the form:

$$D(s)=\det(A-Es)=$$

$$=\begin{vmatrix} -s & 1 & 0 & 0 \\ 0 & -a'_{\psi\psi}v_k-s & -a_{\psi p} & 0 \\ 0 & 0 & -s & 1 \\ kk_1 & kk_2 & -a_{pp} & -a'_{pp}-s \end{vmatrix}, \left(k=\overline{0,n}\right). \qquad \text{(A.21)}$$

Let us expand the determinant (A.21) by the elements of the first row:

$$D(s)=s^4+\left(a'_{pp}+a'_{\psi\psi}v_k\right)s^3+\left(a_{pp}+a'_{pp}a'_{\psi\psi}v_k\right)s^2+$$
$$+\left(a_{pp}a'_{\psi\psi}v_k+a_{\psi p}kk_2\right)s+a_{\psi p}kk_1, \qquad \text{(A.22)}$$
$$\left(k=\overline{0,n}\right).$$

In the characteristic polynomial (A.22), we perform the substitution $s = j\omega$ and obtain the relation for the characteristic vector:

$$D(j\omega)=\omega^4-j\left(a'_{pp}+a'_{\psi\psi}v_k\right)\omega^3-\left(a_{pp}+a'_{pp}a'_{\psi\psi}v_k\right)\omega^2+$$
$$+ja_{pp}a'_{\psi\psi}v_k\omega+ja_{\psi p}kk_2\omega+a_{\psi p}kk_1, \qquad \text{(A.23)}$$
$$\left(k=\overline{0,n}\right).$$

The characteristic vector of a **neutral dynamic system** (a system on the stability boundary) passes through the origin of the complex plane [$X(\omega,k_1,k_2)$, $Y(\omega,k_1,k_2)$], where $X(\omega,k_1,k_2)$ and $Y(\omega,k_1,k_2)$ are the real and imaginary parts of the characteristic vector (A.23), respectively.

Therefore, on the stability boundary of the considered system, the following relations hold:

$$\begin{gathered} X(\omega,k_1,k_2)=R_eD(j\omega)=\omega^4-\left(a_{pp}+a'_{pp}a'_{\psi\psi}v_k\right)\omega^2+a_{\psi p}kk_1=0; \\ Y(\omega,k_1,k_2)=I_mD(j\omega)=-\left(a'_{pp}+a'_{\psi\psi}v_k\right)\omega^2+ \\ +a_{pp}a'_{\psi\psi}v_k+a_{\psi p}kk_2=0, \\ \left(k=\overline{0,n}\right). \end{gathered} \tag{A.24}$$

From relations (A.24), we obtain:

$$\begin{gathered} k_1(\omega)=\frac{1}{a_{\psi p}k}\left\{\left(a_{pp}+a'_{pp}a'_{\psi\psi}v_k\right)\omega^2-\omega^4\right\}; \\ k_2(\omega)=\frac{1}{a_{\psi p}k}\left\{\left(a'_{pp}+a'_{\psi\psi}v_k\right)\omega^2-a_{pp}a'_{\psi\psi}v_k\right\}, \\ \left(k=\overline{0,n}\right). \end{gathered} \tag{A.25}$$

Assume: $v_5 = 0$ m·s^{-1}; $\alpha_{\psi p} = 0{,}135 \cdot 10^{-4}$ N^{-1}·m^2·s^{-2}; $\alpha'_{\psi\psi} = 0{,}0408$ m^{-1}; $\alpha_{pp} = 1{,}03 \cdot 10^4$ s^{-2}; $\alpha'_{pp} = 0{,}56 \cdot 10^2$ s^{-1}; $k = 1{,}03 \cdot 10^9$ B^{-1}·Pa·s^{-1}; $v_0 = 25$ m·s^{-1}; $v_1 = 20$ m·s^{-1}; $v_2 = 15$ m·s^{-1}; $v_3 = 10$ m·s^{-1}; $v_4 = 5$ m·s^{-1}.

Figure A4 shows the stability regions of the closed-loop vehicle directional stability system, constructed for each speed value v_k, $(k=\overline{0,5})$. In Fig. A4, the plotted regions almost merge with each other, indicating a minor influence of the current vehicle speed v_k on the directional stability of motion.

To apply the hatching, we will use the hatching rule by constructing the determinant:

$$\Delta=\begin{vmatrix} \dfrac{\partial X(\omega,k_1,k_2)}{\partial k_1} & \dfrac{\partial X(\omega,k_1,k_2)}{\partial k_2} \\ \dfrac{\partial Y(\omega,k_1,k_2)}{\partial k_1} & \dfrac{\partial Y(\omega,k_1,k_2)}{\partial k_2} \end{vmatrix}=\begin{vmatrix} a_{\psi p}k & 0 \\ 0 & a_{\psi p}k \end{vmatrix}=a_{\psi p}^2k^2>0. \tag{A.26}$$

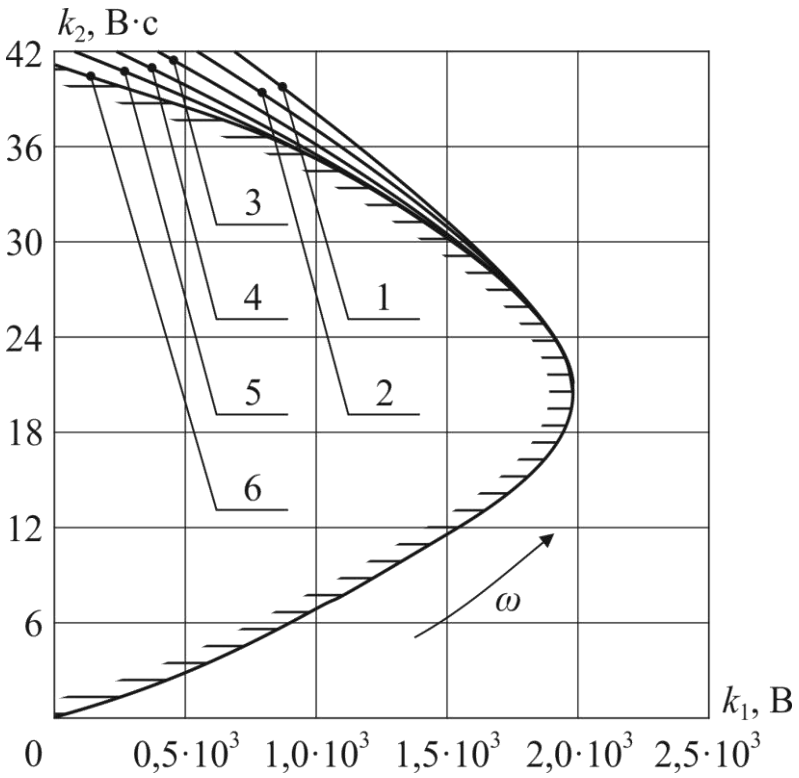

Fig. A4. **Stability regions of the closed-loop vehicle directional stability system:**
1 – v_0 = 25 m·s^{-1}; 2 – v_1 = 20 m·s^{-1}; 3 – v_2 = 15 m·s^{-1};
4 – v_3 = 10 m·s^{-1}; 5 – v_4 = 5 m·s^{-1}; 6 – v_5 = 0 m·s^{-1}.

The determinant (A.26) is positive; therefore, when moving along the stability boundary in the direction of increasing ω, the boundary should be hatched on the left. In this case, the hatching is directed towards the interior of the stability region.

The **object of study** for CGW No. 2 is the processes of angular stabilization of the vehicle body during emergency braking and the selection of values for the variable parameters of the vehicle's directional stability system that ensure motion stability in the given direction.

Bibliography.

1. Aleksandrov Ye., Aleksandrova T., Kostianyk I., Morgun Ya. (2023). Simulation of Random External Disturbance Acting on the Car Body in the Urgent Braking Mode. *Advanced Information Systems*. 7(1). 14 – 17.
2. Aleksandrov, E. E., Bohomolov, V. O., Klymenko, V. I., & Leontiev, D. M. (2025). *Prykladna teoriia kolyvan dlia studentiv avtomobilnykh spetsialnostei vyshchiv: navchalnyi posibnyk* [Applied Theory of Oscillations for Students of Automotive Specialties at Higher Education Institutions: A Textbook].
3. Aleksandrov, E. E. (2010). *Osnovy avtomobil'noi avtomatiki* [Fundamentals of automotive automation]. KhNADU.
4. Aleksandrov, E. E., Aleksandrova, T. E., & Ovcharenko, Yu. E. (2019). *Pidvyshchennia tekhnichnykh ta erhnomichnykh kharakterystyk rukhomykh ob'iektiv viys'kovoho pryznachennia* [Improvement of technical and ergonomic characteristics of military mobile objects]. KhNADU
5. Alexandrov, Ye., Alexandrova, T., & Morgun, Ya. (2019). Parametric Synthesis of the Electronic Control Unit of the Course Stability System of the Car. *Easter-European Journal of Enterprise Technologies*, 6/9(102), 39–45.
6. Aleksandrov, E. E., Aleksandrova, T. E., Hryhor'iev, O. L., & Morhun, Ya. Yu. (2020). Stiikist' ta avtokolyvannia elektronnoi zamknienoi systemy stabilizatsii kursu avtomobilia z tsysternoiu [Stability and self-oscillations of the electronic closed-loop car course stabilization system with a tank]. *Bulletin of NTU "KhPI". Series: "Mathematical Modeling in Engineering and Technologies"*, 1, 44–63.
7. Aleksandrov, E. E., Aleksandrova, T. E., Hryhor'iev, O. L., & Morhun, Ya. Yu. (2021). Pro vplyv kolyvan' vil'noi poverkhni ridyny na kursovu stiikist' avtomobilia-palyvozapravnyka [On the influence of free liquid surface oscillations on the directional stability of a refueling truck]. *Ozbroiennia ta viys'kova tekhnika*, 1, 36–43.
8. Aleksandrov, E. E., Aleksandrova, T. E., Hryhor'iev, O. L., & Morhun, Ya. Yu. (2021). Pro vplyv kolyvan' transportuiemoi ridyny na oblast' stiikosti zamknienoi systemy avtomatychnoho keruvannia kursom avtomobilia [On the influence of transported

liquid oscillations on the stability region of the closed-loop automatic car course control system]. *Bulletin of NTU "KhPI". Series: "System Analysis, Control and Information Technologies"*, 1(5), 29–41.
9. Ihdalov, I. M., Kuchma, L. D., Poliakov, M. V., & Sheptun, Yu. D. (2004). *Rakety-nosii i kosmichni stupeni raket yak ob'iekt keruvannia* [Launch vehicles and space rocket stages as a control object]. ART-PRESS.
10. Eswaran, M., Parulekar, Y.M., Reddy, G.R. (2019). Introduction to Structural Dynamics and Vibration of Single-Degree-of-Freedom Systems. In: Reddy, G., Muruva, H., Verma, A. (eds) *Textbook of Seismic Design*. Springer, Singapore. https://doi.org/10.1007/978-981-13-3176-3_3
11. Kerschen, G., Vakakis, A.F. (2020). *Modal Analysis of Nonlinear Mechanical Systems*. In: Allemang, R., Avitabile, P. (eds) Handbook of Experimental Structural Dynamics. Springer, New York, NY. https://doi.org/10.1007/978-1-4939-6503-8_35-1
12. Linge, S., Langtangen, H.P. (2017). Vibration ODEs. In: Finite Difference Computing with PDEs. *Texts in Computational Science and Engineering*, 16. Springer, Cham. https://doi.org/10.1007/978-3-319-55456-3_1
13. Povstenko, Y. (2024). Essentials of Fractional Calculus. In: Fractional Thermoelasticity. *Solid Mechanics and Its Applications*, 278. Springer, Cham. https://doi.org/10.1007/978-3-031-64587-7_1
14. Volterra, E., Zachmanoglou, E.C., & Kolsky, H. (1965). *Dynamics of vibrations*.
15. Chang, Zongyu & Ali, Rai & Ren, Ping & Zhang, Guangbin & Wu, Peixin. (2015). Dynamics and Vibration Analysis of Delta Robot. *Proceedings of the 5th International Conference on Information Engineering for Mechanics and Materials.* 1408-1417. https://doi.org/10.2991/icimm-15.2015.257
16. Genta, G. (2009). Vibration of Beams. In: Genta, G. (eds) Vibration Dynamics and Control. *Mechanical Engineering Series*. Springer, Boston, MA. https://doi.org/10.1007/978-0-387-79580-5_12

Notes

Notes

Навчальне видання

АЛЄКСАНДРОВ Євген Євгенович
БОГОМОЛОВ Віктор Олександрович
КЛИМЕНКО Валерій Іванович
ЛЕОНТЬЄВ Дмитро Миколайович

ПРИКЛАДНА ТЕОРІЯ КОЛИВАНЬ
для студентів автомобільних спеціальностей вищів

Навчальний посібник
друге видання
(англійською мовою)

Відповідальний за випуск *В.І. Клименко*

Редактор *Д.М. Леонтьєв*

Комп'ютерна верстка *Д.М. Леонтьєв*

Дизайн обкладинки *Д.М. Леонтьєв*

Видавець ФОП Бровін О.В.
Свідоцтво про внесення суб'єкта до Державного реєстру видавців та виготовників видавничої продукції серія ДК 3587 від 23.09.09 р.
Формат 60x84/16 Ум. друк. арк. 9.3. Тир. 100 прим. Зам. 856.

Надруковано з макету замовника ФОП Бровіна І.П.
61022, м. Харків, вул. Трінклера, 2, корп.1, к.19. Т. (066) 822-71-30

СТИЛЬ-ІЗДАТ®
ДРУКАРНЯ
www.stil-izdat.com